Untersuchung der Wechselwirkung von Molekülen (CsCl, NaCl, Benzolderivate) und Atomen (Na) mit gefrorenen Oberflächen (H_2O, CH_3OH, NH_3)

Dissertation

Zur Erlangung des Grades eines
Doktors der Naturwissenschaften

vorgelegt von
Andriy Borodin
aus Stariy Oskol/Rußland

genehmigt von der
Mathematisch-Naturwissenschaftlichen Fakultät
Der TU Clausthal

Tag der mündlichen Prüfung: 30 Juli 2004

Dekan:	Prof. Dr. D. Mayer
Berichterstatter:	Prof. Dr. V. Kempter
Berichterstatter:	Prof. Dr. W. Daum

Diese Arbeit wurde am Institut für Physik und Physikalische Technologien der Technischen Universität Clausthal angefertigt.

Diese Arbeit gründet sich auf den folgenden Veröffentlichen:

Kapitel II. ***Ionization and solvation of CsCl interacting with solid water***

A. Borodin, O. Höfft, S. Krischok, V. Kempter, Journal of Physical Chemistry B 107 (35): 9357-9362 (2003)

Interaction of NaCl with Solid Water

A. Borodin, O. Höfft, U. Kahnert, V. Kempter, A. Poddey, and P.E. Blöchl, Journal of Chemical Physics 121 (18): xxxx (2004)

Kapitel III. ***The interface between benzenes (C_6H_6; C_6H_5Cl; 2-C_6H_4OHCl) and amorphous solid water studied with metastable impact electron spectroscopy and ultraviolet photoelectron spectroscopy (HeI-II)***

A. Borodin, O. Höfft, U. Kahnert, S. Krischok, M. O. Abou-Helal and V. Kempter, Journal of Chemical Physics 120 (11): 5407-5413 (2004)

Kapitel IV. ***The interaction of Na atoms with the molecular surfaces H_2O and CH_3OH: The role of delocalized Na3s electrons***

A. Borodin, O. Höfft, U. Kahnert, V. Kempter, A. Allouche, Physical Surface Engineering Vol. 1 (2): 146-154 (2003)

Electron Solvation by Polar Molecules: The Interaction of Na Atoms with Solid Methanol Films Studied with MIES and Density Functional Theory Calculations

A.Borodin, O. Höfft, U. Kahnert and V. Kempter, Y. Ferro, A. Allouche, Journal of Chemical Physics 120(18): 8692-8697 (2004)

Electron Delocalization by Polar Molecules: Interaction of Na Atoms with Solid Ammonia Films Studied with MIES and Density Functional Theory

A.Borodin, O. Höfft, V. Kempter, and Y. Ferro, A. Allouche
Journal of Chemical Physics 120(18): 8692-8697 (2004)

Inhaltsverzeichnis

Danksagung

Die Arbeit wurde von mir am Institut für Physik und Physikalische Technologien der Technischen Universität Clausthal durchgeführt und sie ist entsanden als Ergebnis der Unterstützung mehrerer Mitarbeiter.
Zunächst bedanke ich mich bei meinem Betreuer Prof. Dr. V. Kempter. Sein Beitrag in der Arbeit kann nicht hoch genug eingeschätzt werden. Er hat mich in jeder Etappe sehr unterstützt und unschätzbare Beträge bei meiner Arbeit geleistet, wie z.B. in der Aufgabenstellung, im theoretischen Ansatz, Besprechen von Ergebnissen.
Ebenso bedanke ich mich bei Prof. Dr. W. Daum für Übernahme des Korreferats.
Mehrere Teile dieser Arbeit sind in der Zusammenarbeit mit Theoretikern entstanden. Dafür einen besonderen Dank an Prof. Dr. A. Allouche von der Universität Saint Jèrôme, Marseille (Kapitel IV – Wechselwirkung mit Natrium) und an Prof. Dr. P. E. Blöchl mit seinem Diplomanden A. Poddey aus dem Institut für Theoretische Physik der TU-Clausthal (Kapitel II – Solvatation von Chlor im Wasser).
Ich möchte auch den ehemaligen und heutigen Mitarbeitern unserer Arbeitsgruppe danken: Dr. habil. W. Maus-Friedrichs, dessen Erfahrung mir oft geholfen hat; Dr. S. Krischok; von ihm habe ich viel über die MIES-Quelle gelernt; O. Höfft, er hat mich tatkräftig unterstützt durch seinen Rat und seine konstruktive Kritik; U. Kahnert, dank ihm ist mir die ehemals fremde Sprache Deutsch verständlich geworden und S. Bahr, durch die Diskussionen mit ihm, habe ich viele Dinge besser verstanden.
Es ist auch zu sagen, dass die Mitarbeiter der Mechanik- und Elektronikwerkstätten viel gemacht haben, damit die Arbeit entstehen konnte. Ich danke den Herren B. Wittenberg, U. Hubert, P. Cyris und R. Zerries.
Ich bedanke mich auch bei meinem ehemaligen wissenschaftlichen Leiter Prof. N. Gladkikh aus Karasin Kharkiv National Universität (Ukraine) für meine Empfehlung an die TU-Clausthal.

Zusammenfassung

Das Verständnis von Prozessen, die zwischen Wasser und verschiedenen Schadstoffen bei tiefen Temperaturen stattfinden, hat heute eine große Bedeutung. Die Untersuchungen haben neben einem rein wissenschaftlichen auch einen ökologischen Aspekt, im Bezug auf den Einfluß verschiedener Schadstoffe auf Eigenschaften der hohen Schichten der Atmosphäre, einschließlich der Entstehung des Ozon-Loches.

Als Haupttechniken für die Untersuchungen wurden Metastable Impact Electron Spectroscopy (MIES) und Photoelektronspektroskopie (UPS) verwendet. Die besonderen Eigenschaften von MIES (Oberflächenempfindlichkeit, zerstörungsfrei, eine einfache Verbindung mit UPS) erlauben, Informationen über die Oberfläche und die adsorbierten dünnen (1-8 Monolagen dicken) Schichten zu bekommen. Die Versuche wurden in der Regel auf einem Wolfram(110)-Substrat bei der Temperatur 80K mit anschließendem Heizen durchgeführt.

Bei Untersuchungen der Solvatation von Alkali-Halogeniden in Wasser wurden CsCl und, als Vergleich, auch NaCl untersucht. Es wurde festgestellt, dass bei 80K keine Reaktion zwischen den Salzen und Wasser stattfindet. Erst oberhalb 100K werden Wassermoleküle beweglich; im Bereich zwischen dieser Temperatur und der Temperatur der Wasserdesorption dissoziieren Salzmoleküle auf der Wasseroberfläche und dringen als Ionen in den Wasserfilm ein. Wird die Salz-Sättigungskonzentration noch nicht erreicht, so besteht der Film aus den solvatisierten Ionen, und es gibt keine Möglichkeit, Salz in Ionen- oder Molekularform auf der Wasseroberfläche zu sehen. Es ist auch interessant, dass Eigenschaften der Wasseroberfläche sogar durch kleine Mengen Salz wesentlich geändert werden. Dies betrifft insbesondere die Ausbildung des Wassernetzwerkes über H-Brückenbindungen. Nach der Wasserdesorption ist auf dem Substrat nur eine Salzschicht, deren Eigenschaften

sich nicht von der eines ohne Wasser aufgebrachten Salzes unterscheiden, zu sehen.

Untersuchungen der Wechselwirkung zwischen verschiedenen Benzolderivaten (Benzol, Chlorbenzol und 2-Chlorphenol) und festem Wasser wurden im Temperaturintervall 80-200K durchgeführt. Die Filme wurden bei 80K in verschiedener Reihenfolge aufgebracht und danach bis 200K geheizt. Bei 80K kann eine geschlossene Schicht aufgebracht werden. Im Bereich von ca. 104K bis zur Desorption findet eine Bewegung der Moleküle statt; demzufolge wird der Film wesentlich verändert, z.B. Wasser kann von unteren Lagen durch eine Chlorbenzolschicht auf die Filmoberfläche gelangen, sodass eine geschlossene Lage von Wasser auf der Chlorbenzoloberfläche gebildet wird. Besonderheiten der Wechselwirkung werden für jedes System durch die Profile der freien Energie beschrieben.

Es wurde die Wirkung von Na auf festem Wasser, Methanol und Ammoniak untersucht. Detaillierte Information über Na wurde aus der Na3s-Emission, die sich in MIES gut beobachtet lässt, gezogen; man kann den normalen und solvatisierten Zustand unterscheiden. Es wurde festgestellt, dass Natrium durch das solvatisierte Elektron zur Dissoziation des Wassers bzw. Methanols führt. Im Fall mit Ammoniak tritt zwar keine Reaktion auf; es treten jedoch zwei Na3s-Strukturen auf, bei denen Delokalisation und Solvatation des 3s-Elektron von Na eine Rolle spielen. Aus dem Vergleich mit Dichtefunktional-Rechnungen kann man schließen, dass Na-Dimere beim Solvatationsprozess eine wesentliche Rolle spielen.

1 Kapitel I. Grundlagen und Einführung in die Messmethoden

1.1 Einleitung

Es ist immer wichtig, zu verstehen, welche Prozesse in der Natur stattfinden, und wie die Menschheit auf die Umwelt wirkt. Es muss nicht betont werden, dass sich die Natur heute bereits im wesentlichem geändert hat. Es geht nicht nur um solche Dinge wie Verschmutzung von Landschaften oder die Unterbrechung vielen selbstorganisierter Prozesse, wie z.B. der Erhaltung der chemischen Zusammensetzung der Atmosphäre, die Selbstreinigung der Flüsse, u. s.w. Jetzt ist schon klar, dass der Naturschutz viel bedeutet; sich darauf zu beschränken, reicht aber nicht. In der Tat lässt sich der technische Vorschritt nicht verhindern, und eine aktuelle Frage lautet: Wie soll man Betriebsprozesse führen, damit so wenig wie möglich Schadstoffe produziert werden, bzw. so ungiftig wie möglich. Dafür soll man eine gute Vorstellung über die Wirkung von verschiedenen Schadstoffen auf die Natur haben.

Die Ergebnisse der Arbeit sind in drei Teilen mit den unterschiedlichen Themen dargestellt; jedoch hat jeder Teil einen Bezug zu den Fragen der Ökologie. Prozesse, die untersucht wurden, finden bei tiefen Temperaturen an der Oberfläche von dünnen Wasserschichten statt. In der Natur entspricht es den Eiskristallen in hohen Schichten der Atmosphäre.

Im Kapitel II wird die Wechselwirkung von Alkali-Halogeniden mit Wasser bei solchen Bedingungen behandelt. Die Halogene in verschiedenen Verbindungen sind ein großer Teil von den Schadstoffen, die riesige Auswirkungen nach sich ziehen können; weit bekannt ist z.B. die Entstehung des Ozon-Loches. Es wurden Versuche mit verschiedenen Salzen (CsCl, NaCl) durchgeführt. Dabei wurde Dissoziation und Solvatation von den Salzen untersucht.

Die Frage vom Kapitel III ist: Welche Wechselwirkung kann bei solchen Bedingungen zwischen Wasser und verschiedenen Benzolderivate stattfinden. Es ist bekannt, dass sich aus mehreren solcher Moleküle unter der Wirkung von ultravioletter Strahlung sehr giftige Dioxin-Verbindungen bilden können. Wie funktioniert das und gibt es überhaupt die Wechselwirkung auf der Wasseroberfläche bei tiefer Temperatur? Es wurden die Systeme mit Benzol, Chlorbenzol und 2-Chlorphenol untersucht.

Im Kapitel IV werden die Versuche mit Natrium durchgeführt. Natrium ist ein Material mir sehr großer chemischer Aktivität; deswegen wird es bei katalytischen Prozessen breit verwendet. Die Wirkung von Natrium wurde anhand von Wasser, Ammoniak und Methanol untersucht. Das ist besonders wichtig für das Verständnis der Rolle des Na3s-Elektrons, durch das viele Reaktionen mit Na verursacht werden. Weiteres Interesse an der Methanol-Natrium Wechselwirkung liegt darin, dass sich dabei als Reaktionsprodukt Methoxy beobachten lässt. Dies könnte der erste Schritt für die Produktion von Bimethylether (ein “Zukunfts”-Kraftstoff) sein.

1.2 Experimentelle Grundlagen

1.2.1 Aufbau der Messapparatur.

Die zu dieser Doktorarbeit gehörigen Messungen wurden an der Apparatur von der Abteilung Atom- und Molekülphysik an Oberflächen des Instituts für Physik und Physikalische Technologien (IPPT) der Technischen Universität Clausthal (TU-Clausthal) durchgeführt.
Die in dieser Apparatur genutzten Methoden sind:
MIES (Metastable Impact Electrom Spectroscopy)
UPS (Ultraviolet Photo Electron Spectroscopy)
TPD (Thermal Programmed Desorption)

Die Anlage besteht im wesentlichem aus folgenden Teilen:

- Hauptkammer;
- Probenhalter;
- Einrichtungen (Gaseinlass, Verdampfern) fürs Auftragen der untersuchten Materialien;
- verschiedenen Quellen für die Versorgung der oben erwähnten Methoden;
- Halbkugelanalysator.

Alle Komponenten von der Anlage werden in den entsprechenden Kapiteln ausführlich beschrieben.

1.2.2 Ultrahochvakuumkammer

Die Hauptkammer hat die Form eines Zylinders mit dem Durchmesser 14´´. Die Kammer wird durch eine Turbomolekularpumpe mit einer Pumpleistung von 510l/s gepumpt. Der Basisdruck in der Kammer liegt im Bereich ca. $2 \cdot 10^{-10}$Torr. Um den Druck kurzfristig zu verbessern, ist die Anlage mit einem Ti-Filament ausgestattet. Durch das Filament wird auf einer, auf 80K gekühlten Oberfläche, eine Ti-Schicht erzeugt. Dank den guten Adsorptionseigenschaften von Titan wird das Vakuum so verbessert, dass während eines Versuches der Druck den Wert um $5 \cdot 10^{-11}$Torr erreichen kann.

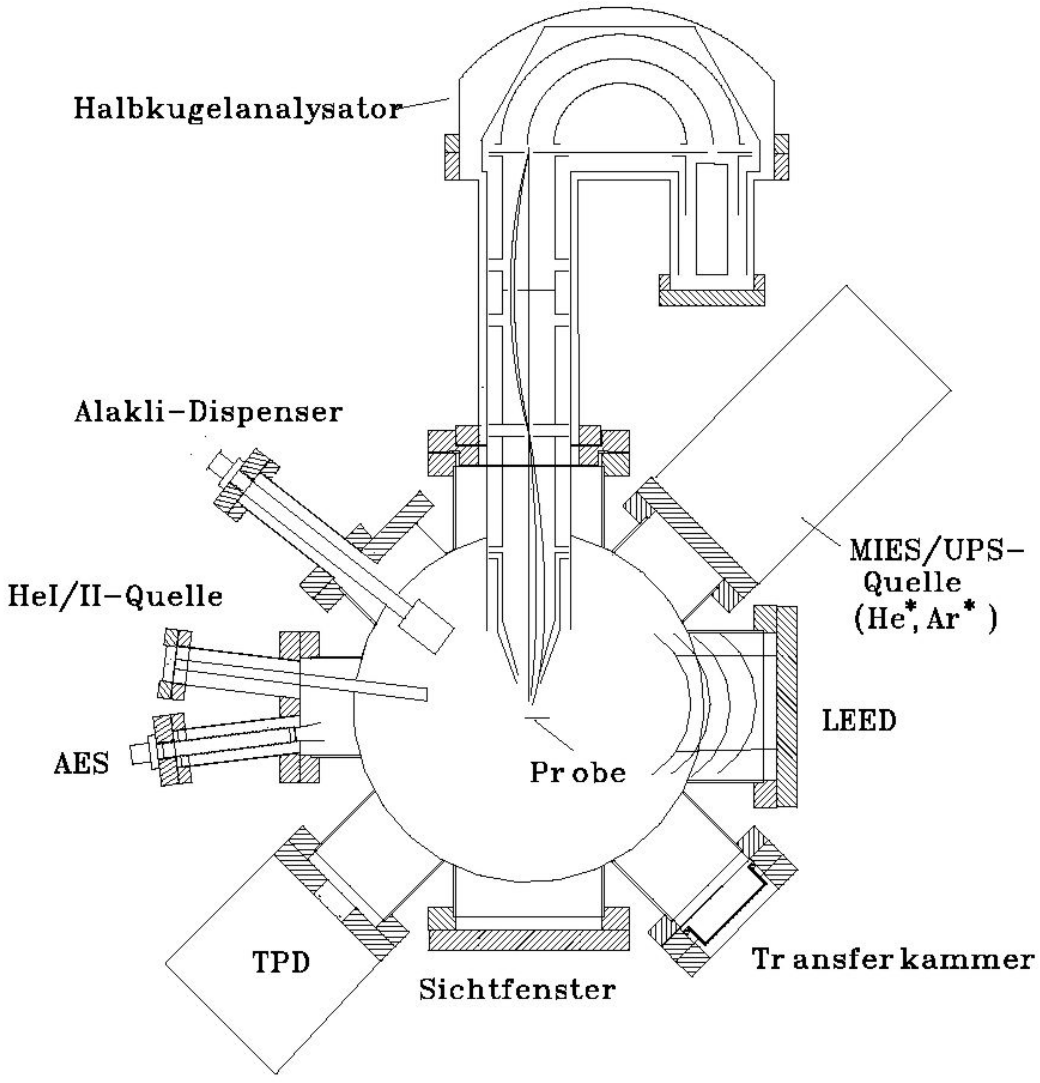

Abbildung 1.1 Schnitt der Hauptkammer

1.2.3 Substrathalter

Von einem für die Messungen aus der Arbeit geeigneten Substrathalter ist das Folgende erforderlich:

- Die Probe soll sich möglichst tief, bis zu 80K kühlen lassen;
- Es soll eine Möglichkeit geben, Messungen bei einer ausgewählten Temperatur durchzuführen;
- Das Heizen der Probe soll die thermische Reinigung der Substratsoberfläche erlauben;
- Die Temperatur von der Probe soll möglichst genau messbar sein.
- die Probe soll sich einstellen lassen;
- Substratpotential soll frei wählbar sein;

Um die Forderungen zu erfüllen, wurde die auf der Abb. 1.2 dargestellte Konstruktion entwickelt: Auf einen mit flüssigem Stickstoff gekühlten Kupfer-Behälter wird eine Molybdän-Halteplatte geschraubt. Auf der Platte wird ein Wolfram(110)-Kristall mit Schrauben und flexiblen Platten befestigt, die ebenso aus Molybdän hergestellt wurden. Auf der anderen Seite der Platte wird durch die stromisolierenden Keramikscheiben eine Konstruktion aus einem W-Filament (Wolfram-Draht Ø=0.3mm) mit einem Molybdän-Schirm geschraubt. Beim Ausheizen werden Elektronen von der W-Drahtoberfläche emittiert, durch ein zwischen dem Draht und der Probe angelegtes Potential (0.5-1.5kV) beschleunigt und auf die Probe gerichtet. So wird die Probe intensiv geheizt. Wird kein intensives Heizen gebraucht, kann man ohne Hochspannung nur mit der Ausstrahlung vom W-Draht die Probe heizen.

Die ganze Konstruktion wird auf einem Manipulator montiert. Um Wärmeverluste zu verhindern, sind zwischen der Probe und dem Manipulator als Wärmeisolation zwei Edelstahlbolzen eingebaut. Damit auch das Potential der Probe frei wählbar ist, ist die Probe vom Manipulator durch ein Keramikstück isoliert.

Der Manipulator lässt sich in drei orthogonalen Richtungen schieben und um die senkrechte Achse drehen. Es gibt die Möglichkeit, die Bewegungen mit einem Rechner zu steuern.

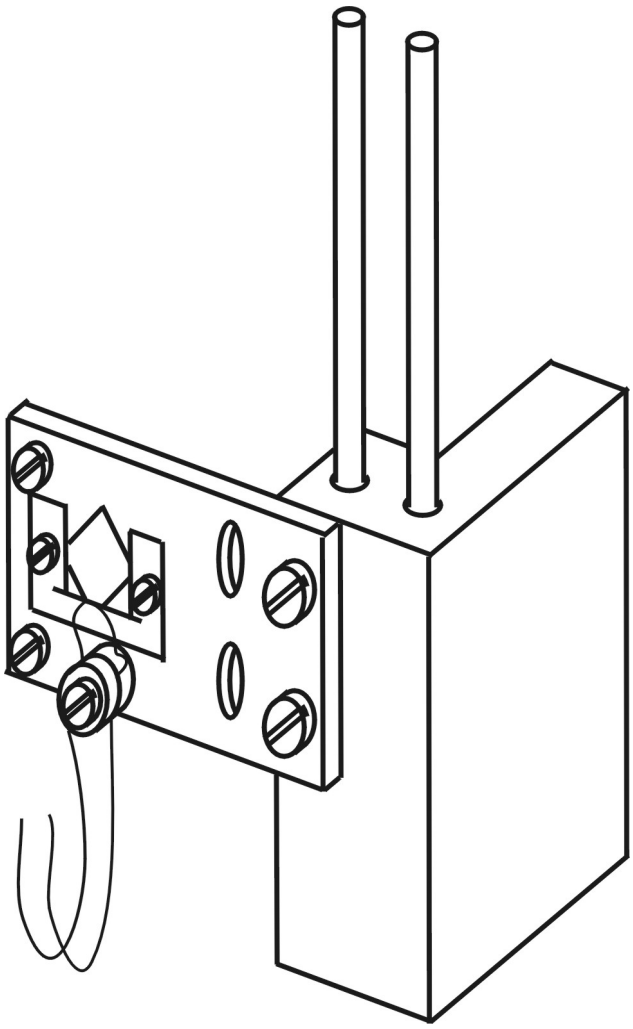

Abbildung 1.2 Probenhalter

1.2.4 Gaseinlasssystem

Um verschiedene Gase anzubieten, wurde die Anlage mit einem Gaseinlasssystem ausgestattet. Der Gaseinlass besteht aus zwei unabhängigen, fast identischen Hälften. Jede von denen hat ein Nadelventil für die Feindosierung des angebotenen Gases. Das Ventil ist über die 6mm-Edelstahlröhre mit Ventilen von den Gas/Flüssigkeit-Gefäßen und mit einem Ventil für das Anpumpen des Gaseinlass verbunden. Die Ventile von den Gas/Flüssigkeit-Gefäßen haben die „Swagelok"-Anschlüsse, wodurch verschiedene Gefäße oder Ballone mit verflüssigten Gasen am Gaseinlass angeschlossen werden können. Das System wird durch eine Vorvakuumpumpe angepumpt. Um den Ölanteil im Restgas zu vermindern, wird in Reihe nach der Pumpe eine Kuhlfalle angeschlossen.

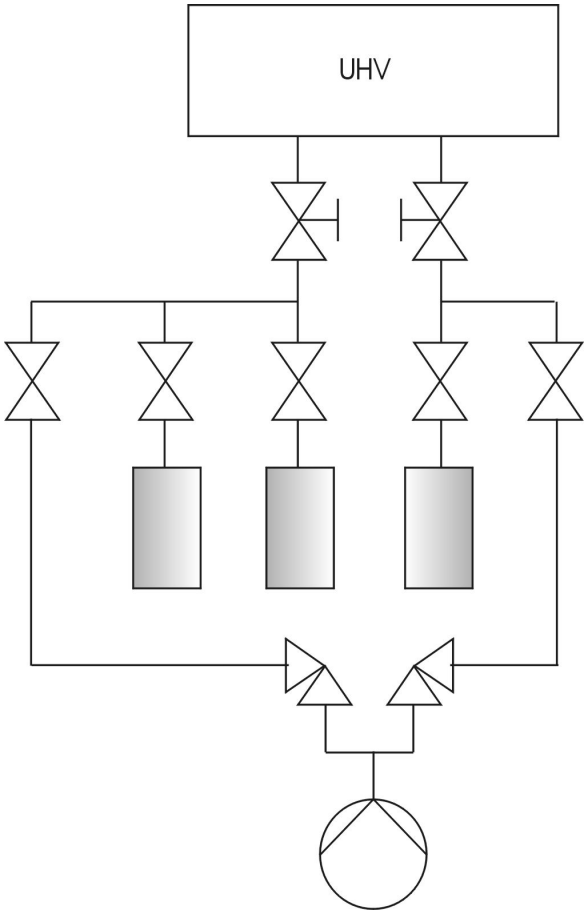

Abbildung 1.3 Gaseinlasssystem.

1.2.5 Verdampfer

Um die Probe mit solchen Adsorbaten wie Alkalimetalle und Salze zu bedampfen, wurden spezielle Verdampfer genutzt. Sie sind so eingebaut, dass während eines Auftragens Spektren immer abgelesen werden können.
Fürs Aufbringen der Alkalimetalle wurden Dispenser von „SAES Getters“ ausgewählt. Eine Beschreibung eines Dispensers dieses Typs ist in den Datenblättern des Herstellers zu entnehmen.
Für das Angebot eines Salzes wurde ein selbstgebauter Verdampfer verwendet. Die Konstruktion wird auf einem KF63-Flansch montiert und besteht aus einem mit Salz (z.B. CsCl) ausgefüllten Quarzglasrohr, um welches ein Wolfram-Draht (Ø=0.3mm) gewickelt ist. Das Teil befindet sich in einem Gehäuse mit einem schmalen Ausgagspalt, der mit einem beweglichen „Shutter“ innerhalb der Vorheizzeit zugemacht werden kann.

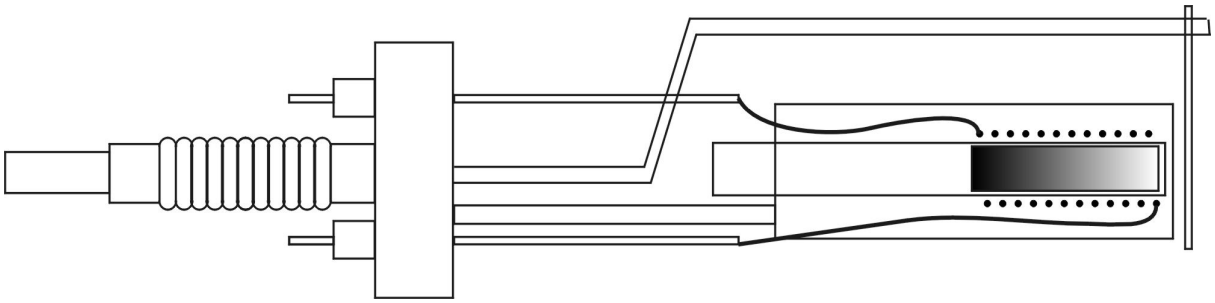

Abbildung 1.4 Salzverdampfer.

1.2.6 Halbkugelanalysator

An der Anlage wird ein Halbkugelanalysator (HKA) vom Typ EA10/100 von Fa. Leybold verwendet. Eine schematische Darstellung der Flugbahn der analysierten Elektronen für den HKA ist auf Abb. 1.5 gezeigt:

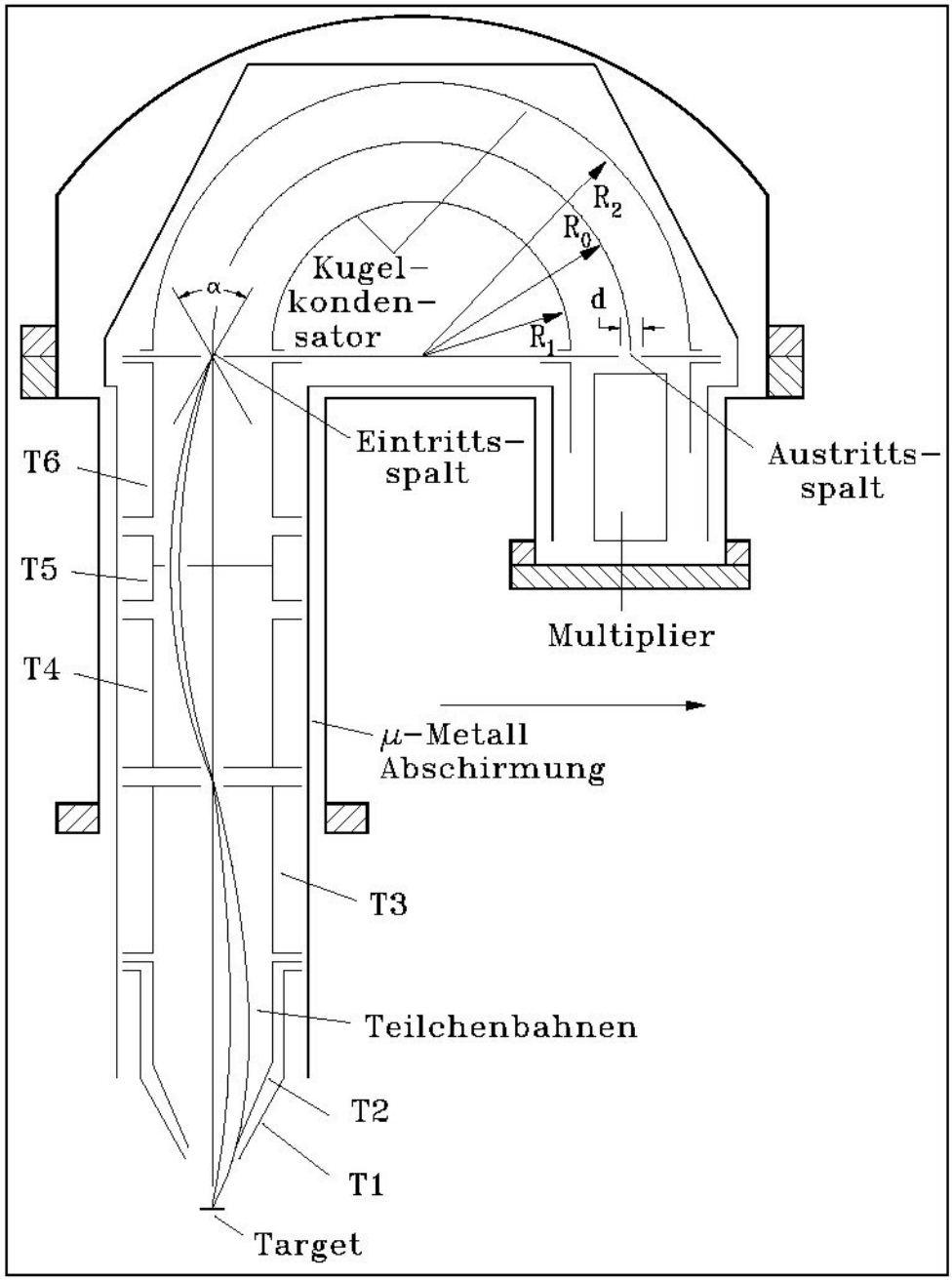

Abbildung 1.5 Schnittzeichnung des Halbkugelanalysators. R_0=97mm, Akzeptanzwinkel α=16°, Ein- bzw Austrittspalt d=0.5mm

Da die elektrostatischen Eigenschaften des Analysators schon mehrmals [1, 2, 3] beschrieben wurden, kann man die wichtigsten Eigenschaften in einer Tabelle (Tab. 1.1.) zusammenfassen:

$\frac{\Delta E}{E_{Kin}} = const$ (CCR)	$\Delta E = const$ (CPE)
Transmission nicht konstant $\mathbf{I} \sim E_{Kin}$	Transmission nicht konstant $\mathbf{I} \sim \frac{1}{E_{Kin}}$
Zu hohe Auflösung für kleine Energien $\Delta E \sim E_{Kin}$	Optimale Auflösung für kleine Energien $\Delta E = const.$
Bei konstantem Retadierungsfaktor bleibt der betrachtete Probenbereich konstant $F_S = const.$	Für alle Energien bleibt der betrachtete Probenbereich konstant $F_S = const.$
Bei konstantem Retardierungsfaktor bleibt der Raumwinkel konstant $\Omega_S = const.$	Veränderlicher Raumwinkel $\Omega_S \sim \frac{1}{E_{Kin}}$
Schlechtes Signal-Rausch Verhältnis bei kleinen Energien	Optimales Signal-Rausch Verhältnis bei kleine Energien
Die Sekundärelektronenausbeute (des Multipliers) ist nur dann konstant, wenn das Potential der ersten Multiplierdynode an die Passenergie gekoppelt ist	Die Sekundärelektronenemission (des Multipliers) ist konstant. Mit der Auflösung muß auch das Potential der ersten Multiplierdynode geändert werden

Tabelle 1.1. Eigenschaften des HKA in seinen zwei Betribsmodi.

Die Tabelle erklärt wohl, warum für die Valenzbandspektroskopie (MIES, UPS – E ~ 0÷40eV) ein Modus mit konstanter Passenergie ausgewählt wird.

1.2.6.1 Korrekturspannung zur Austrittarbeitskompensation.

Ein wichtiger Parameter beim Betrieb des HKA ist die Spannung zwischen der Probe und dem Analysator. Im Fall der unmittelbaren elektrischen Verbindung werden die Ferminiveaus von den beiden ausgeglichen. Demzufolge werden die Vakuumniveaus von der Probe und vom Analysator (bei den unterschiedlichen Austrittarbeiten) unterschiedlich. Bei den fast immer erfüllten Umständen, dass Austrittarbeit des Analysators größer als die vom Substrat ist, führt es zum Ausschneiden eines Teils der Spektren im tiefenergetischen Bereich. Dies wird im EA10/100 durch ein internes Netzteil verhindert. Die Spannung wird normalerweise so eingestellt, dass das Ferminiveau der Probe mit dem

Vakuumniveau des Analysators übereinstimmt. In dem Fall stört es nicht, die niederenergetischen Elektronen zu beobachten. An dieser Apparatur wird zusätzlich an die Probe noch eine negative Spannung (ca. 15V) gelegt. Dies ruft die entsprechende Verschiebung der Spektren hervor und lässt die Intensität steigen.

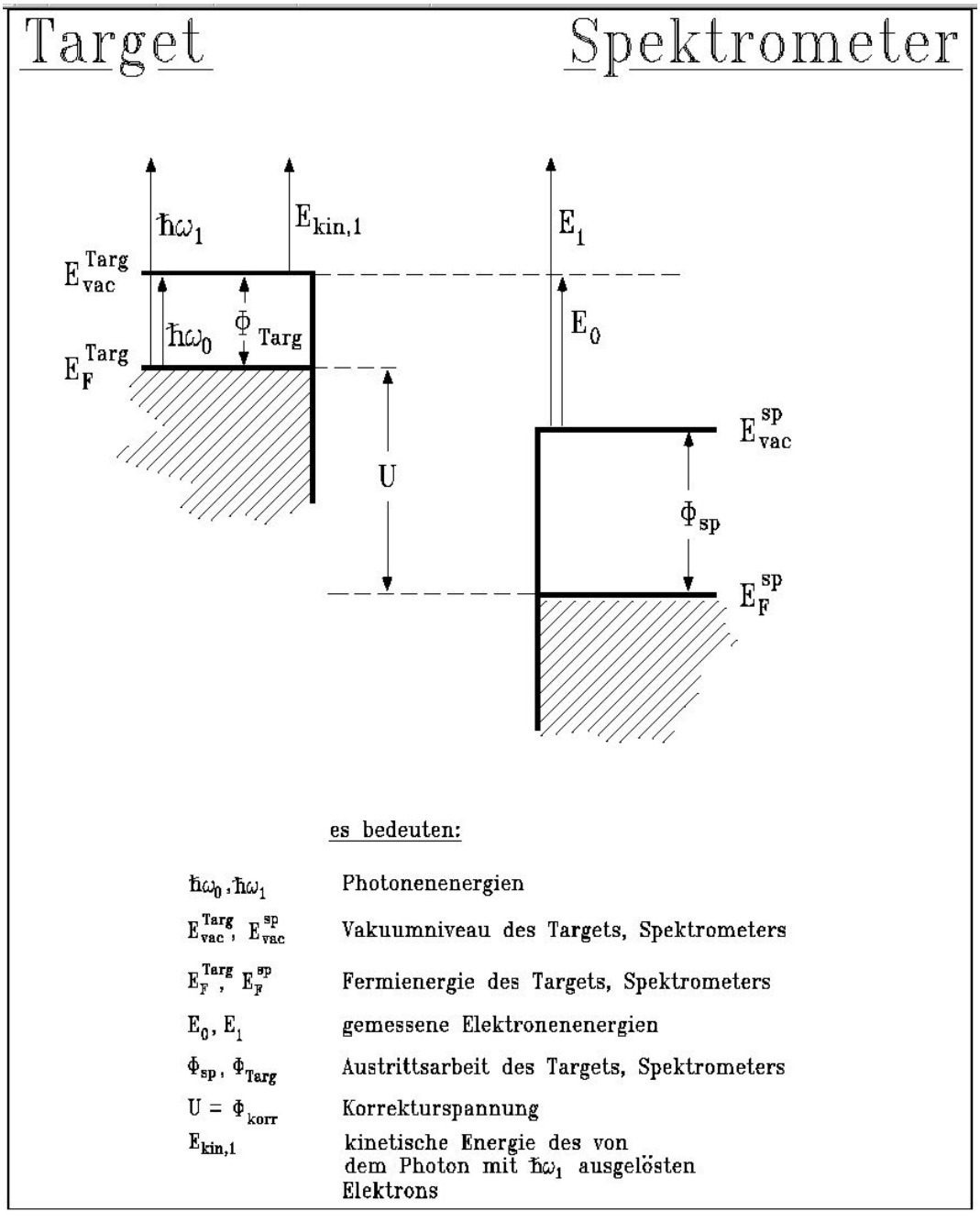

Abbildung 1.6 Kompensation der Austrittarbeit durch die Korrekturspannung

1.2.7 Quelle für metastabile He*-Atome

Diese MIES-Quelle ist ein Ergebnis von weiteren Modifizierungen einer von den Arbeitsgruppen A.Niehaus, H. Hotop und H. Morgner [4, 5, 6] entwickelten Quelle. Sie wurde bereits in mehreren Diplom- und Doktorarbeiten beschrieben [7].

1.2.7.1 Funktionsweise von MIES-Quellen.

Die metastabile He*-Atome können auf verschiedene Weise produziert werden. Diese MIES-Quelle gehört zur Kategorie der kontinuierlich arbeitenden Quellen, die die He*-Atome bei einer Gasentladung produzieren. In solchen Quellen werden auch Photonen (HeI-Photonen) zusätzlich erzeugt, sodass bei einer Messung gleichzeitig zwei Spektren (von MIES und von UPS(HeI)) abgelesen werden.

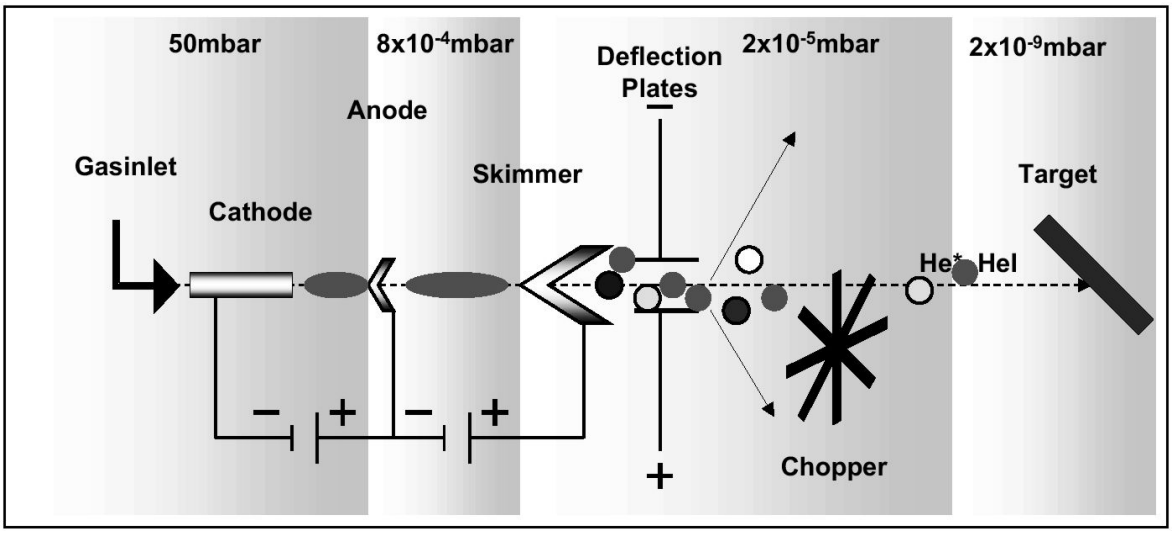

Abbildung 1.7 Schematische Darstellung einer MIES-Quelle.

Wie es auf Abb.1.7 zu sehen ist, können in der Quelle drei Regionen unterschieden werden.

In der ersten Region (Entladungskammer) herrscht der Druck ca. 70Torr, unter dem die richtige Art der Gasentladung stattfindet und neben den erwünschten metastabilen He*-Atome und HeI-Phononen als auch Rydbergatome und He^+-Ionen erzeugt werden. Die unter der Gleichspannung (ca. 300V) gezündete Entladung befindet sich im Bereich zwischen einer Kathode und einer Anode. Als Kathode dient ein Wolfram-Rohr mit einem inneren Durchmesser von 0,8mm, durch das wird He-Gas eingelassen und auf ein Loch in der Anode gerichtet. Durch das, als eine Differentielpumpstufe mit einem Durchmesser ca. 0,15mm dienende, Anodenloch treten die Entladungsprodukte in die 2. Region ein. Der Bereich wird über einer Turbomolekularpumpe bepumpt und hat einen Druck ca. $1{,}3\cdot10^{-3}$Torr. Um den Anteil der metastabilen He*-Atome um einen Faktor 30 weiter zu steigern, gibt es in der Region noch eine Entladung. Die Entladung wird zwischen der Anode der Quellekammer und einem Skimmer erzeugt. Durch ein Skimmerloch mit einem Durchmesser von 0,8mm gelangen Produkte von den zwei Entladungen in die dritte so genannte Puffer-Kammer. Da der Druck in der Kammer ca. $1\cdot10^{-5}$Torr (Hochvakuum) beträgt, und da alle Löche auf einer optischen Achse liegen, wird in der Pufferkammer aus Helium ein schmaler (ca. 4mm breit) Strahl erzeugt. Bevor der Strahl durch ein Ventil in die Hauptkammer trifft, wird er durch einen Chopper unterbrochen, was für eine Trennung (s. weiter) der Metastabilen von den HeI-Photonen notwendig ist. Außer dem Chopper befinden sich in der Pufferkammer zwei Ablenkplatten, die gebraucht werden, um geladene Spezies vom Helium-Strahl abzutrennen.

Teilchen	Elektronischer Zustand bzw. Übergang	Anregungsenergie	Ionisationspotential
He Grundzustand	1^1S_0	0eV	24.59eV
He* (Triplett)	2^3S_1	19.82eV	4.77eV
He* (Singulett)	2^1S_0	20.62eV	3.97eV
HeI Photon	$2^1P_1 \longrightarrow 1^1S_0$	21.2eV	–

Tabelle 1.2 Anregungsenergien und Ionisationspotentiale der von der MIES-Quelle emmitierten Teilchen

1.2.7.2 Messelektronik der Flugzeittrennung

Die Trennung der He*-Atome von den HeI-Photonen wird aufgrund der unterschiedlichen Fluggeschwindigkeiten der Atome und der Photonen möglich: Nehmen wir zuerst an, dass der Chopper sich vor kurzem so drehte, dass der Weg von der Quelle bis zum untersuchten Substrat frei wurde. Dann, innerhalb der nächsten 250µs (Flugzeit von metastabilen Atomen auf der 50cm-Strecke für ihre mittlere Geschwindigkeit bei der Raumtemperatur), lässt sich im gemessenen Spektrum nur der UPS(HeI)-Anteil beobachten. Wird nach den 250µs der Chopper zugemacht, so bekommt man zwar keine HeI-Photonen mehr, aber immer noch innerhalb der nächsten 250µs die He*-Atome. Also kommt der MIES-Anteil des Spektrums. Der zweiteilige Prozess kann eine beliebig lange Zeit wiederholt werden.

Die Elektronik für die Trennung MIES von UPS soll folgende Funktionen erfüllen:

1) Die Steuerung der Chopperfrequenz;
2) Das Ablesen der Chopperposition;
3) Das Umschalten, je nach der Chopperposition, des Signals vom HKA in den MIES- oder UPS-Kanal;
4) Da in Wirklichkeit die Metastabilen keine bestimmte Geschwindigkeit besitzen, sondern eine Geschwindigkeitsverteilung (Maxwell-Bolzmanverteilung) haben, soll man die Zeit, die während des UPS-Anteils eines Spektrums gemessen wird (so genannte UPS-Fenster), einschränken. Da ein Messfehler beim Ablesen der Chopperposition entstehen kann, soll das MIES-Fenster sich auch einstellen lassen. Auf Grund der möglichen Änderungen von der Raumtemperatur bzw. von der Flugzeit soll die Chopperfrequenz auch einstellbar sein.

Ein Gerät, in dem das alles realisiert ist, stellt die Abbildung 1.8 dar.

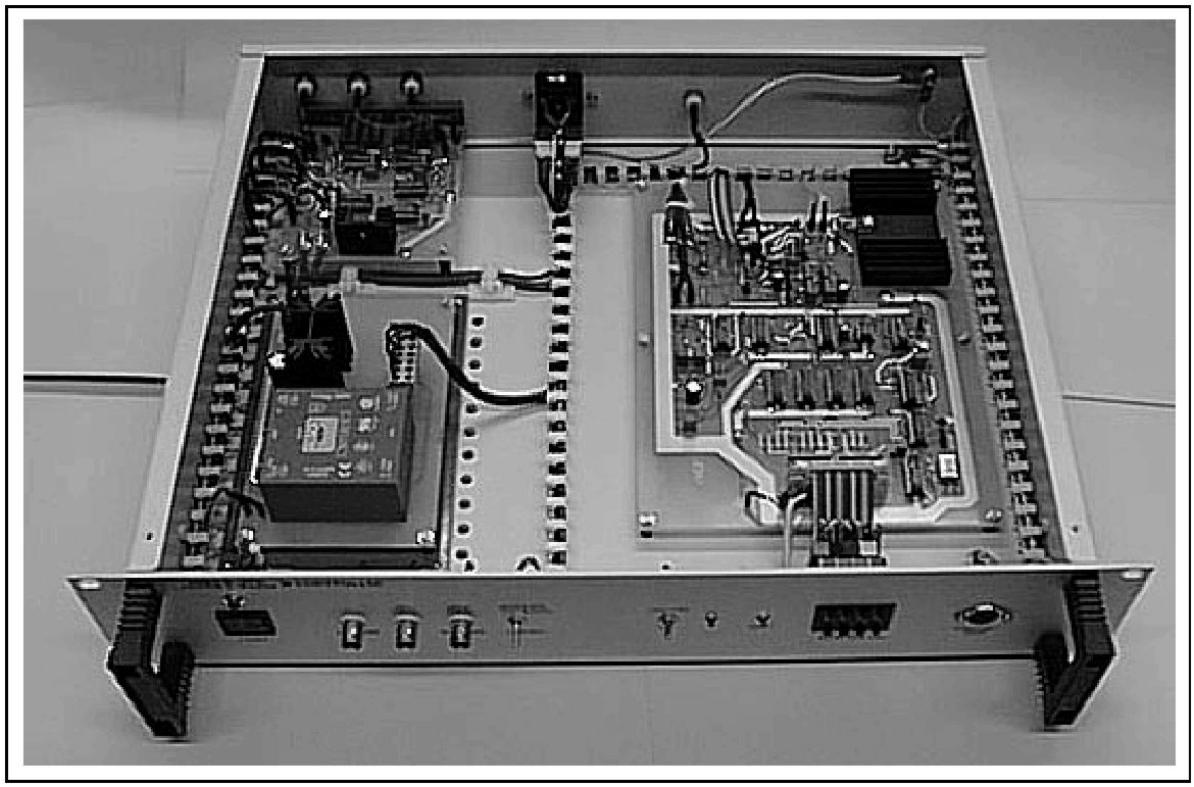

Abbildung 1.8 Das Gehäuse der Chopperelektronik

Ein richtiges Einstellen der oben erwähnten MIES- und UPS-Fenster stellt bei dem W-Substrat und bei einem zur Verfügung stehenden Alkaliverdampfer kein Problem dar:

1) Beim Einstellen des MIES-Fensters nutzt man die 5d-Emission von Wolfram. Die im Analysator eintreffende UPS-Elektronen, die von dem Teil des Valenzbandes kommen, besitzen Energien, die bei MIES nie erreicht werden können. Taucht in einem MIES-Spektrun eine Struktur mit höherer Energie als Fermienergie auf, ist über den UPS-Anteil zu reden. Also, eine Einstellung des MIES-Fensters läuft daraus hinaus, dass das Fenster so breit eingestellt wird, wie es möglich ist, ohne Elektronen mit „Überfermieenergie“ nachzuweisen.
2) Für die Einstellung des UPS-Fensters soll man zuerst eine Alkalischicht (z.B. Cäsium) auf das Substrat aufbringen. Emission von einem s-Elektron (Cs6s) lässt sich in UPS, im Gegensatz zu MIES, nie beobachten. Also, beim Einstellen des UPS-Fensters soll der Anteil des 6s-Elektrons von MIES

minimiert werden. Es ist immer ein Kompromiss zwischen einer guten Statistik der Spektren und relativem Gehalt von MIES in UPS, wegen der breiten Geschwindigkeitverteilung sogar bei einem schmalen UPS-Fenster immer ein wenig von MIES in UPS zu finden ist. Der Grenzwert liegt ca. bei 1% MIES in UPS.

Die folgende Tabelle zeigt einen typischen Betriebsmodus der MIES-Quelle.

Größe	Wert
Entladungsstrom I	60mA
Entladungsstrom II	60mA
Entladungsspannung I	300V
Entladungsspannung II	80V
He-Druck in Quellenkammer	$1.3 \cdot 10^{-3}$Torr
He-Druck in Pufferkammer	$1.8 \cdot 10^{-5}$Torr
Strahlquerschnitt auf dem Target	4mm
Verhältnis He*(2^3S_1) zu He*(2^3S_1)	7:1
Chopperfrequenz	2kHz
Intensität	$1 \cdot 10^{16}$ Atome/sr

Tabelle 1.3 Typische Betriebsparameter der MIES-Quelle.

1.2.8 UPS(HeII)-Quelle

Eine in dieser Arbeit oft benutzte Quelle für die Valenzbandspektroskopie ist die kommerzielle UPS(HeI/HeII)-Quelle Typ HIS13 von Fa. Omicron. Die Quelle erzeugt Ultraviolettphotonen in einer Kaltkathoden-Kappilarentladung. Linien, die sich beim Betrieb beobachten lassen, sind in der Tab. 1.3 dargestellt:

Linien	Energy [eV]	rel. Intensitäten [%]	Wellenlänge [nm]	Satellitenshift [eV]
HeI α	21.22	100	58.43	0
HeI β	23.09	1.2..1.8	53.70	1.87
HeI γ	23.74	0.5	52.22	2.52
HeII α	40.81	100	30.38	0
HeII β	48.37	≤ 10	25.63	7.56
HeII γ	51.02	n.a.	24.30	10.2

Tabelle 1.4 Position, Energien und Intensitäten der beobachteten Linien.

Die Quelle lässt sich in zwei Modi betrieben:

1) Beim HeI-Betrieb werden nur die HeI-Ultraviolettphotonen produziert.
2) Bei so genanntem HeII-Betrieb werden neben den HeII-Photonen auch die von HeI produziert. Dabei ist die Intensität von HeI etwa um einen Faktor 7 höher als die von HeII. Demzufolge, obwohl die Energie von HeII-Photonen 40,81eV beträgt, ist das Valenzband im Bindungsenergiebereich von 40,81eV bis 21,22eV tatsächlich nicht untersuchbar, weil sich dort der HeI-Anteil des Spektrums befindet, durch welchen die HeII-Strukturen überdeckt werden.

In welchem der zwei Modi die Quelle funktionieren soll, wird durch die Betriebsparameter bestimmt. Den verschiedenen Arbeitsdrücken und Arbeitsspannungen entsprechen unterschiedliche Verhältnisse vom HeII- zum HeI-Anteil. In folgender Tabelle werden die Betriebsparameter dargestellt, bei denen die HeI-, bzw. HeII-Intensität jeweils maximal ist.

Linie	Zünddruck [mbar]	Arbeitsdruck [mbar]	Stromstärke [mA]
HeI	5×10^{-2}	8×10^{-2}	30
HeII	5×10^{-2}	1.5×10^{-2}	100

Tabelle 1.5 Betriebsparameter der HeII-Quelle.

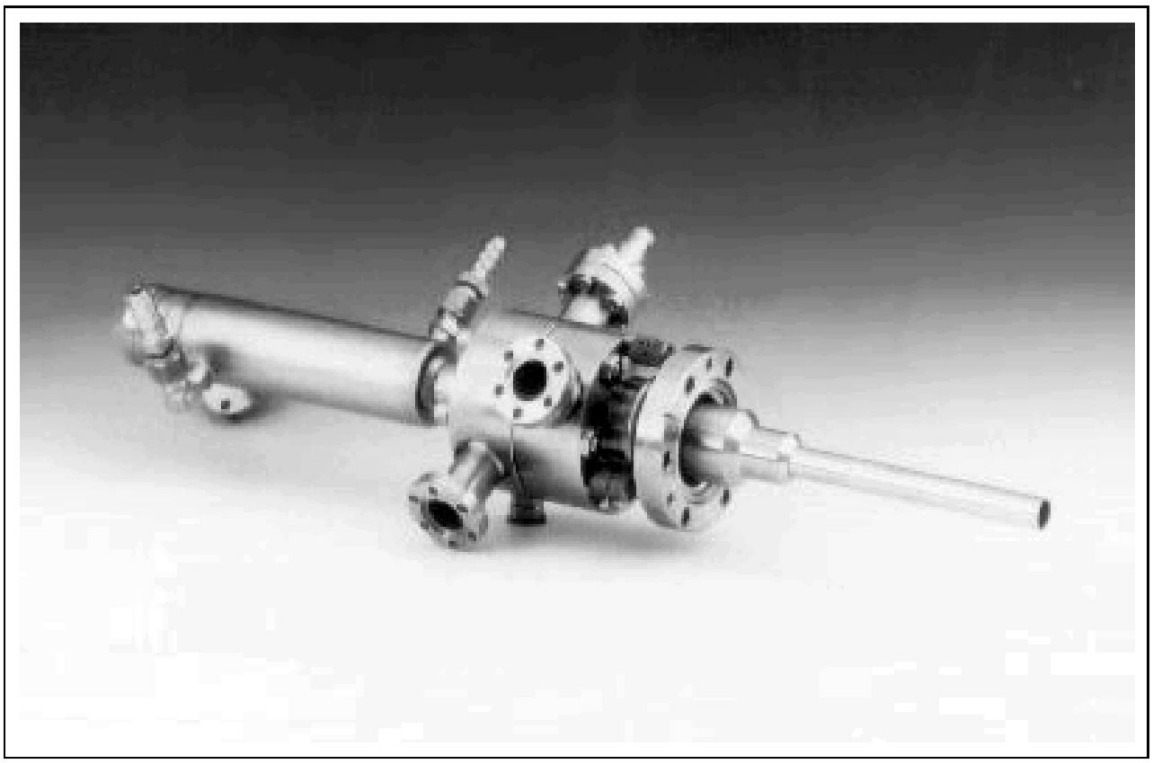

Abbildung 1.9 Die HeII-Quelle

1.3 Physikalische Grundlagen der Messmethoden

Wie es aus den vorigen Kapiteln bereits zu sehen war, ist diese Apparatur für die Untersuchungen mit den spektroskopischen Methoden geeignet. Berücksichtigend, dass der Hauptteil von Messungen im Rahmen dieser Arbeit in MIES und UPS durchgeführt wurde, ist es als sehr wichtig zu erachten, über die physikalischen Aspekte der Spektroskopie, insbesondere über MIES und UPS, zu reden. Auf die elektronischen Prozesse bei den zwei Arten der Spektroskopie wird in diesem Kapitel näher eingegangen.

1.3.1 Metastable Impact Electron Spectroscopy (MIES)

Die im folgenden beschriebenen elektronischen Prozesse sind schon lang bekannt [8, 9] und werden in dem Unterkapitel am Beispiel eines metastbilen He*-Atoms erläutert. Also, es werden Wechselwirkungen vom Substrat mit den Projektilen beschrieben, die für die im weiteren zu interpretierenden Spektren verantwortlich sind.

1.3.1.1 Resonanter Transfer (RT)

Nähert sich ein Projektil einer Oberfläche, wechselwirkt die Wellenfunktion vom Projektil mit der Oberfläche so stark, dass die Wahrscheinlichkeit des Tunnelns eines Elektrons von 2s-Heliumsniveau in einen unbesetzten Resonanzzustand der Oberfläche nicht mehr zu vernachlässigen ist. Daher muss das 2s-Niveau von Helium oberhalb der Fermienergie (bei einem Metall) oder oberhalb des Minimums vom Leitungsbandes (bei einem Substrat mit Bandlücke) liegen.

Die Übergangsrate für den RT-Prozess beträgt typischerweise $1 \cdot 10^{16} s^{-1}$ [10].

1.3.1.2 Auger Neutralisation

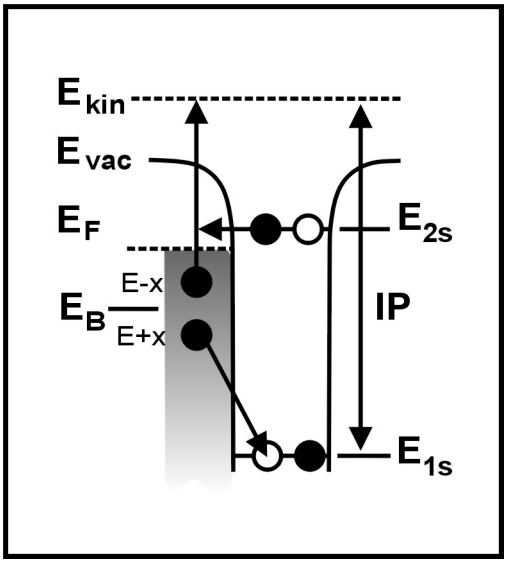

Abbildung 1.10 Resonanter Transfer und Augerneutralisation

Die oben beschriebene Situation kann sich weiter entwickeln. Dabei bekommt das, sich an der Oberfläche befundene, He^+-Ion in seinen halbbesetzten 1s-Zustand, ein Elektron von der Oberfläche. So findet eine Augerneutralisation statt; die dabei befreite Überschussenergie wird durch die Emission eines Elektrons von der Oberfläche abgegeben.

Um die Energiebilanz dieses Prozesses zu beschreiben, werden die folgenden Bezeichnungen verwendet:

Φ_{Pr} – die Austrittsarbeit der Probe (untersuchte Oberfläche);

Φ_{Sp} – die Austrittsarbeit des Spektrometers;

E_F, E_{1s}, E_{2s} und E – die Fermienergie, die Energie von He* 1s, 2s-Niveau und von einem Probeelektron gegen Vakuumniveau.

IP – das Ionisierungspotential; $IP = \Phi_{Pr} + E_F - E_{1s}$

Für die AN-Prozess: (als E wird die mittlere Energie der beteiligten Probenelektronen bezeichnet):

$E_{kin,Pr} + \Phi_{Pr} + E_F - (E-x) = (E+x) - E_{1s}$

$E_{kin,Pr} = IP - 2 \cdot (\Phi_{Pr} + E_F - E)$

$E_{kin,Sp} = IP - \Phi_{Pr} - \Phi_{Sp} - 2 \cdot (E_F - E)$

Entspricht die mittlere Energie der Energie vom höchsten besetzten Orbital ($E = E_F + \Delta E$) oder (bei metallischem Substrat) der Fermienergie ($E = E_F$; $\Delta E = 0$), so bekommt das emittierte Elektron die größte kinetische Energie:

$E_{kin,Sp} = IP - \Phi_{Pr} - \Phi_{Sp} - 2 \cdot \Delta E$

Damit folgt die Breite eines AN-Spektrums:

$E_{kin,Sp}\ (E = E_F + \Delta E) - E_{kin,Sp}\ (E_{kin,\,Pr} = 0) = IP - 2 \cdot \Phi_{Pr} - 2 \cdot \Delta E$

1.3.1.3 Auger Deexcitation

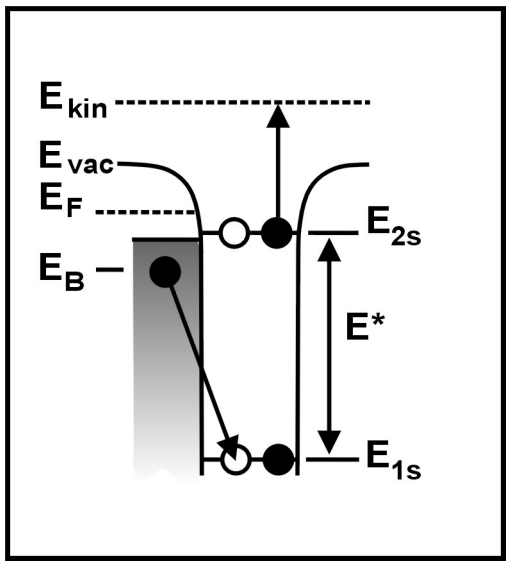

Abbildung 1.11 Augerabregung

Bei dem Prozess kommt ein Probeelektron aus dem Zustand mit der Bindungsenergie E_B in den unbesetzten 1s He*-Zustand. Das 2s-Elektron erhält dann in einem Augerprozeß die Überschußenergie und wird ins Vakuum emittiert.

Die Energiebilanz: ($E^* = E_{1s} - E_{2s}$):

$E^* + (E_B - E_{1s}) = (E_F - E_{1s}) + E_{kin,Pr} + \Phi_{Pr}$

$E_{kin,Pr} = E^* - \Phi_{Pr} - (E_F - E_B)$

$E_{kin,Sp} = E^* - \Phi_{Sp} - (E_F - E_B)$

Der AD-Prozeß ist immer möglich. Die typische Übergangsrate ist etwa $3 \cdot 10^{14} s^{-1}$[10].

1.3.1.4 Autodetatchment

Bei einer kleinen Austrittsarbeit (weniger als 2eV) findet eine Resonanz zwischen einem besetzten Zustand vom Substrat und dem 2s-Niveau vom Helium statt. In dem Fall ist es möglich, dass ein Elektron vom Substrat in das 2s-Niveau vom Helium tunnelt. So entsteht ein kurzlebiges He^{*-}-Ion ($He^{*-}(2s2s^2)$), welches nach einem intraatomaren Augerprozeß zerfällt: $He^{*-}(2s2s^2) \rightarrow He^0(1s^2) + e^-(E_{kin})$.

Dabei kommt eines der 2s-Elektronen in den unbesetzten 1s-Zustand und das andere wird mit der Überschussenergie ins Vakuum emittiert.

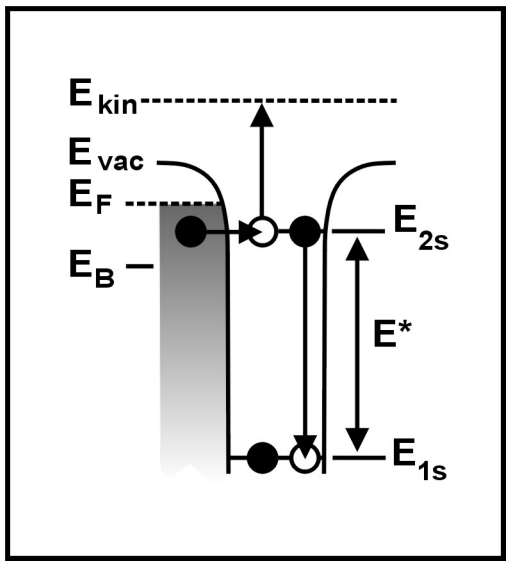

Abbildung 1.12 Autodetatchment

1.3.2 Ultraviolet Photoelectron Spectroscopy

Bei dieser Art der Valenzbandspektroskopie verwendet man die Ultraviolettphotonen mit der Energie von 3 bis 100eV (in Ramen dieser Arbeit die von HeI - 21,12eV und von HeII - 40,80eV). Durch die Bestrahlung werden Photoelektronen aus dem Valenzband ausgelöst.

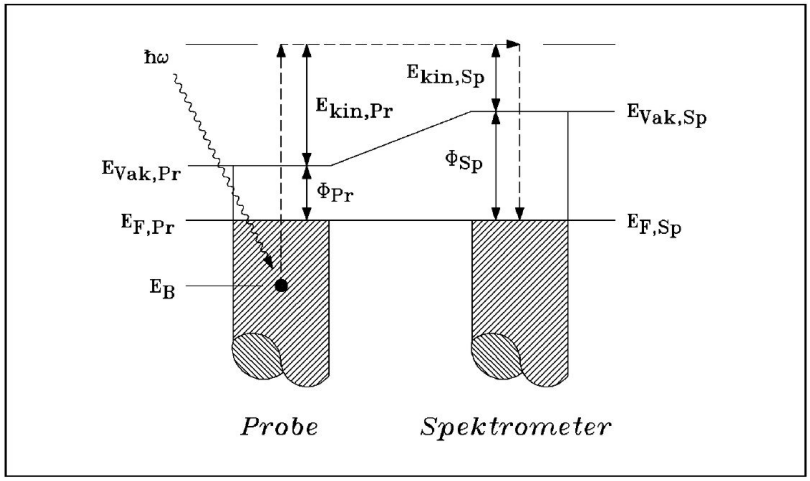

Abbildung 1.13 Energiediagramm einer UPS-Messung. Der Analysator und die Probe sind leitend miteinander verbunden.

Die Energiebilanz des Prozesses:

$E_{kin,Pr} = \hbar\omega + E_B - \Phi_{Pr}$

Wie bereits erwähnt, wird an der Messapparatur eine Spannung zwischen der Probe und dem Analysator so angelegt, dass das Vakuumniveau des Analysators auf das Ferminiveau der Probe fällt. Dann ist die gemessene Energie:

$$E_{kin,Sp} = E_{kin,Pr} + \Phi_{Pr}$$

$$E_{kin,Sp} = \hbar\omega + E_B$$

Bei der so ausgewählten Korrekturspannung wird die maximale gemessene kinetische Energie

$E_{kin,Sp} = \hbar\omega$ (für die Substrate mit der Bandlücke $E_{kin,Sp} = \hbar\omega - (E_F - VBM)$); und die minimale Energie:

$E_{kin,Sp} = \Phi_{Pr}$.

1.4 Literaturverzeichnis

[1] H. Brenten. PhD thesis, TU Clausthal, Physikalisches Institut, 1992.

[2] H. G. Nöller, H. D. Polaschegg, and H. Schillalies. A step towards quantitative electron spectroscopy measurements by improved electron optics. J. of Elec. Spec. and Rel. Phen., 5:705-723, 1974.

[3] K. Berresheim, M. Mattern-Klosson, and M. Wilmers. A standard form of spectra for quantitative ESCA analysis. Fresenius J. Anal. Chem., 341:121-124, 1991.

[4] H. Hotop, E. Kolb, and J. Lorenzen. J. Elec. Spec. and Rel. Phen., 16:213, 1979.

[5] O. Leisin, H. Morgner, and W. A. Müller. Z. Phys. A, 304:23, 1982.

[6] W. Keller, H. Morgner, and W. A. Müller. Mol. Phys, 58:1039, 1986.

[7] W. Maus-Friedrichs, S. Dieckhoff, and V. Kempter. Suf. Sci., 249:149, 1991.

[8] A. L. Shluger, P. V. Sushko, and L. N. Kantorovich. Phys. Rev. B, 59:2417, 1999.

[9] L. N. Kantorovich, A. L. Shluger, P. V. Sushko, and A. M. Stoneham. Surf. Sci, 444:31-51, 1999.

[10] G. Doyen. Surf. Sci, 117:85, 1982.

2 Kapitel II. Wechselwirkung von Alkali-Halogeniden mit festem Wasser

2.1 Ionization and Solvation of CsCl Interacting with Solid Water

Ionization and solvation of CsCl interacting with solid water, A. Borodin, O. Höfft, S. Krischok, V. Kempter, Journal of Physical Chemistry B 107 (35): 9357-9362 (2003)

The interaction of CsCl with solid water, deposited on tungsten at 130K, was investigated. Metastable Impact Electron Spectroscopy (MIES) and UPS(HeI) were applied to study the emission from the ionization of Cl3p and Cs5p and $1b_1$, $3a_1$, and $1b_2$ of molecular water. Below a critical stoichiometry of about $CsCl{\cdot}6H_2O$ the UPS spectra are quite similar to those for codeposition of water and CsCl on tungsten, also studied here, and from chlorides solvated in liquid water in as much as the relative positions and intensities of the water and salt features are concerned. Very little emission from Cl3p and Cs5p is observed with MIES. We propose that CsCl dissociates, and the resulting ions become solvated in solid water. For over-critical stoichiometries Cs and Cl appear at the solid water surface, and become accessible by MIES. CsCl-induced destruction of the water network takes place at the surface, and water molecules interact mainly with Cs and Cl, rather than with other water molecules. When heating under-critical films above 135K the water-induced part of the spectrum changes its shape and becomes more gasphase-like. Beyond 160K no water can be detected anymore with MIES. Above this temperature only Cs and Cl are found on the surface and desorb around 450K. We have also studied water adsorption at 130K on CsCl films. CsCl becomes solvated, and migrates into the water overlayer.

2.1.1 Introduction

So far, the study of molecular surfaces, with water as an important example, has found comparatively little attention [1, 2, 3, 4, 5]. On the other hand, such systems are of considerable interest for our atmosphere: the processes taking place at the surface and in the near-surface region of icy particles can catalyze processes that are suspected to be responsible for the ozone "hole" formation over the polar regions. Under atmospheric conditions (180 to 250K, relevant partial pressures) it has proved difficult to separate and study each of the elementary reaction steps which might be involved in surface-induced transformations (adsorption, solvation, reaction and desorption processes). Recently, sophisticated surface-analytical techniques were applied to study the interaction of atoms and molecules with solid water films. Explicitely, we mention the application of TPD [6], FTIR [7], low-energy reactive ion scattering [8], and NEXAFS [9] to the interaction of HCl with solid water, of the electron-stimulated desorption to the ion release from solid argon, partially covered by NaCl [10], and of the low-energy reactive ion scattering to the hydration of Cs^+ ions scattered from ice films [11], and to ionic dissociation of NaCl on solid water [12]. In the past, electron spectroscopic techniques have been demonstrated to be a powerful tool to study the physics and chemistry on surfaces [1, 13]. For insulating substrates the problem of the surface charge-up could be circumvented by perform- ing the experiments on sufficiently thin films deposited on conducting substrates. We study the surface chemistry on water films under UHV conditions with Metastable Impact Electron Spectroscopy (MIES) and UPS(HeI). The films are grown "in situ" via deposition onto a tungsten substrate at 130K. As was pointed out previously, this approach has several advantages: (1) it is a relatively simple matter to investi-gate both surface and bulk phenomena for films when using the particular technique combination MIES and UPS [5], (2) surface charging is eliminated

when using sufficiently thin films [5], and (3) condensation of water molecules below about 135K results in the formation of an amorphous form of solid water (SW) [6, 14]. To a large extent the properties of SW are believed to be comparable to those of liquid water, in particular with regard to its molecular orientation; SW can therefore be considered as a liquid water substitute, however with a significantly lower water pressure. This makes a comparison of the results with those obtained by UPS on liquid water surfaces and aqueous solutions meaningful [15, 16, 17, 18]. Previous studies carried out under similar conditions were on the interaction of SW with Na atoms and CH_3OH [5]. We report here combined MIES/UPS-studies for CsCl molecules interacting with ultrathin SW films prepared as indicated above. Among the electron spectroscopic tools MIES is characterized by its extremely high surface sensitivity because the He-probe atoms interact with the edge of the surface when still 3 to 5 a.u. away from the surface [18, 19]. Consequently, only the species adsorbed on top of the film will be seen with MIES, in contrast to UPS which will detect both the surface-adsorbed species and those within about 3 layers below the top of the film. Thus, the combination of MIES and UPS appears well suited to study the adsorption and dissociation of salt molecules at and the penetration of the resulting ions into solid water surfaces. As compared to other chlorides, CsCl offers the advantage that cation and anion are both accessible to ionization with the techniques employed inthis study. We present evidence for ionic dissociation of CsCl during its interaction with water at 130K, followed by migration of solvated species into the layer. The stoichiometry up to which the film surface still resembles closely to condensed water is approx. $CsCl{\cdot}6H_2O$. Beyond, interaction of water is mainly with solvated ions, rather than among themselves. A preliminary account of some of the results can be found in Ref. [20].

2.1.2 Experimental remarks

Experimental details were given previously [21, 22, 23, 24, 25]. Brie y, the appa- ratus is equipped with a cold-cathode gas discharge source for the production of metastable He*(^{3}S/^{1}S) (E*=19.8/20.6eV) atoms with thermal kinetic energy and HeI photons (E=21.2eV) as a source for ultraviolet photoelectron spectroscopy (UPS). The intensity ratio ^{3}S/^{1}S is found to be 7:1. In MIES metastable He*1s2s atoms are utilized to eject electrons from the surface. Since the metastables approach the surface with near-thermal kinetic energy (60 to 100meV), this technique is non-destructive and highly surface sensitive (see Refs. [18, 19] for more detailed introductions into MIES and its various applications in molecular and surface spectroscopy). A discharge serves both as source for an intense beam of He*1s2s atoms for MIES and as a HeI photon source for UPS (HeI with 21.2eV). The spectral contributions from metastables and photons are separated be means of a time-of-flight technique. MIES and UPS spectra were acquired with incident photon/metastable beams 45° with respect to the surface normal; electrons emitted in the direction normal to the surface are analyzed. Collection of a MIES/UPS spectrum requires approximately 100s. The measurements were performed using a hemispherical analyzer (Leybold EA10/100). In order to minimize charge-up phenomena, we worked with low beam currents densities, and thus an energy resolution of 600meV was employed for MIES/UPS. The spectra showed no basic changes at 250meV resolution. By applying suitable biasing electrons emitted from the Fermi level, E_F , are registered at 19.8eV (the potential energy of He*(2^3S)). Consequently, the onset of the spectra at low kinetic (high binding) energies occurs at the work function of the sample. The variation of the onset of the spectra at low kinetic energies with exposure gives then directly the exposure dependence of the surface work function. The sample can be cooled with LN_2 to 130K. The temperature was measured with a thermocouple in direct contact with

the front of the tungsten single crystal. The surface was exposed to water by backfilling the chamber. The water was cleaned by several freeze-pump-thaw cycles. The cleanliness of the water was checked with a quadrupole mass spectrometer. The amount of surface-adsorbed water is estimated on the basis of our previous results concerned with the water-titania interaction [25]: essentially, we make use of the fact that (a) water adsorption leads to an initial work function decrease up to half coverage of the surface, and (b) the MIES signal from water saturates for full coverage of the surface. From this we conclude that at 2L exposure the surface is covered by one bilayer (BL) of water. At 5L emission from the tungsten substrate has essentially disappeared in the UPS(HeI) spectra. The CsCl exposure is given in units of monolayer equivalents (MLE); at 1MLE the surface would be covered by one CsCl layer if it would not be for penetration effects.

Our previous results for salt adsorption on tungsten indicate that the observed work function minimum occurs at 0.5MLE [26, 27, 28, 29]. Annealing of the prepared films is done stepwise; during the collection of the MIES/UPS spectra the substrate temperature is kept constant.

2.1.3 Results

This section starts with the discussion of the spectral features expected from the ionization of CsCl and water, and a comparison with the information available in the literature on these and similar species. All results are presented as function of the binding energy, EB, of the emitted electrons. Electrons from the Fermi level would appear at zero energy in the MIES and UPS spectra. The change of the work function (WF) with exposure is determined from the cut-off of the MIES spectra at large binding energies. In the present paper we confine ourselves to a qualitative analysis of the MIES spectra: the comparison of the MIES and UPS spectra indicates that the spectral features seen in MIES are due to Auger Deexcitation of He*[18, 19]. In this case the position of the spectral

feature gives the binding energy of the electron emitted from the considered species, and the intensity of the feature is a direct image of the density of states related with the species. Quantitative methods are available to either synthesize MIES spectra [30, 31] (see Ref. [32] for an example) or to deconvolute them [18].

2.1.3.1 Signature of CsCl and water species on W(110)

The spectra for a CsCl-exposed tungsten surface will be presented below when discussing the adsorption of water on CsCl films. Peaks are seen from the Cs5p (11.5 and 13eV for $Cs5p_{3/2}$ and $Cs5p_{1/2}$, respect.) and Cl3p (5eV) ionization. Although the relative intensities of the Cs5p fine structure components are different in MIES and UPS, the overall similarity of the spectra suggests that the MIES spectra are due to the Auger Deexcitation process. Combined MIES/UPS results for other alkali halides on tungsten are available for NaCl [26], CsI [27], and LiF [28, 29], and the energetic positions of Cl3p and Cs5p reported here and in Refs. [26, 27] agree well. Water exposure at 130K produces the three features $1b_1$, $3a_1$, and $1b_2$ seen both with MIES and UPS (see spectra presented below). Combined MIES/UPS results were published for the water adsorption on MgO [5] and TiO_2 [25]; the spectra from water multilayers are rather similar in all cases studied so far with MIES/UPS. It should also be noticed that our UPS date for SW films are rather similar to those for liquid water [15]. First principles calculations carried out on ice [33] suggest that the $1b_2$ peak represents an intra-molecular bonding combination between O2p and H1s orbitals. The $1b_1$ peak can be assigned to lone-pair electrons on oxygen atoms; the hydrogen contribution is much smaller than in $1b_2$. The $3a_1$ feature (which appears considerably more diffuse in the spectra than $1b_1$ and $1b_2$) corresponds to delocalized states with inter-molecular contributions from different water molecules interacting via hydrogen bonds. Thus, the broad $3a_1$ feature is characteristic for condensed water, either in the liquid or solid phase, and signals the presence of a water network, formed by hydrogen bonds.

2.1.3.2 The water-CsCl interaction

In the following we present three sets of MIES/UPS results that give information on the CsCl-water interaction at 130K: (1) codeposition of water and CsCl on tungsten (fig.1), (2) CsCl deposition on solid water films (fig.3), and (3) water deposition on CsCl films (fig.4). Also shown are results obtained during the annealing of the films produced in (1) to (3) (fig.2).

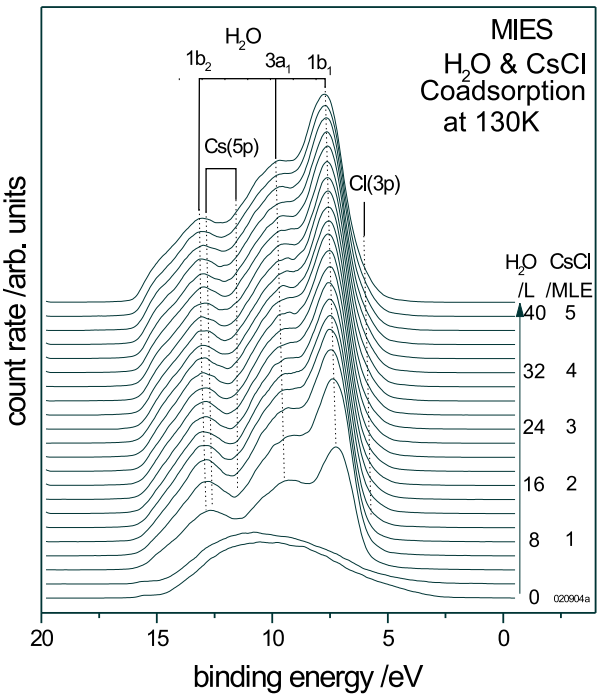

Fig. 1(a): MIES spectra obtained during the codeposition of CsCl and water onto W(110) held at 130K. Exposure is given in Langmuirs (L) (1 L=10^{-6}Torr/s)

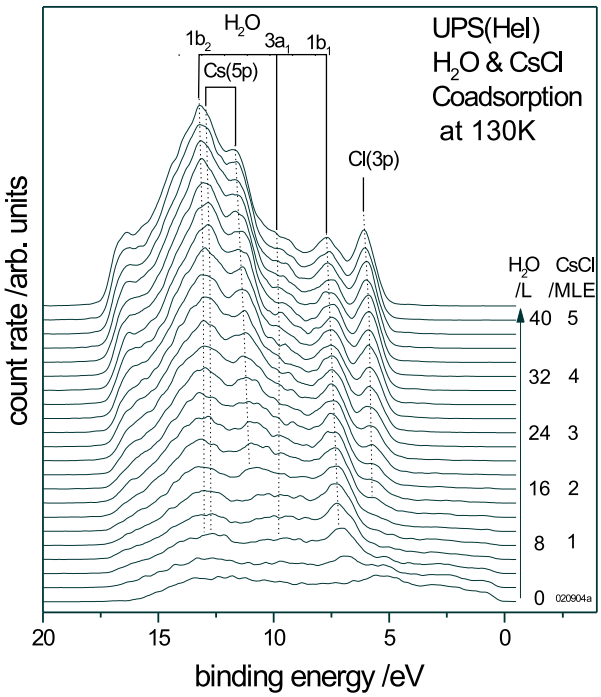

Fig. 1(b): UPS(HeI) spectra obtained during the codeposition of CsCl and water onto W(110) held at 130K

For a comparison with UPS data for aqueous liquid salt solutions we have studied the codeposition of water and CsCl (see Fig.1 for MIES (a) and UPS (b)). We have deliberately chosen a CsCl exposure rate at which little emission from Cs and Cl appears in the MIES spectra. Nevertheless, Cl3p and Cs5p emission is clearly seen in the UPS spectra. Since we still see weak Cl3p emission in MIES (as suggested by the onset of the $1b_1$ water peak which is

softer than for pure water), we conclude that the Cl3p species, covered by not more than one water layer, exist near the film surface. The estimated stoichiometry is $CsCl \cdot 6H_2O$. In order to arrive at this estimate, we have taken into account the diffierent surface density of the molecules in water and CsCl layers, and assumed a homogeneous depth distribution of the salt species. Alternatively, we can compare the peak areas in the UPS spectra; when assuming equal cross sections for photoionization of Cl3p and the three water states $1b_1$ to $1b_2$, we arrive at the same stoichiometry.

We can compare our UPS(HeI) results with those for a $CsF \cdot 2.6H_2O$ solution which is close to the salt saturation concentration [16]. As far as the Cs- and water-induced spectral features are concerned, the spectra compare well with ours. It should however be noted that a different interpretation is given in Ref. [16] to that part of the spectra where the $1b_2$ and $Cs5p_{1/2}$ features overlap. It was already questioned in ref. [15] that the small feature seen at 12.5eV kinetic energy is due to F2p ionization. Indeed, we find that for CsF adsorption on SW the spectral features F(2p) and $1b_1$ almost coincide, and that their intensity ratio is comparable to that of Cl(3p) and $1b_1$ in the present work [34].

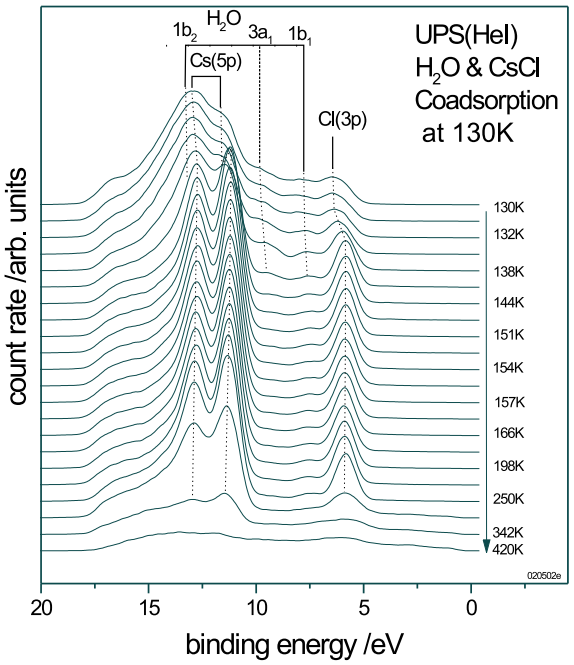

Fig. 2(a): Spectral changes observed with MIES when annealing the top spectrum of fig. 1(a)

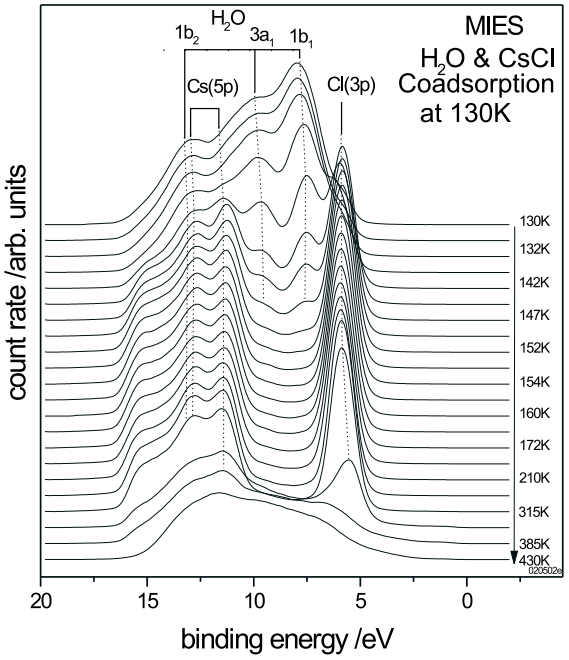

Fig. 2(b): Spectral changes observed with UPS(HeI) when annealing the top spectrum of fig. 1(b)

Concerning the Cl3p emission we can compare with the HeI spectra of a 3molar KCl aqueous solution [15] (stoichiometry about KCl·18H2O). The Cl-induced part is rather similar to CsCl, both as far as the energetic positions and the shape of the Cl^- and water-induced features are concerned. The Cl/water-intensity ratio is about three times smaller than in the present case. The similarity of the present UPS results suggests that, as in liquid aqueous salt solutions, ionic dissociation takes place for codeposition of CsCl and water at 130K, and Cs^+ and Cl^- are present as solvated species. Fig. 2 presents MIES and UPS results obtained when heating the film, characterized by the top spectra in fig.1, from 130 to 430K. Before heating, the signature of the Cs and Cl species can barely be seen in MIES. However, above 140K the signature of Cs and Cl can clearly be noticed also in MIES indicating that these species are now accessible to interaction with the He probe atoms. The $3a_1$ structure (which is diffuse for pure

water, see fig.3) becomes rather well defined. In fact, the water part in MIES reminds to gasphase-like water spectra [1, 3]. This indicates that direct interaction of water with Cs and/or Cl species dominates over water-water interactions and no hydrogen-bonded network exists anymore at these temperatures. The shift in the onset of Cl(3p) with increasing temperature seen in Fig.2(b) could re ect the fact that the binding energy of solvated Cl-species is larger by 0.6eV than that in isolated CsCl molecules. In Born's model this situation is modeled by embedding the Cl-species in a cage formed by the surrounding dielectric medium [15]. However, small changes in the onset of the spectra at large binding energies and of the Cl(3p) energetic position could also be caused by charge-up phenomena. They would shift the spectral features Cl(3p) and $1b_1$ to $1b_2$ from water simultaneously which is not the case, neither in fig.2 nor in fig.4. Thus, we tend to believe that the observed shift may indeed re ect the change in binding energy of the Cl3p electron upon solvation. According to MIES, most of the water has desorbed around 155K (the small feature seen in UPS near the position of $1b_1$ is due to incomplete separation of the MIES and UPS contribution to the spectra). Above 160K only Cs and Cl species can be detected by MIES and UPS and desorb around 350K. We do not detect any OH-fragments which could, as in the case of solid water on MgO, be produced at the water/tungsten interface [5].

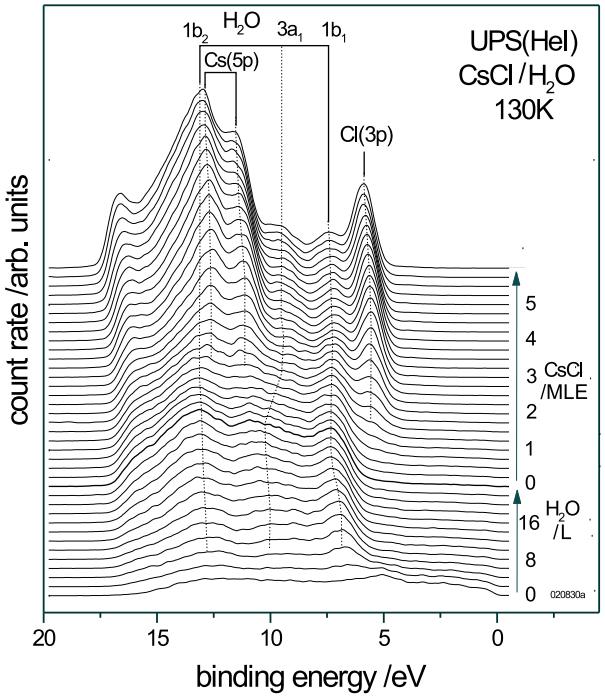

Fig. 3(a): MIES spectra during the growth of water films (approx. 12 bilayers thick) on W(110) at 130K, followed by the exposure to CsCl

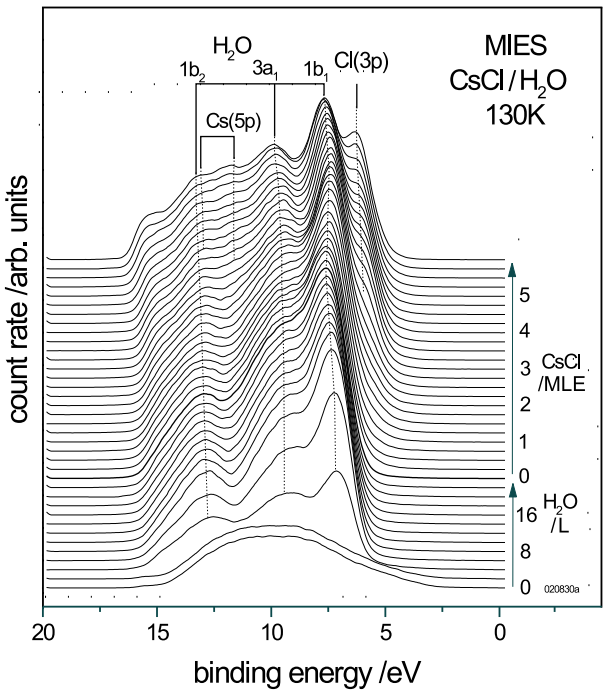

Fig. 3(b): UPS(HeI) spectra during the growth of water films (approx. 12 bilayers thick) on W(110) at 130K, followed by the exposure to CsCl

Fig.3 displays the results obtained during the deposition of CsCl onto SW (12 bilayers). Already during the early stage of exposure pronounced Cl3p emission develops in the UPS spectra at E_B=5.8eV (fig. 3(b)) while it remains rather weak in the MIES spectra up to 3MLE (7 percent of the total emission), and merely produces the small shoulder on the rise of the strong $1b_1$ peak from water (fig. 3(a)). Moreover, while the Cs5p emission is the dominant spectral contribution to UPS, it cannot be detected unambiguously with MIES at this stage. Up to 3MLE the SW spectral features change little in MIES as far as their energetic position and shape is concerned. This, together with the weak Cl3p emission and the absence of Cs5p emission in the MIES spectra at this stage, indicates that the toplayer must consist of water molecules mainly; they shield the Cl and Cs species efficiently from their interaction with the He* probe atoms. According to

MIES, water-water interaction dominates in the toplayer. This implies migration of the adsorbed species into the water film after deposition. At this stage both the MIES and UPS spectra resemble closely those obtained by codeposition of CsCl and water (fig.1). For codeposition we have evidence that ionic dissociation of CsCl may take place. Therefore, the stated similarity is indication that for small exposures solvation and dissociation of the adsorbed CsCl take place prior to the migration of Cs and Cl into the film. For exposures beyond 3MLE the $3a_1$ feature seen with MIES narrows considerably and becomes a well-defined peak, very similar to what is seen in fig. 2 when heating films produced by codeposition. Clearly, CsCl-induced destruction of the water network takes place at the surface. At 3MLE the nominal stoichiometry corresponds to that chosen in fig.1 for coadsorption, namely $CsCl{\cdot}6H_2O$; in the following it will be called the critical stoichiometry. Nevertheless, Cl(3p) is twicw as large as in fig.1(b). This indicates that under the conditions of fig.3 the depth distribution of the salt molecules is not homogenous. When heating the film represented by the top spectrum of fig.3 (over-critical stoichiometry) the MIES and UPS spectra become similar to those in fig. 2, in particular above 140K.

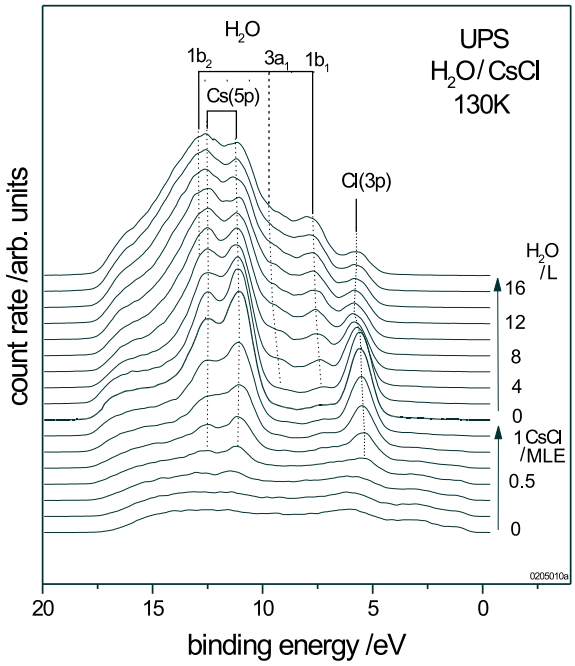

Fig. 4(a): MIES spectra obtained for the condensation of water onto a CsCl film deposited on W(110) at 130K

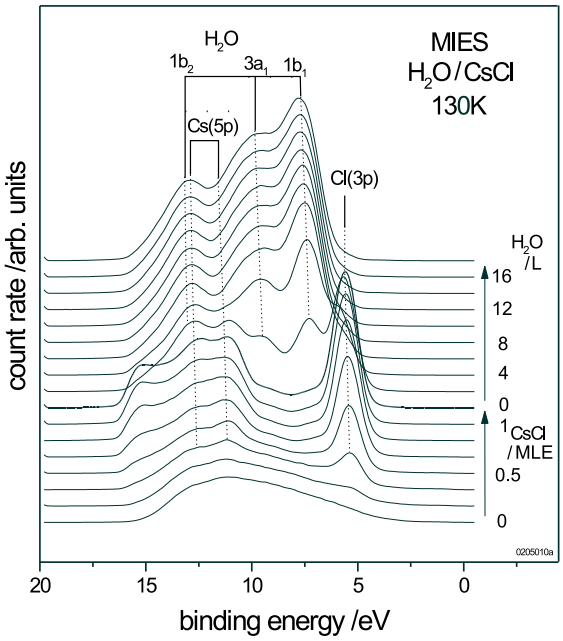

Fig. 4(b): UPS(HeI) spectra obtained for the condensation of water onto a CsCl film deposited on W(110) at 130K

Fig. 4 shows MIES (a) and UPS (b) results for the condensation of water on a CsCl film (1 monolayer) on tungsten held at 130K. Below about 4L the water-induced features $1b_1$, $3a_1$, and $1b_2$ remain well-defined peaks in MIES; for larger exposures, however, the spectrum typical for condensed water develops, displaying, in particular, the rather diffuse $3a_1$ feature. Beyond about 6L both Cl3p and Cs5p have disappeared in MIES almost completely. In contrast, their signature is still clearly seen in UPS, and the respective UPS intensities show only a weak exposure dependence at least up to 18L, i.e. up to exposures where 9 water BL would have built up on tungsten. We notice the water-induced shift of Cl(3p) of 0.6eV at 3L already seen in fig.2(b).

Taking into account the combined LEED and UPS results [36], and the ion-scattering data for water condensation on NaCl [12], we are led to the following interpretation: initially, 2D water condensation takes place whereby the interaction is predomi- nantly with Cs and Cl species. At this stage the existence

of gas phase like water features, in particular the well-defined $3a_1$ peak, excludes water clusters. In the case of NaCl the LEED re exes from, in particular, the water superstructure disappear at this stage, indicating that a transition from 2D to 3D condensation takes place around 3L. For CsCl the $3a_1$ feature becomes diffuse in MIES around 6L, indicating that now water-water interaction begins to dominate in the toplayer, and a transition from 2D to 3D condensation has taken place. Since the Cs and Cl-induced emission has almost completely disappeared in MIES at 6L, but persists in UPS up to at least 18L, we conclude that CsCl becomes solvated into the deposited water film. This view is supported by the observed water-induced shift of the Cl(3p)-peak. For a NaCl surface at 273K, covered by more than about 2 BL of water, it was demonstrated by IR spectroscopy that ions from the substrate are indeed incorporated into the film [37].

2.1.4 Solvation and Dissociation of CsCl on Solid Water

We concentrate now on the fate of CsCl adsorbed on SW at 130K. MIES reveals that the CsCl species tend to become covered by molecules of the water film. From our results alone cannot exclude that molecular hydration, followed by the migration of the hydrated molecular CsCl into the film takes place. However, when combining our data with previous work, mainly on NaCl, it appears more likely that at 130K, as for NaCl [11, 12], ionic dissociation of CsCl takes place at under-critical stoichiometries; the Cl and Cs species form complexes with water molecules, penetrate the surface and become embedded into the film: The dissociation is suggested by the close similarity of the UPS results of fig.3 with those for codeposition (fig.1) and liquid salt solutions [15, 16]. This view is supported by the following facts: (1) at least for NaCl no hydrated molecular species exist [12, 35], (2) at 15K $Na^+ \cdot (H_2O)_n$-complexes are formed when NaCl and H_2O molecules are codeposited on solid Ar [10], and (3) low-energy

reactive ion scattering experiments show that NaCl dissociates almost completely on SW surfaces, even at 110K, forming solvated ions [12]. $Cs(H_2O)_n$ complex formation, as a precursor for solvation, even on the time scale of 10^{-13}s, was demonstrated very directly by scattering Cs+ ions from SW [11]. The surface penetration follows from the fact that, as verified by MIES, water forms the toplayer (except for over-critical stoichiometries). Inspection of theoretical results for the penetration of pollutants into SW films suggests that the ions may mostly be located within the first two water bilayers [38]. On the other hand, for NaCl on SW of 110K the diffusion of Na^+ into the water film is insignificant, although efficient dissociation of NaCl still takes place [12].

The solvation is suggested by the fact that our results for salt and water codeposition (fig.1) and for CsCl adsorption on solid water (fig.3) are rather similar. Also the water-induced shift of Cl(3p) seen in figs.2 and 4 supports this view. Solvation may be accompanied by the transport of water molecules from inside the film to the surface as suggested in Ref. [7], thus restoring the composition and topology of the surface, and, consequently, allowing additional water molecules to become accommodated at the surface. New data taken by us between 80 and 150K show that the probability for hydration and penetration of CsCl is greatly reduced below 115K.

A molecular dynamics simulation is available for a concentrated aqueous CsF solution [17]. The surface of the system was found to consist of nearly pure water; this region extended about 0.2nm below the surface. It was concluded that the F^- and Cs^+ ions are solvated, and keep their solvation shell intact at the surface. A tendency was found that the Cs ions are located somewhat closer to the surface than the F ions. In the present case a similar tendency cannot be substantiated. The annealing experiments (fig.2) suggest that water is present in two different environments, (i) hydrogen-bonded, without direct interaction with the salt components, and (ii) involved into the solvation of the ions. The results for water deposition on CsCl films (see fig.4) are consistent with the scenario

proposed above: CsCl dissociation takes place at the (H_2O-CsCl) interface. The resulting solvated Cs and Cl ions migrate into the water adlayer. MIES will not be able to detect these species because they retain their solvation shells. On the other hand, UPS will register those solvated ions that become located within the information depth of UPS underneath the top of the water layer. A scenario similar to that discussed above appears to describe the HCl interaction with SW: at 130K HCl is dissociated as suggested by the occurrence of broad IR bands characteristic for hydronium ion (H_3O^+) formation [7] as well as from the reactive ion scattering spectra which display hydronium ions [8]. Above about 125K rapid migration into the water film takes place which leads to the formation of a trihydrate phase $HCl{\cdot}3H_2O$ [7].

2.1.5 Summary

We have shown that MIES, in combination with UPS(HeI), can be employed success- fully to investigate processes between salt molecules, CsCl in the present case, and solid water. We have studied the adsorption of CsCl on water, and the codeposition of CsCl and water on tungsten, both at 130K. The UPS spectra are rather similar to the corresponding ones for liquid salt solutions. The following scenario describes our results consistently: the CsCl molecules dissociate into Cl^- and Cs^+ upon adsorption. With MIES we establish that up to a critical stoichiometry of CsCl·6H2O very little Cl and Cs is located at the surface, and, thus, the ions become solvated in the water film. The water top layer is formed by the Cl and Cs ions solvation shells which remain intact at the surface. Above the critical stoichiometry, besides water, Cl and Cs species are found in the toplayer, indicating that the migration of CsCl species is largely suppressed. In this range the water contribution to the spectra becomes more gas phase-like; the $3a_1$ structure, in particular, develops into a well-defined peak, indicating that above the critical stoichiometry ion-induced destruction of the

hydrogen-bonded water network takes place at the surface, andion-water, rather than water-water interactions dominate. When heating the film, MIES provides information on the solvation shells: it is found that they consist of water molecules which bond among each other via hydrogen bonds, on the one hand, and water molecules that interact directly with the ions, on the other hand. We have also studied the water adsorption on CsCl films at 130K. Initially, 2D condensation takes place whereby the water interaction is mainly with the ions of the CsCl film. According to UPS solvated Cs and Cl species are formed at larger water exposures and migrate into the water film.

2.1.6 References

[1] V. E. Henrich, P. A. Cox: The surface science of metal oxides (Cambridge University Press, Cambridge, 1994)

[2] G. E. Brown Jr. et al.: Chem. Rev. 1999, 99, 77

[3] P. A. Thiel, T. E. Madey: Sur. Sci. Rep. 1987, 7, 211

[4] M. A. Henderson: Surf. Sci. Rep. 2002, 285, 1-308

[5] J. Günster, S. Krischok, V. Kempter, J. Stultz, D. W. Goodman: Surf. Rev. Lett. 2002, 9, 1511

[6] J. D. Graham, J. T. Roberts: J. Phys. Chem. 1994, 98, 5974

[7] S. Haq, J. Harnett, A. Hodgson: Phys. Chem. B 2002, 106, 3950

[8] H. Kang, T.-H. Shin, S.-C. Park, I.K. Kim, S.-J. Han: J. Am. Chem. Soc. 2000, 122, 9842

[9] F. Bournel, C. Mangeney, M. Tronc, C. Lafion, P. Parent: Phys. Rev. B 2002, 65, 201404

[10] R. Souda: Phys. Rev. B 2002, 65, 245419

[11] T.-H. Shin, S.-J. Han, H. Kang: Nucl. Instr. Meth. B 1999, 157, 191

[12] S.-C. Park, T. Pradeep, H. Kang: J. Chem. Phys. 2000, 113, 9373

[13] G. Ertl, J. K. uppers: Low Energy Electrons and Surface Chemistry (VCH Publs., 1985)

[14] J. P. Devlin: Int. Rev. Phys. Chem. 1990, 9, 29

[15] M. Faubel, in: Photoionization and Photodetachment, Part I (C. Y. Ng, Ed., World Scientific, Sing.) 2000 634

[16] R. Böhm, H. Morgner, J. Overbrodhage, M. Wulf: Surf. Sci. 1994, 317, 407

[17] J. Dietter, H. Morgner: Chem. Phys. 1997, 220, 261

[18] H. Morgner: Adv. Atom. Mol. Opt. Phys. 2000, 42, 387

[19] Y. Harada, S. Masuda, H. Osaki: Chem. Rev. 1997, 97, 1897

[20] A. Borodin, O. Höfft, S. Krischok, V. Kempter: Nucl. Instrum. Meth. Phys. Res. B 2002, xxx, in print

[21] W. Maus-Friedrichs, M. Wehrhahn, S. Dieckhoff, V. Kempter: Surf. Sci. 1991, 249, 149

[22] D. Ochs et al.: Surf. Sci. 1996, 365, 557

[23] D. Ochs, M. Brause, B. Braun, W. Maus-Friedrichs, V. Kempter: Surf. Sci. 1998, 397, 101

[24] D.Ochs, B.Braun, W. Maus-Friedrichs, V. Kempter: Surf.Sci.1998,417,390

[25] S. Krischok, O. Höfft, J. Günster, J. Stultz, D. W. Goodman, V. Kempter: Surf. Sci. 2001, 495, 8

[26] S. Dieckhoff, H. Müller, H. Brenten, W. Maus-Friedrichs, V. Kempter: Surf. Sci. 1992, 279, 233

[27] A. Hitzke, S. Pülm, H. M. uller, R. Hausmann, J. Güunster, S. Dieckhoff, W. Maus-Friedrichs, V. Kempter: Surf. Sci. 1993, 291, 67

[28] S. Pülm, A. Hitzke, J. Günster, H. Müller, V. Kempter: Rad. Efi. Def. Solids 1994, 128, 151

[29] D. Ochs, M. Brause, P. Stracke, S. Krischok, F. Wiegershaus, W. Maus-Friedrichs, V. Kempter, V. E. Puchin, A.L.Shluger: Surf.Sci. 1997, 383 , 162

[30] P. Eeken, J. M. Fluit, A. Niehaus, I. Urazgil'din: Surf. Sci. 1992, 273, 160

[31] L. N. Kantorovich, A. L. Shluger, P. V. Sushko, J. G. unster, P. Stracke, D. W. Goodman, V. Kempter: Faraday Disc. 1999, 114, 173

[32] M. Brause, S. Skordas, V. Kempter: Surf. Sci. 2000, 445, 224

[33] S. Casassa, P. Ugliengo, C. Pisani: J. Chem. Phys. 1997, 106, 8030

[34] A. Borodin, O. Höfft, V. Kempter: J. Phys. Chem., in preparation

[35] D. J. Cziczo, J. P. D. Abbatt: J. Phys. Chem. A 2000, 104, 2038

[36] S. Fölsch, A. Stock, M. Henzler: Surf. Sci. 1992, 264, 65

[37] M. Foster, G. E. Ewing: Surf. Sci. 1999, 427-428, 102

[38] C. Girardet, C. Toubin: Surf. Sci. Rep. 2001, 44, 159

2.1.7 Zusammenfassung des Unterkapitels 2.1

Die Untersuchung der molekularen Oberflächen, z.B. die Oberfläche von Wasser, ist heute besonders relevant, weil es in unserer Atmosphäre eine Menge kleiner Wasserpartikel gibt, deren Oberfläche eine wichtige Rolle in verschiedenen Prozessen spielen kann. Ein weit bekanntes Problem ist z.B. die Entstehung des Ozon-Loches.

Im Rahmen der Untersuchungen der Solvatation von Alkali-Halogeniden in Wasser wurde CsCl untersucht. Die Filme wurden *in situ* bei 130K unter MIES/UPS-Kontrolle auf dem W(110)-Oberfläche präpariert und einschließlich bis auf 300-450K geheizt. Die Spezies wurden in verschiedener Reihenfolge auf das Substrat aufgebracht, auch wurden Messungen mit der Codeposition von Wasser und CsCl durchgeführt.

Durch die Kombination MIES-UPS und aufgrund der verschiedenen Informationstiefen (die Oberflächenempfindlichkeit für MIES und ca. 1nm bei UPS), ist in einem Experiment gleichzeitig der Zustand der Oberfläche und der integrierte Zustand der letzten 2 bis 3 Monolagen zu erkennen.

Die Ergebnisse von den Versuchen lassen die folgenden Schlüsse zu:

CsCl dissoziiert im Wasser zu Cs^+- und Cl^--Ionen, welche mit Wasser solvatisiert werden. Die Wasserhülle ist ziemlich dicht. Bei MIES wird nur ca. 15% der normalen Intensität des Chlors nachgewiesen.

Der mit Salz gesättigte Wasserfilm hat eine starke Vernetzung. Wenn die Konzentration von CsCl einen kritischen Wert erreicht ($CsCl:6\cdot H_2O$), bleiben die neu ankommenden Salzmoleküle auf der Oberfläche des Films. Es ist keine weitere Dissoziation und Solvatation zu sehen.

Sogar eine kleine Konzentration von CsCl im Wasser kann im wesentlichen die Struktur von der Wasserschicht ändern. Der $3a_1$-Peak von Wasser wird während des CsCl-Angebots schmaler. Der Peak hat einen Bezug zu den

Wasserstoffbrücken zwischen den Wassermolekülen: Er wird durch die Bindungen verbreitert. Beobachtet man den $3a_1$-Peak in dem System, so kann man schließen, dass das Wassernetzwerk durch CsCl zerstört wird.

Ergänzende Messungen werden für CsF und CsI mit derselben Methodik durchgeführt. Sie bestätigen die vorstellenden Schlüsse. Diese Messungen werden derzeit für die Veröffentlichung aufbereitet.

2.2 Interaction of NaCl with Solid Water

Interaction of NaCl with Solid Water, A. Borodin, O. Höfft, U. Kahnert, V. Kempter, A. Poddey, and P.E. Blöchl, Journal of Chemical Physics 121 (18): xxxx-xxxx (2004)

The interaction of NaCl with solid water, deposited on tungsten at 80K, was investigated with Metastable Impact Electron Spectroscopy (MIES) and UPS(HeI). We have studied the ionization of 3pCl and the $1b_1$, $3a_1$, and $1b_2$ bands of molecular water. The results are supplemented by first-principles DFT calculations of the electronic structure of solvated Cl-ions. We have prepared NaCl/water interfaces at 80K, NaCl layers on thin films of solid water and H_2O ad-layers on thin NaCl films; they were annealed between 80 and 300K. At 80K, closed layers of NaCl on H_2O, and vice versa, are obtained; no interpenetration of the two components H_2O and NaCl was observed. However, ionic dissociation of NaCl takes place when H_2O and NaCl are in direct contact. Above 115K solvation of the ionic species Cl-becomes significant. Our results are compatible with a transition of Cl-species from an interface site (Cl in direct contact with the NaCl lattice) to an energetically favored configuration, where Cl species are solvated. The DFT calculations show that Cl-species, surrounded by their solvation shell, are nevertheless by some extent accessed by MIES because the Cl3p-charge cloud extends through the solvation shell. Water desorption is noticeable around 145K, but is not complete before 170K, about 15K higher than for pure solid water. Above 150K the NaCl-induced modification of the water network gives rise to gas phase-like structures in the water spectra. In particular, the $3a_1$ emission turns into a well-defined peak. This suggests that under these conditions water molecules interact mainly with Cl-rather than among themselves. Above 170K only Cl is detected on the surface and desorbs around 450K.

2.2.1 Introduction

The understanding of the interaction of salt molecules with water and vice versa,of water molecules with NaCl surfaces, is of interest in various fields, ranging from biological systems to catalysis and environmental sciences. Hydrated NaCl particles extracted from the ocean may become part of the atmosphere or deposited on the ocean shore. In both situations they play an important role as providers for chloride species and/or catalysts for pollution reactions involving (N-O)-compounds [1, 2].

In the chemistry of aerosols and clouds the surface layers to be investigated are usually extremely thin. Low-energy reactive ion scattering (RIS) has proven to be a sensitive tool for monitoring surface species [3]. In RIS a low-energy Cs^+ ion beam (3 to 100eV) is surface-scattered, and the scattered ions are mass-analyzed. Association products of Cs^+ with neutral species adsorbed at the surface, here water, and, in addition, ions pre-existing at the surface are ejected. For NaCl exposed to solid water (SW) at 100K, RIS showed that NaCl dissociates almost completely, forming Na^+-water complexes [3]. It was concluded that these solvated species do not migrate across one water bilayer of the water film over several minutes.

In the past, electron spectroscopies have been demonstrated to be a powerful tool to study the physics and chemistry on surfaces [4, 5]. For insulating substrates the problem of surface charging could be circumvented by working with suficiently thin films deposited on conducting substrates. In the Metastable Impact Electron Spectroscopy (MIES) metastable He atoms with thermal energy interact exclusively with the topmost layer via Auger processes [6, 7]). Their probability depends essentially on the overlap between the 1sHe orbital and those of the outermost surface layer that contribute to the charge density in the toplayer. Thus, the ejected electrons bear information on the electronic structure

of the surface top layer. So far, the combination of MIES and UPS(HeI) was applied to the study of the interaction of SW with Na atoms and CH_3OH [8], of SW with CsCl [9, 10], and, supported by cluster DFT calculations, to the interaction of Na with CH_3OH [11, 12].

It is the aim of the present work to study details of the solvation process, in particular its temperature dependence, for NaCl interacting with SW by combining MIES and UPS. Films of SW, held at 80K, were exposed to NaCl, and the change of the electronic structure with the temperature of the NaCl-exposed film was monitored under the in situ control of MIES and UPS. Additional information on the solvation process was obtained from the interaction of water molecules with NaCl films produced at 80K. The interpretation of the MIES data obtained for Cl^- in aqueous environment required First Principles DFT calculations to disentangle the contributions resulting from the ionization of $1b_1$ water and the Cl3p orbitals, both contributing to the charge density in the surface toplayer.

All films are grown via in situ deposition onto a tungsten substrate. As was pointed out previously, this approach has several advantages: (1) it is a relatively simple matter to investigate both surface and bulk phenomena with the technique combination MIES and UPS [8], (2) surface charging is eliminated for suficiently thin films [8], and (3) condensation of water molecules below about 135K results in the formation of an amorphous form of SW [13, 14]. Its properties are believed to be similar to those of liquid water, in particular with regard to its molecular orientation; therefore, SW can be considered as a model for liquid water with a very low vapor pressure and, thus, accessible to analysis with surface analytical techniques. This makes a comparison with UPS results on liquid water surfaces and aqueous solutions meaningful [6, 15, 16, 17].

2.2.2 Experimental and Theoretical Methods

2.2.2.1 Experimental remarks

Experimental details can be found elsewhere [18, 19, 20, 21, 22]. Brie y, the apparatus is equipped with a cold-cathode gas discharge source for the production of metastable He*(^{3}S/^{1}S) (E*=19.8/20.6eV) atoms with thermal kinetic energy and HeI photons (E*=21.2eV) as a source for ultraviolet photoelectron spectroscopy (UPS). The intensity ratio ^{3}S/^{1}S is found to be 7:1. Since the metastables approach the surface with near-thermal kinetic energy (60 to 100meV), this technique is non- destructive and highly surface sensitive (see Refs. [6, 7] for more detailed introductions into MIES and its various applications in molecular and surface spectroscopy). The spectral contributions from metastables and photons are separated by means of a time-of-flight technique. MIES and UPS spectra were acquired with incident photon/metastable beams 45° with respect to the surface normal; electrons emitted in the direction normal to the surface are analyzed. Collection of a MIES/UPS spectrum requires approximately 100s. The measurements were performed using a hemispherical analyzer. In order to minimize charge-up phenomena, we worked with low beam currents densities, and thus an energy resolution of 600meV was em- ployed for MIES/UPS. The spectra showed no basic changes at 250meV resolution. A second photon source is at our disposal providing HeI and HeII (40.8eV) photons.

By applying suitable biasing electrons emitted from the Fermi level, E_F , are registered at 19.8eV (the potential energy of He*(2^3S)). Consequently, the onset of the spectra at low kinetic (high binding) energies occurs at the work function of the sample. The variation of the onset of the spectra at low kinetic energies with exposure gives then directly the exposure dependence of the surface work function.

The sample can be cooled with LN_2 to 80K. The temperature, measured with a thermocouple in direct contact with the front of the tungsten single crystal, is estimated to be accurate within +/-10K. The surface was exposed to water by backfilling the chamber. The water was cleaned by several freeze-pump-thaw cycles. The amount of surface-adsorbed water is estimated on the basis of our previous results for the water-titania interaction [22]: essentially, we make use of the fact that (a) water adsorption leads to an initial work function decrease up to half coverage of the surface, and (b) the MIES signal from water saturates for full coverage of the surface. From this we conclude that at 2L exposure the surface is covered by one bilayer (BL) of water. At 5L emission from the tungsten substrate has essentially disappeared in the UPS(HeI) spectra.

Exposure of NaCl molecules was made by thermal evaporation of polycrystalline material at approx. 700K (for details see [23]). Evaporation of monomers takes place as concluded from the fact that the UPS spectra for adsorption on tungsten in the submonolayer regime resemble closely those of gaseous NaCl molecules [23]. The NaCl exposure is given in units of monolayer equivalents (MLE); at 1MLE the saturation coverage of the surface would be reached if it would not be for penetration effects. Our previous results for salt adsorption on tungsten indicate that the observed work function minimum occurs at 0.5MLE [23, 24, 25, 26]. For the exposure of NaCl on solid water we assume that the sticking coefficient is the same as on tungsten. Annealing of the prepared films is done stepwise; during the collection of the MIES/UPS spectra the substrate temperature is kept constant.

2.2.2.2 Computational details

We performed density functional theory (DFT) calculations [27, 28] using PBE gradient corrections [29] on the electronic structure of a chlorine ion in liquid water. The calculations have been performed using the CP-PAW implementation of the projector augmented wave (PAW) method [30]. We used

one projector function and one pair of partial waves per angular momentum (*l*,, m) for the s- and p-orbitals of chlorine and oxygen, respectively, and two projector functions for the hydrogen s-orbital. The plane wave cutofi for the wave functions has been 30 Ry. We used a super-cell with lattice constant a=15A, containing 111 water molecules and one Cl-ion, corresponding to the density of liquid water. Our calculations therefore refer to the dilute limit of Cl-ions. The slow relaxation times of liquid water mandates large equilibration times before a realistic structure of liquid water is obtained. Therefore, the initial structure for the density functional calculations has been obtained from a classical molecular-dynamics simulation using the TIP3P model [31] for water and a force field consisting of a Van-der-Waals interaction with the water oxygen atoms and an electrostatic interaction with all other atoms in the system for Cl [32] (see Table 1 for the TIP3P parameters). The system has been equilibrated for 0.87ns between 200 and 300 K, following a heating-cooling cycle lasting about 0.27ns. From this structure we started a PAW calculation and quenched the structure within 1.15ps into a nearby local minimum state. In order to analyze the decay of the Cl-related state at the top of the water valence state we projected the three Cl(3p) states onto the individual water molecules. The projection is such that the one center expansion at each atom of a molecule is integrated out to a radius which is 1.1 times larger than the covalent radius [30].

q_O	-0.834	$c_6(O-O)$	1.9235	$c_{12}(O-O)$	143.0775
q_H	0.417	$c_6(Cl-O)$	1.2745	$c_{12}(Cl-O)$	101.6710
q_{Cl}	-1	$d(O-H)$	1.8088	$d(H-H)$	2.8614

Table 1: Parameters used for the force field calculations in Hartree atomic units ($e = \hbar = m_e = 4\pi\varepsilon_0 = 1$). The internal structure of the water molecules, defined by the intramolecular distances $d(O-H)$ and $d(H-H)$, are kept rigid. The Van–der–Waals interaction between Cl and O atoms are defined by $V_{VdW} = c_{12}r^{-12} - c_6 r^{-6}$. In addition the intermolecular electrostatic interaction between the atoms with charges q_H, q_O q_{Cl} have been considered.

2.2.3 Results and Discussion

This section starts with the discussion of the spectral features expected from the ionization of NaCl and water. In the present paper, we confine ourselves to a qualitative analysis of the MIES spectra: the comparison of the MIES and UPS spectra indicates that the spectral features seen in MIES are due to Auger Deexcitation (AD) of He*[6, 7]. Here, the potential energy of a surface electron is utilized to eject the 2sHe electron. In this case, the position of the spectral feature gives the experimental binding energy of the electron emitted. All results are presented as function of the binding energy, E_B, of the emitted electrons; electrons from the Fermi level would pear at zero energy in the MIES and UPS spectra. Quantitative methods are available to either synthesize MIES spectra [33, 34] (see Ref. [35] for an example) or for their deconvolution [6]. For a qualitative analysis of the present data we suppose that the intensity of the spectral features from the AD process reflects directly the density of states initially populated. Thus, we compare the MIES results directly with the DFT-DOS (section 3.2). In contrast, the UPS results depend upon both the DOS of the initial and final states involved in the photoionization process.

2.2.3.1 Signature of NaCl and water species in MIES and UPS

Water exposure produces the three features $1b_1$, $3a_1$, and $1b_2$ seen in MIES and UPS as well as in the DOS of the water film (for previous studies on SW with MIES/UPS see Refs. [8, 22]). It should be noted that the UPS data for SW films are rather similar to those for liquid water [15]. According to the first-principles calculations carried out on ice in Ref. [40], the $1b_2$ peak represents bonding orbitals between O and H atoms in the water molecule. The $3a_1$ peak is attributed to the in-plane O(2p) orbital. The $1b_1$ peak represents the O(2p) orbital perpendicular to the plane of the water molecule. The $3a_1$ feature (considerably more diffuse than $1b_1$ and $1b_2$) corresponds to delocalized states with inter-

molecular contributions from different water molecules interacting via hydrogen bonds. Apparently, the broad 3a1 feature is characteristic for condensed water, either in the liquid or solid phase, and signals the presence of a water network, formed by hydrogen bonds (see also section 3.2).

Combined MIES/UPS results for alkali halide films on tungsten are available for NaCl [23, 39], CsI [24], and LiF [25, 26]. The Na species cannot be detected directly with our techniques because Na is present as ionic species; 3sNa is empty, and, thus, not accessible to UPS and MIES. The available potential energy of the HeI photons and the metastable He atoms is not suficient to ionize the Na2p shell. The energetic position of the Cl(3p)-emission seen in the present work agrees well with literature. The overall similarity of the MIES and UPS(HeI) spectra suggests that the MIES spectra are due to the AD process. In general, the transition $Cl^-(3p^6)$- $Cl^0(3p^5)$ displays a "fine structure" that can give information on the chemical environment of the chloride species. The fine structure splitting of the transition $Cl^-(3p^6)$ - $Cl^0(3p^5; 2P_{3/2;1/2})$ in the free Cl^- -ion is 0.11eV [36], too small to be observed in the present work. The free NaCl molecule displays a $(^2\Sigma - {}^2\Pi)$-Stark splitting of 0.46eV in UPS [36], originating from the strong axial field in the NaCl molecule. The spectra of solid NaCl, films or single crystals, between 5 and 10eV originate from the ionization of the Cl3p states of the valence band, and show a "double-peak" structure that reflects the valence band density of the states [37, 38]. The peak separation is 0.9eV in the HeII spectra [37]. Our UPS(HeI) spectra also show this splitting. On the other hand, the MIES spectra from NaCl films do not display this splitting; instead, a single peak is found that is asymmetric towards larger binding energies ([23, 39] and present work).

Solvated Cl^- -species can be expected to experience an essentially isotropic environment. Therefore, the situation will resemble to that of a free ion, and a single peak can be expected from the $Cl^-(3p^6)$ - $Cl^0(3p^5)$ transition (apart from the small fine structure splitting which cannot be resolved). On the other hand,

the UPS spectra from solvated molecular NaCl species would show the ($^2\Sigma$ - $^2\Pi$)-Stark splitting of 0.46eV. Finally, for NaCl films on SW the UPS spectra should display the double-peak structure of the Cl3p valence band emission, provided that the film has solid state properties, expected for more than two NaCl layers [23]. In summary, the shape of the Cl3p emission, in particular in the UPS spectra, will provide information on the chemical identity of the adsorbed species and on its molecular or dissociative adsorption. Although we have applied UPS with HeII radiation to NaCl/H_2O, these results are not presented here: the low efficiency for Cl3p ionization by HeII makes a separation of the contributions $1b_1$ and Cl3p between 5 an<d 6eV difficult.

2.2.3.2 Electronic Structure of Solvated Cl-Species

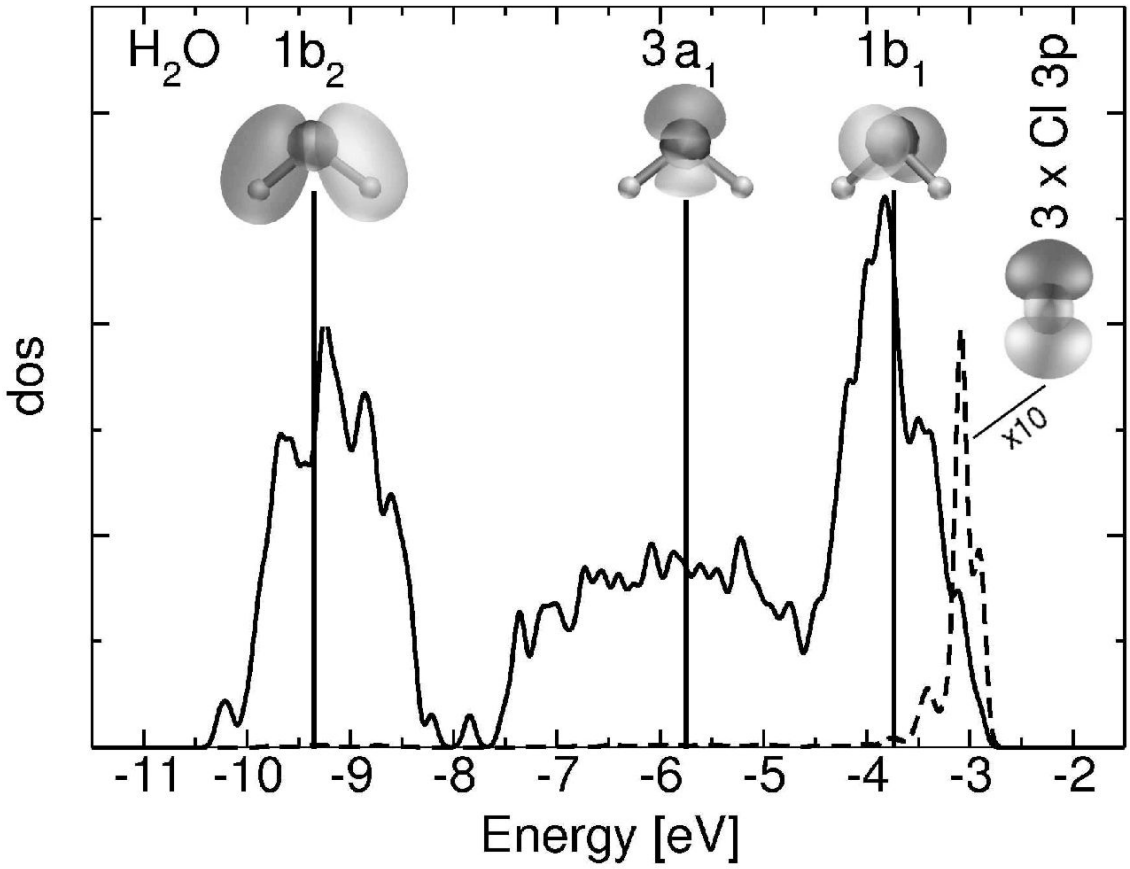

Fig. 1: Density of states of a Cl ion solvated in water. The density of states projected onto Cl(3p) shown as dashed line is magnified by a factor of 10. The vertical lines correspond to the states of an isolated water molecule, shifted globally, so that the center of the oxygen p-band align with that of the bulk water.

The DFT calculations reproduce the characteristic three-peak structure of the oxygen p-band (Fig.1). The three peak structure corresponds to the antisymmetric O-H bonds ($1b_2$), the symmetric O-H bonds ($3a_1$) with the p-orbital lying in both mirror planes of the water molecule, and the p-orbital oriented perpendicular to the bond plane ($1b_1$). The peak of the 2sO-band lies well separated below the p-band.

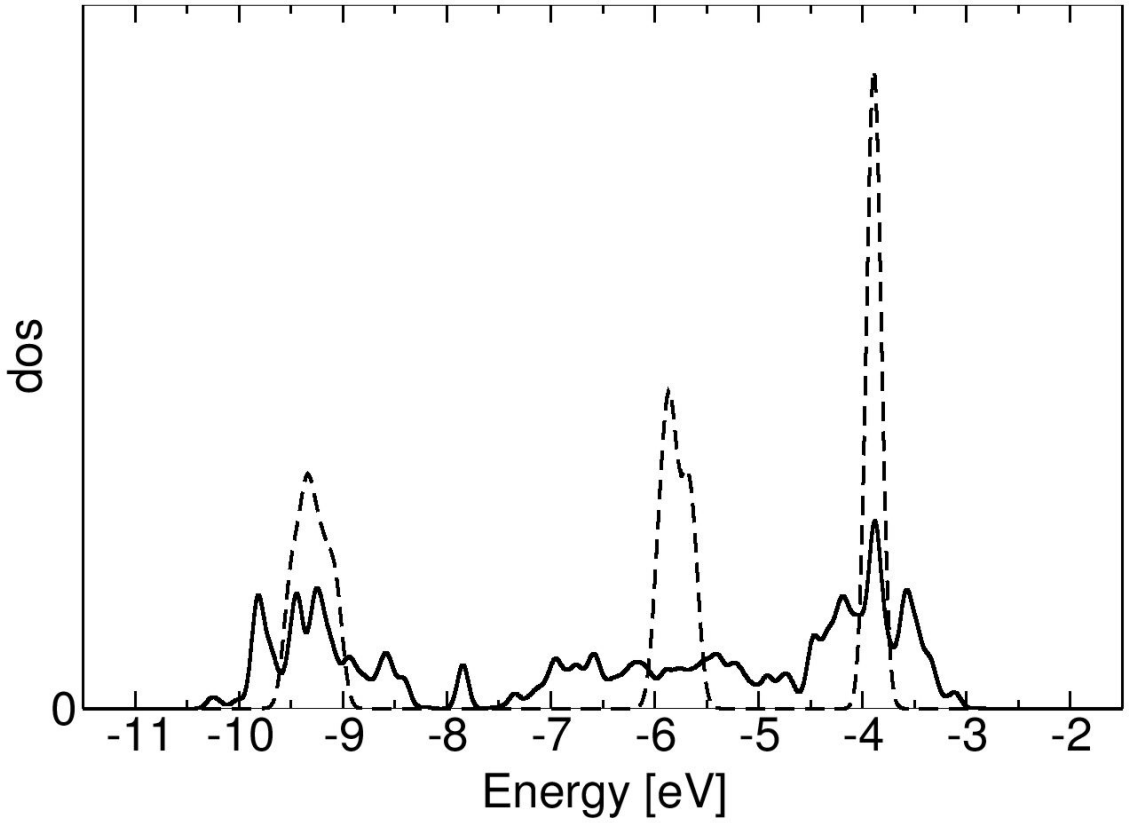

Fig. 2: Sum of the density of states of five randomly selected water molecules, once in bulk water (full line) and secondly as isolated molecules in the same intramolecular geometry as in the bulk cell (dashed line). See text for further details.

There has been a discussion about the origin of the wide broadening of the $3a_1$ band as compared to the $1b_1$ and $1b_2$ bands [40]. We investigated if this broadening can be related to structural changes or to the hydrogen bond network. For that purpose we randomly selected five water molecules, and compared their density of states, once in bulk water and secondly as isolated molecules in the same geometry as in the bulk cell (Fig.2). The broadening of $3a_1$ band in the solid is substantially larger than for the other two. We clearly see that this broadening is due to the coupling with the neigboring water molecules, and not to intramolecular structural distortions, because the width of the $3a_1$

states in isolation is comparable to that of the other two bands. We attribute the particularly large broadening of the $3a_1$ band to the nature of the contributing states, which can couple to the neighboring water molecules both via the hydrogen atoms and via the oxygen lone pair. The $1b_1$ and $1b_2$ states, on the other hand, can only couple either via the hydrogen atoms ($1b_2$) or via the oxygen p-orbitals ($1b_1$). Thus, the $3a_1$ state is in the best position to form delocalized wave functions that extend over many water molecules, which is the origin for the width of the $3a_1$ band.

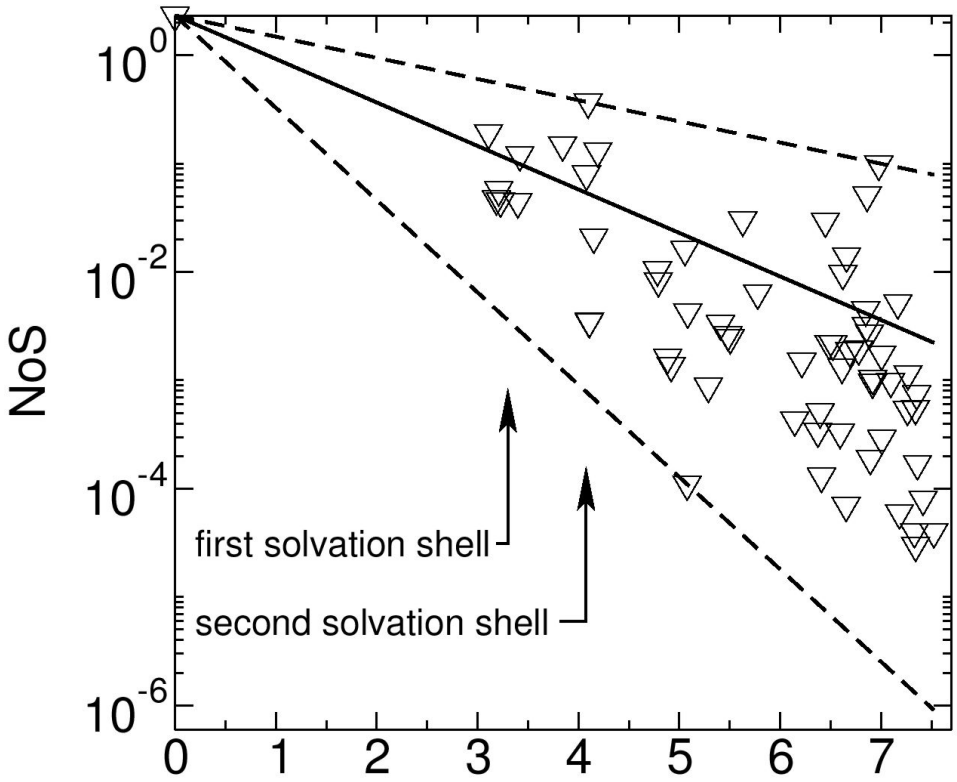

Fig. 3: Decay of the Cl(3p) states in water. Logarithmic plot of the water-projected number of states of those three states with predominant Cl(3p)-character. This weight decays with a factor of 0.4-0.25 for everyA distance from the Cl-atom. The Cl-O distances for the first solvation shell lie between 3.12 and 3.42A . The oxygen atoms of the water molecules in the second solvation shell are found between 3.84 and 4.15A . See text for further details.

The 3pCl-states form a rather narrow band located at the top of the valence band of the water molecules. Although these states are fairly localized on the Cl atoms, the tails of the wave function extend over several water molecules into the solvation shell. They couple nearly exclusively to the $1b_1$ orbitals of the neighboring water molecules. This is because the 3pCl-orbitals hybridize predominantly with those states of the solvent that are energetically close.

Our main interest was to quantify the decay of the Cl-state into the bulk of the water. This will provide a measure for the relative intensities of the MIES spectra from the Cl ions depending on its position at the surface or in the subsurface. He* metastables interact only with the tails of the wave function of the outermost surface atoms. The wave functions attributed to the chlorine atoms extend to the surface and contribute approximately proportional to their weight to the surface atoms. We evaluated the weight of the three wave functions with predominantly 3pCl-character, which are located within an energy window of width <0.2 eV at the top of the upper occupied band of water, on the water molecules, shown in Fig.3. We find a decay corresponding to a factor 0.4(-0.25) per Angstrom distance from the Cl atom. The decay has been obtained from a fit of $W_{Cl}e^{-\lambda r}$, where W_{Cl} is the weight of the states on the Cl atom (full line). The dashed lines correspond to the maximum and minimum values of λ obtained from individual data points. The position of the oxygen atom has been used to calculate the distance from the Cl atom. The wide spread stems from the inhomogeneous coupling of the 3pCl-orbitals along the hydrogen bond network.

Interestingly, the largest weight is not found on the first, but the second solvation shell. The electron on the Cl atom couples to the high-lying $1b_1$ orbitals. The lobes of the latter orbitals point perpendicular to the hydrogen bonds. This implies that the $1b_1$ orbitals on the molecules in the first solvation shell are oriented unfavorably for an efficient coupling to the Cl orbitals. As the water molecules in the second shell do not have this orientational relationship,

the Cl(3p) orbitals can extend more efficiently into $1b_1$ states of the water molecules in the second shell.

The first solvation shell consists of six water molecules. The H-bonds to the first solvation shell range from 2.17 to 2.63A. The next Cl-H distance lies well separated by 3.19A. Our finding difiers from previous calculations at finite temperatures that obtain a solvation shell of five molecules [41]. We attribute this difference to the fact that our structure is obtained from a quench into the groundstate. At this point we cannot exclude that, due to the rapid quenching, our calculation still reflects some structural features of the TIP3P model.

2.2.3.3 Interaction at NaCl-Water Interfaces

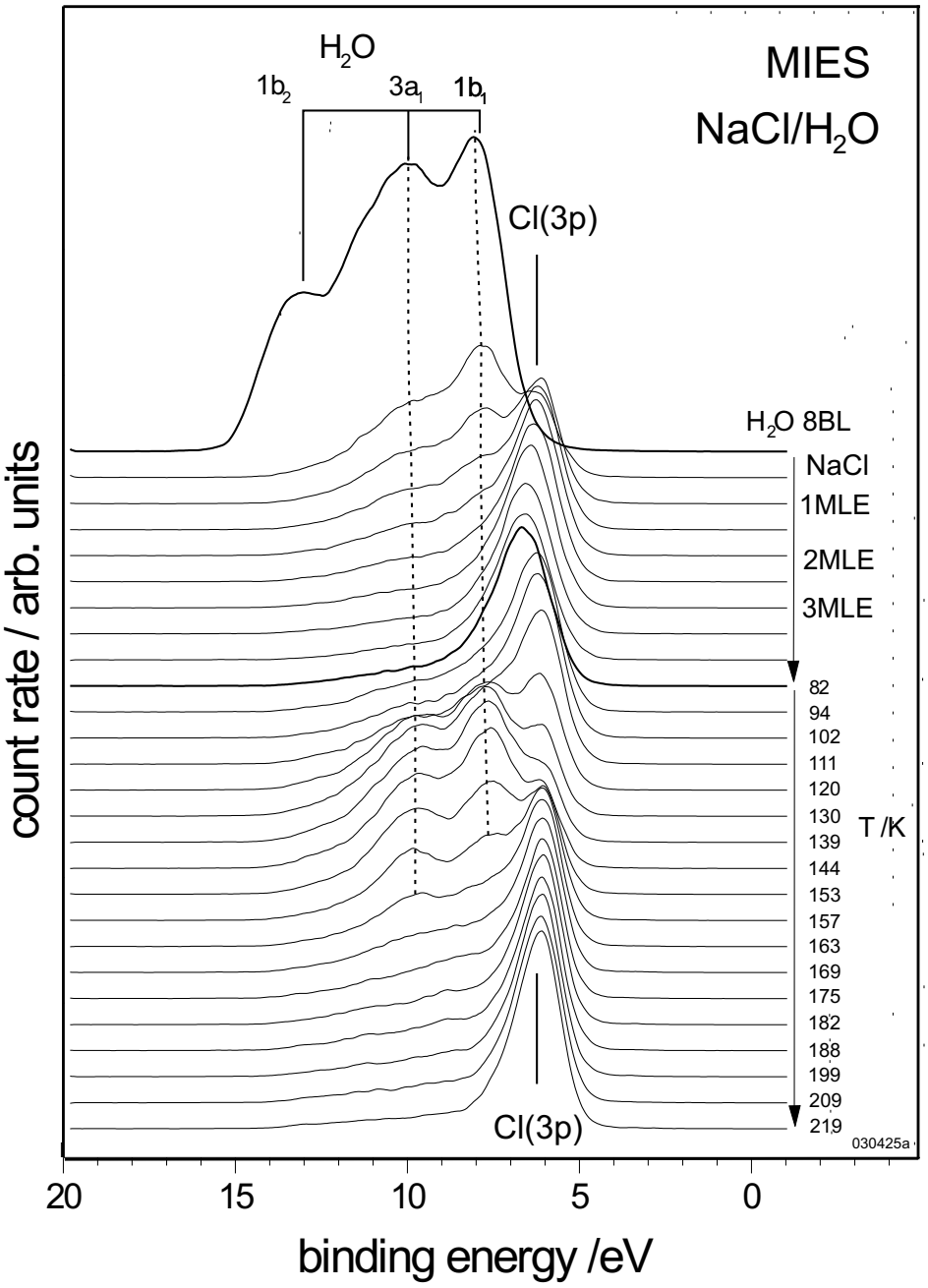

Fig. 4: MIES spectra for solid H_2O (3BL) on tungsten kept at 80K (top spectrum), and for NaCl exposure of the H_2O film. Lower part: spectra obtained during annealing of the NaCl-exposed film (80 to 210K).

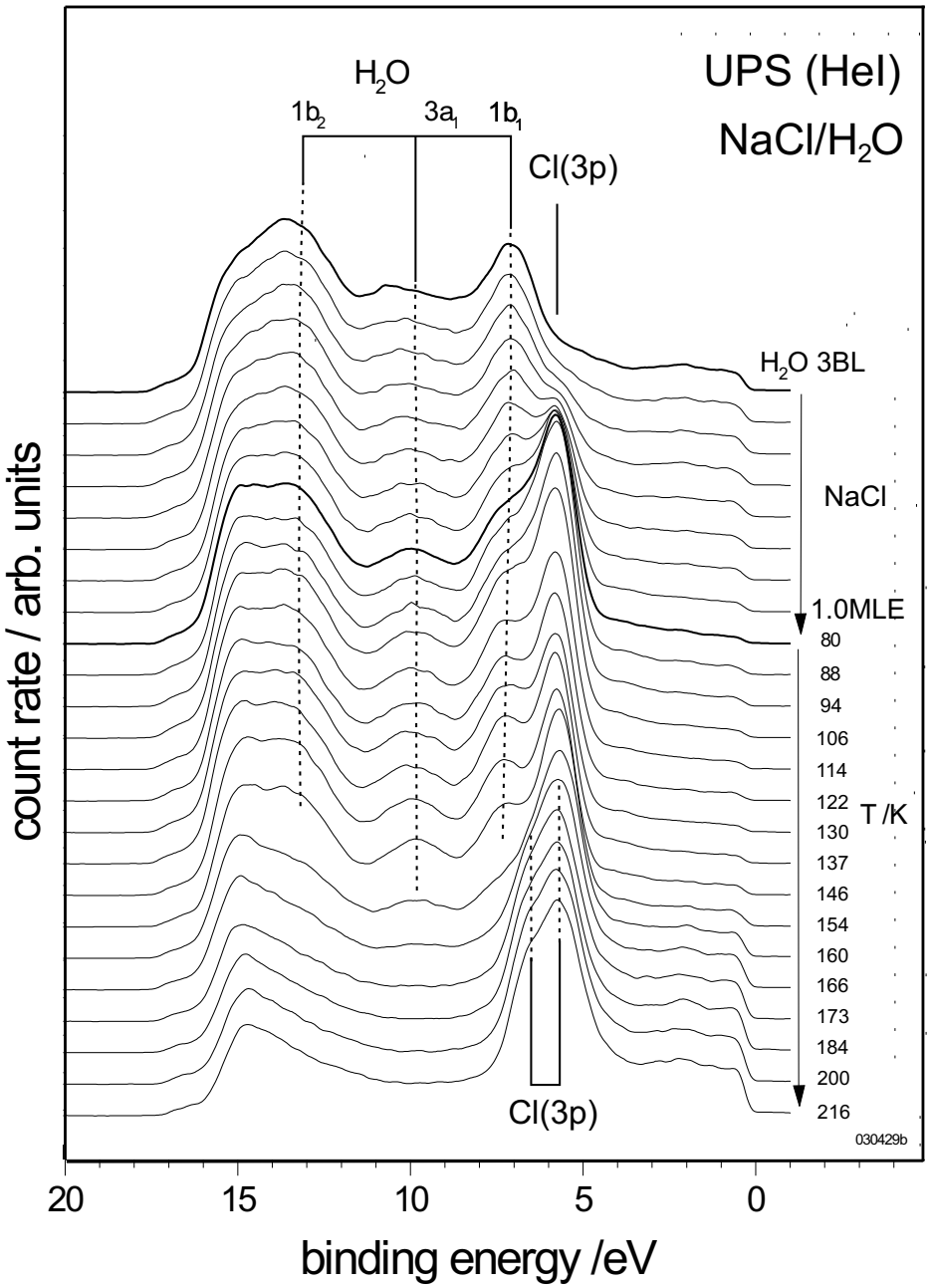

Fig. 5: As fig.4, but UPS(HeI) spectra

Figs. 4 and 5 summarize the MIES and UPS results obtained for a film of SW, held at 82K (abbreviated by NaCl/H_2O), during its exposure to NaCl, followed by film heating to 210K. The top spectrum of fig.4 is for SW(8BL)(BL: bilayer). The following 9 spectra display the changes occurring during the exposure of 4MLE NaCl. A shoulder develops at the right side of $1b_1$ and turns into the peak denoted by Cl(3p), identified as emission from the Cl(3p) orbital. Apparently, a

closed NaCl layer can be produced on SW at this temperature (10^{th} spectrum from top). This was not possible for CsCl at 130K where a mixed layer formed, consisting of H_2O, Cs and Cl species [9, 10]. When heating beyond 110K, the spectral features of water reappear gradually, and become the dominant structures in the spectra between 120 and 140K; clearly, water species penetrate deep enough into the NaCl toplayer to become accessible to MIES. Around 145K water desorption becomes significant as signaled by the renewed rise of Cl(3p), concurrent with the decrease of the water features; around 170K, according to MIES, all water has desorbed, and Cl(3p) is seen only. Auxiliary experiments carried out for SW on tungsten show that the water desorption in that case is completed about 20K earlier than for $NaCl/H_2O$.

Additional information on the first step of the NaCl interaction with SW comes from the HeI results of fig.5. The top spectrum is for water (3BL) on tungsten. Besides the emission from the water states $1b_1$, $3a_1$, and $1b_2$, contributions from the tungsten substrate can be noticed between the Fermi level (E_B=0eV) and E_B=5eV. The Cl(3p) feature is seen as a single, sharp peak at E_B=5.6eV; its shoulder towards larger binding energies is clearly due to $1b_1$ water emission. When most of the water has desorbed (T>166K), Cl(3p) develops the double-peak structure typical for the NaCl bulk, here for NaCl film formation on the W substrate. As outlined in 3.1, the sharp Cl(3p) peak found in aqueous environment can be considered as evidence for ionic dissociation during NaCl adsorption. Apparently, on SW the resulting species Cl^- and Na^+ adsorb independently without much mutual lateral interaction. This is in full accord with the findings of RIS where dissociative adsorption of NaCl on SW, followed by the formation of Na^+-water clusters, was found at 100K [3]. Support for cluster formation comes also from the study of the ions emitted during ESD from NaCl and water, coadsorbed on a condensed Ar substrate (35K) [42]. It was demonstrated that solvated Na^+ ions, $Na^+(H_2O)_n$ (n=1 to 4), desorbed more intensively than bare Na^+ ions.

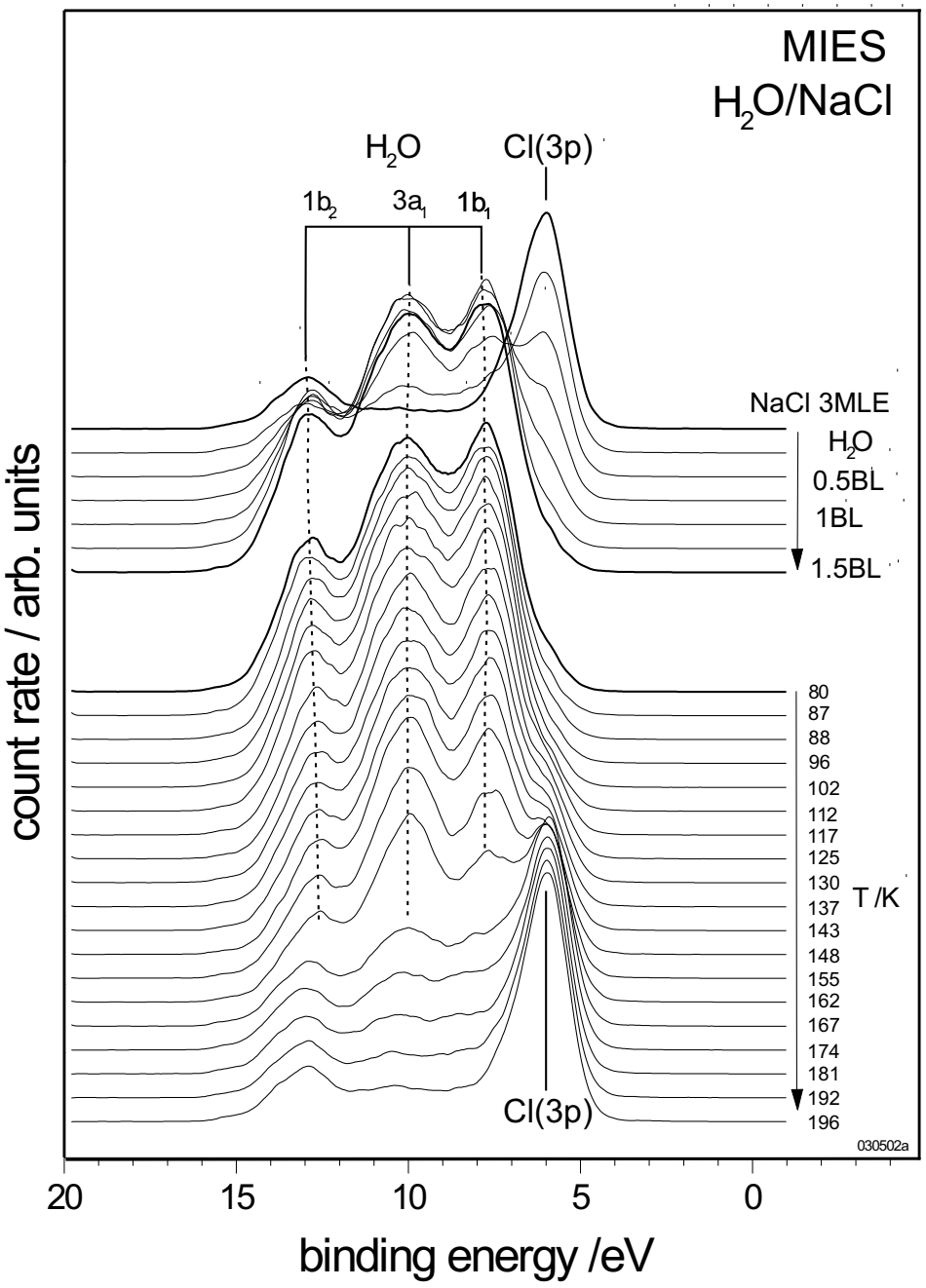

Fig. 6: MIES spectra for a NaCl film (3MLE) on tungsten kept at 80K (top spectrum), and during H_2O exposure (1BL) of the NaCl film. Lower part: spectra obtained during annealing of the H_2O-exposed NaCl film (80 to 210K).

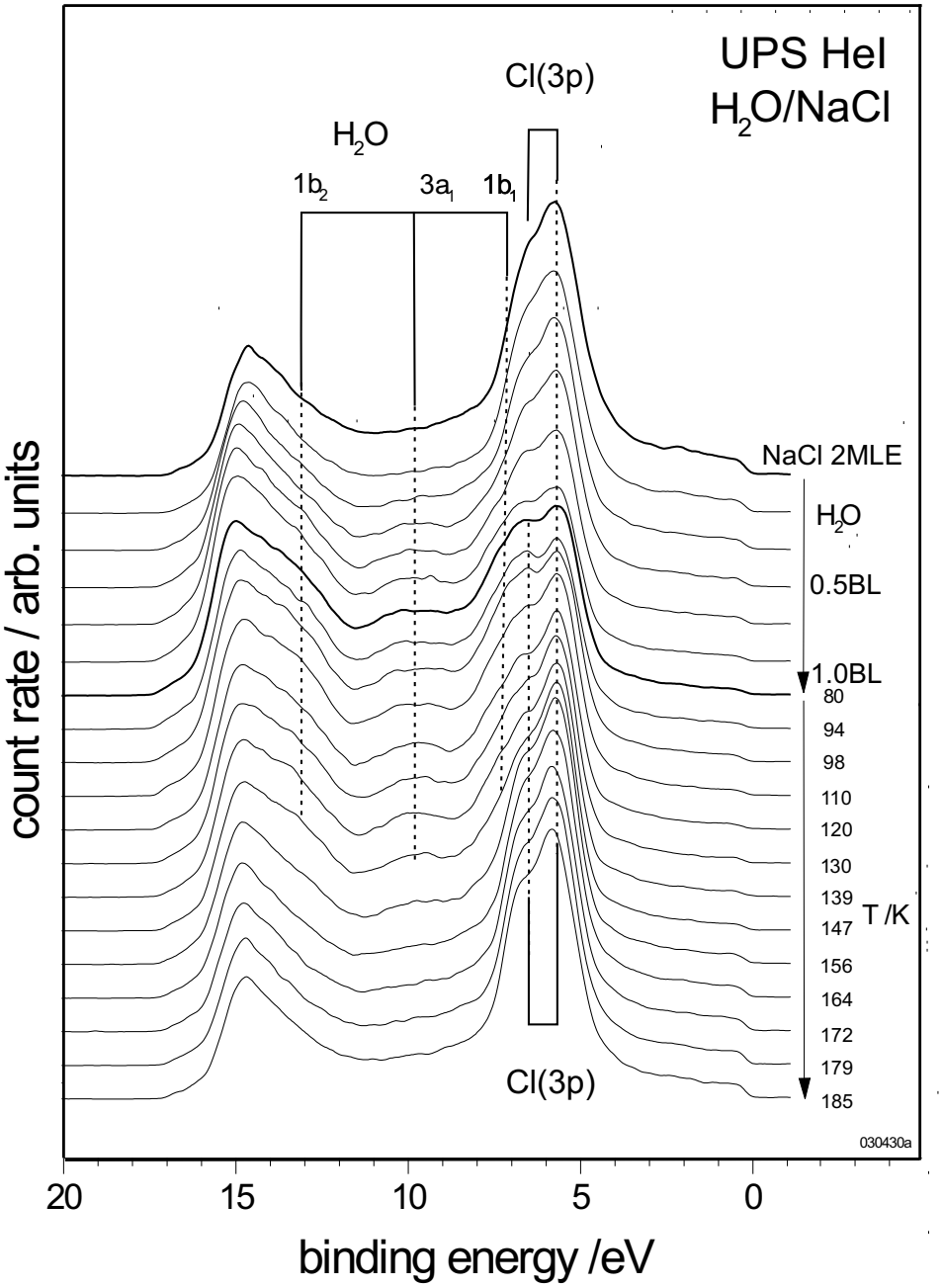

Fig. 7: As fig.6, but UPS(HeI) spectra

Figs.6 and 7 summarize the results collected for water films deposited on NaCl films at 80K (abbreviated by H_2O/NaCl). We find that the exposure required for a closed layer is comparable to that required on tungsten. Therefore, water penetration into the NaCl film does not take place at 80K. The MIES data obtained during the annealing to 300K reveal that above 105K both species H_2O and Cl are seen with MIES, even if at 80K, as in fig. 6, practically only H_2O

species were present in the outermost layer. The HeI results also demonstrate that Cl(3p) becomes more pronounced as a consequence of the annealing, and, thus, Cl-species must become located closer to the surface. While Cl(3p) is a sharp peak in aqueous environment, the double-peak structure of the NaCl bulk develops when the water desorbs.

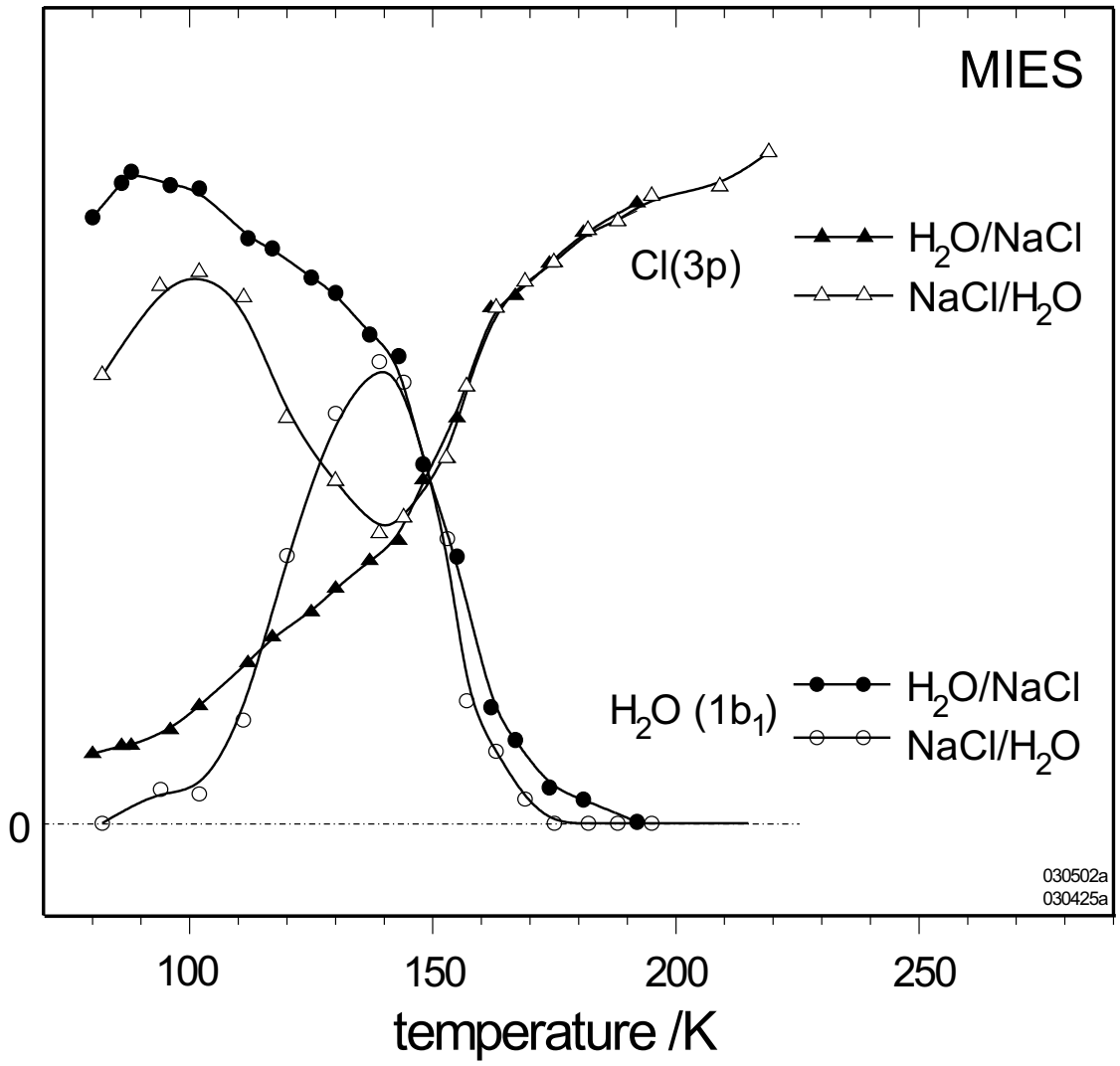

Fig. 8: Intensities of $1b_1$ of H_2O and Cl(3p) from Cl-as a function of the annealing temperature (80 to 210K) for (a) NaCl(1MLE)/H_2O(3BL) and (b) H_2O(1BL)/NaCl(3MLE). Data from the MIES spectra of figs.4 and 6.

Fig.8 displays the intensities of $H_2O(1b_1)$ and Cl(3p), extracted from the MIES data, versus the annealing temperature. In the case of $NaCl/H_2O$ the rise of $1b_1$ above 105K is correlated with a decrease of Cl(3p). Clearly, water species are now present in the top layer. On the other hand, for $H_2O/NaCl$ the rise of Cl(3p) is correlated with a decrease of $1b_1$ in the same temperature range. Above 145K the temperature dependence of the signals is the same for both $NaCl/H_2O$ and $H_2O/NaCl$. This suggests that the composition of the top layer is the same. The Cl(3p) intensity present at 140K, shortly before water desorption becomes significant, does not necessarily imply that the shielding of the Cl-species by water is incomplete. Instead, 3pCl-charge density may extend through the solvation shell, rendering the solvated Cl-species accessible to MIES. This viewpoint is supported by two observations:

(1) Mixed NaCl/water films produced by co-deposition of the two components at 80K on tungsten (not shown) also display a shoulder identified as $1b_1$ which in shape and intensity resembles that seen in figs.4 and 5 at annealing temperatures above 120K.

(2) As far as Fig.4 is concerned, the result most relevant from our first-principles calculations on Cl^- species in bulk water (section 3.2), is the penetration of the charge density with 3pCl character through the first solvation shell. The projected DOS reproduces qualitatively the MIES spectra in the region between 5 and 10eV binding energy both in relative position and shape of the spectral features. The calculations indicate, that the residual Cl(3p) intensity seen around 140 K (before water desorption becomes significant), does not necessarily imply incomplete Cl solvation. The intensity of the wave function beyond the solvation shell may even be higher than that on the solvation shell. The decay of the wave function is however strongly anisotropic, and the angular average is most relevant. From the calculations we obtain an average decay of the wave function from Cl to a water molecule of the first solvation shell by a factor of 0.036. The factor from Cl to a water of the second solvation shell is 0.045.

Thus, the first-principles results displayed in Fig.3 support that a substantial contribution of the Cl(3p) band is accessed by MIES, even if the Cl ion is fully solvated and located one or two layers beneath the surface of the $NaCl/H_2O$ film. Under these conditions, MIES would detect the charge density extending into the vacuum, consisting of the Cl3p charge density leaking via intermediate water molecules through the solvation shell. A drop of the intensity to about few percent up to few tens percent seems compatible with the calculated scenario. A scenario for the interaction at interfaces between NaCl and water will now be discussed on the basis of a qualitative free energy profile for the $Cl^-(Na^+)$/ice film interaction. So far, free energy profiles appear to be available only for Na^+ (Cl^-) adsorption at the water/NaCl crystal interface [43]. The profile of Fig.9 presents the change $\Delta F(z)$ of the free energy, F(z), felt by the $Cl^-(Na^+)$ion with respect to the vacuum. It possesses two minima, one for adsorption at a "surface" site, denoted by S_1, and another, denoted by S_2, for adsorption at a "solvent-separated" site; it was found that the ions are more stably adsorbed under "solvent-separated" conditions, -i.e. as fully solvated species [43]. As discussed for HCl/ice [44], the details of $\Delta F(z)$ will depend on temperature because of the decrease of the entropic contribution with rising temperature. No significant intermixing of the species takes place at the interface as long as the temperature stays below about 105K. However, already at 80K there is strong interaction between NaCl and water species at the interface: the NaCl species become dissociated ionically, as already concluded from RIS results obtained at 100K [3]. In our work the dissociation is suggested by the peculiar shape of the Cl(3p) emission in UPS under conditions where NaCl is in close contact with water. As demonstrated by RIS, (Na^+-water) complexes are formed at the interface.

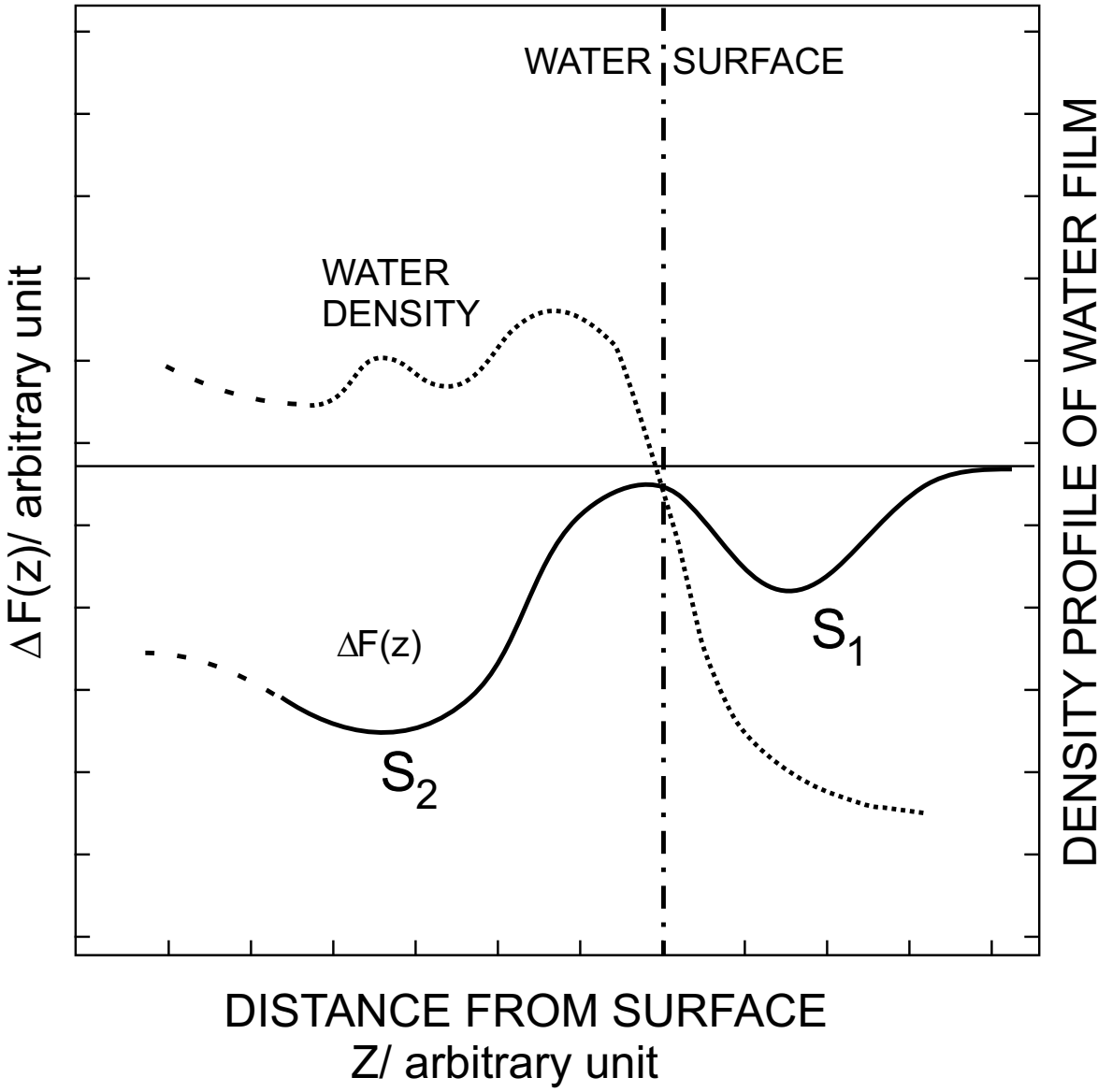

Fig. 9: Qualitative free energy profile, ΔF(z), versus the $Cl^-(Na^+)$ distance from the water surface. The dashed curve refers to the density profile of the water film.

With respect to fig.9 the adsorbed ions occupy site S1 up to about 110K. Above 115 K the mobility of the water molecules is suficiently enhanced for the transition S_1 - S_2 to take place, -i.e. the Cl^- ions become embedded into the water film, completing their solvation shell. The reason may be that around 110K, as a consequence of the increase in disorder of the water film, the barrier between S_1

and S_2 has become greatly reduced or has even disappeared, similar to what has been found for HCl/ice [44]. The transition S_1 - S_2 appears to be related to the amorphous/crystalline transition seen in pure water (135K) as consequence of the increased water mobility [13, 14].

For H_2O/NaCl we see a decrease of $1b_1$ above 105K, accompanied by a rise of Cl(3p). This indicates that Cl^--species become accessible to MIES. This does not necessarily imply that Cl becomes part of the top layer, but rather that the Cl species are located suficiently close to it so that, as suggested by our DFT results, MIES can detect the Cl3p charge density extending through the respective solvation shell. Following ref. [43], this can be interpreted as the transition of Cl^- from a site at the H_2O-NaCl interface ("direct" adsorption) to an energetically more favorable, "water-separated" site where the Cl^- species is fully solvated.

Water desorption becomes sizeable above 140K because feature Cl(3p) increases, and, at the same time, $1b_1$ decreases. On the other hand, desorption is not complete before about 170K. The MIES spectra of water in the range between 140 and 170K are gas phase like, featuring well-defined peaks. This applies in particular to the $3a_1$ emission which was unstructured and diffuse for condensed water [9, 10, 40]. This indicates that, at this stage, the water emission originates from water species that are no longer involved in a H-bonded water network, but are stabilized by their electrostatic interaction with the salt ions. Consequently, the $3a_1$ hybridization becomes less important, and the $3a_1$ structure becomes sharper.

2.2.4 Summary

We have shown that MIES, in combination with UPS(HeI), can be employed successfully to investigate processes between salt molecules (NaCl) and solid water. We have prepared NaCl/water interfaces at 80K, namely NaCl layers on thin films of solid water and water adlayers on thin NaCl films; they were annealed between 80 and 300K. All experiments were carried out under in situ control of MIES and UPS. The spectroscopy results are backed-up by First-Principles DFT calculations concentrating on the electronic structure of solvated Cl^- ions; the DFT-DOS is compared with the MIES spectra caused by the Auger deexcitation process. The following scenario describes our results consistently: at 80K there is no interpene- tration of the two components water and NaCl; however, ionic dissociation of NaCl takes place when water and NaCl are in direct contact. Above 110K the solvation of the ionic species Cl^- and Na^+ becomes significant. The DFT calculations suggest that Cl^- species which are surrounded by their solvation shell are to some extent accessed by MIES because the 3pCl-charge cloud extends through the solvation shell. The desorption of water from the mixed film takes place between 145 and 170K; those water species bound ionically to Na^+ and Cl^- are removed last.

2.2.5 References

[1] A.R. Ravishankara, Science 276, 1058, (1997) [2] E.E. Gard et al., Science 279, 1184, (1998)

[3] S.-C. Park, T. Pradeep, H. Kang, J. Chem. Phys. 113, 9373, (2000)

[4] V. E. Henrich, P. A. Cox, The surface science of metal oxides (Cambridge University Press, Cambridge, 1994)

[5] G. Ertl, J. K. uppers, Low Energy Electrons and Surface Chemistry (VCH Publs., 1985)

[6] H. Morgner, Adv. Atom. Mol. Opt. Phys. 42, 387, (2000)

[7] Y. Harada, S. Masuda, H. Osaki, Chem. Rev. 97, 1897, (1997)

[8] J. G. unster, S. Krischok, V. Kempter, J. Stultz, D. W. Goodman, Surf. Rev. Lett. 9, 1511, (2002)

[9] A. Borodin, O. Höfft, S. Krischok, V. Kempter, Nucl. Instr. Meth. B 203, 205, (2003)

[10] A. Borodin, O. Höfft, S. Krischok, V. Kempter, J. Phys. Chem. B 107, 9357, (2003)

[11] A. Borodin, O. Höfft, U. Kahnert, V. Kempter, Y. Ferro, A. Allouche, J. Chem. Phys. 120, 8692, (2004)

[12] Y. Ferro, A. Allouche, V. Kempter, J. Chem. Phys. 120, 8683, (2004)

[13] J. D. Graham, J. T. Roberts, J. Phys. Chem. 98, 5974, (1994)

[14] J. P. Devlin, Int. Rev. Phys. Chem. 9, 29, (1990)

[15] M. Faubel, in Photoionization and Photodetachment, Part I (C. Y. Ng, Ed., World Scientific, Sing., 2000), p. 634

[16] R. Böhm, H. Morgner, J. Overbrodhage, M. Wulf, Surf. Sci. 317, 407, (1994)

[17] J. Dietter, H. Morgner, Chem. Phys. 220, 261, (1997) [18] W. Maus-Friedrichs, M. Wehrhahn, S. Dieckho_, V. Kempter, Surf. Sci. 249, 149, (1991)

[19] D. Ochs, et al., Surf. Sci. 365, 557, (1996)

[20] D. Ochs, M. Brause, B. Braun, W. Maus-Friedrichs, V. Kempter, Surf. Sci. 397, 101, (1998)

[21] D. Ochs, B. Braun, W. Maus-Friedrichs, V. Kempter, Surf. Sci. 417, 390, (1998)

[22] S. Krischok, O. Höfft, J. Günster, J. Stultz, D. W. Goodman, V. Kempter, Surf. Sci. 495, 8, (2001)

[23] S. Dieckhoff, H. Müller, H. Brenten, W. Maus-Friedrichs, V. Kempter, Surf. Sci. 279, 233, (1992)

[24] A. Hitzke, S. P. ulm, H. M. uller, R. Hausmann, J. G. unster, S. Dieckho_, W. Maus-Friedrichs, V. Kempter, Surf. Sci. 291, 67, (1993)

[25] S. Pülm, A. Hitzke, J. G. unster, H. Müller, V. Kempter, Rad. E_. Def. Solids 128, 151, (1994)

[26] D. Ochs, M. Brause, P. Stracke, S. Krischok, F. Wiegershaus, W. Maus-Friedrichs, V. Kempter, V. E. Puchin, A. L. Shluger, Surf. Sci. 383, 162, (1997)

[27] P. Hohenberg, W. Kohn, Phys. Rev. 136, B864, (1964)

[28] W. Kohn, L. J. Sham, Phys. Rev. 140, A1133, (1965)

[29] J. P. Perdew, K. Burke, and M. Ernzerhof, Phys. Rev. Lett. 77, 3865, (1996)

[30] P. E. Blöchl, Phys. Rev. B 50, 17953, (1994)

[31] W. L. Jorgensen, J. Chandrasekhar, J. D. Madura, R. W. Impey, and M. L. Klein J. Chem. Phys. 79, 926, (1983)

[32] M. Patra, M. Karttunen, arXiv:physics/0211059 v2 2003

[33] P. Eeken, J. M. Fluit, A. Niehaus, I. Urazgil'din, Surf. Sci. 273, 160, (1992)

[34] L. N. Kantorovich, A. L. Shluger, P. V. Sushko, J. G. unster, P. Stracke, D. W. Goodman, V. Kempter, Faraday Disc. 114, 173, (1999)

[35] M. Brause, S. Skordas, V. Kempter, Surf. Sci. 445, 224, (2000)

[36] W.C. Price, in Electron Spectroscopy: Theory, Techniques and Applications, Vol. 1 (Academic Press, C.R. Brundle and A.D. Baker, Eds., 1977)

[37] T. Poole, J.G. Jenkins, J. Liesegang, C.G. Leckey, Phys. Rev. B 11, 5179, (1975)

[38] N.O. Lipari, A.B. Kunz, Phys. Rev. B 3, 491, (1971)

[39] T. Munakata, T. Hirooka, K. Kuchitsu, J. Electr. Spectr. Rel. Phenom. 18, 51, (1980)

[40] S. Casassa, P. Ugliengo, C. Pisani, J. Chem. Phys. 106, 8030, (1997)

[41] J.M. Heuft, E.J. Meijer, J. Chem. Phys., 119, 11788, (2003)

[42] R. Souda, Phys. Rev. B 65, 245419, (2002)

[43] H. Shinto, T. Sakakibara, K. Higashitani, J. Chem. Engin. Jap. 31, 771, (1998)

[44] C. Toubin, S. Picaud, P.N.M. Hoang, C. Girardet, R.M. Lynden-Bell, J.T. Hynes, J. Chem. Phys. 118, 9814, (2003).

2.2.6 Zusammenfassung des Unterkapitels 2.2

Bei den MIES- und UPS(HeI)-Untersuchungen der Wechselwirkung von NaCl mit festem Wasser wurden Filme, die bei 80K in verschiedenem Reihenfolge (Wasser/NaCl und NaCl/Wasser) auf das W(110)-Substrat aufgebracht wurden, charakterisiert. Strukturen, die sich in dem System gut beobachten lassen, sind $1b_1$, $3a_1$, $1b_2$ von Wasser und 3p von Chlor.

Beim Auftragen der Schichten bei 80K, gleich in welcher Reihenfolge, wird nur ein normales Lagewachstum festgestellt. Es wurden keine Effekte wie Eindringen, Dissoziation oder Solvatation gesehen. Die Spektren zeigen, dass eine Schicht oberhalb der anderen wächst. Bei Wasser ist die $3a_1$-Peakverbreiterung gut zu sehen; dies weist auf die vorhandenen Wasserstoffbrücken zwischen Moleküle von Wasser hin. Bei Cl in den UPS(HeI)-Spektren ist deutlich ein Aufspalten des 3p-Peak zu erkennen, dies bedeutet, dass sich NaCl in einer undissoziierten Form am Substrat befindet.

Nach der Präparation wurde der Film geheizt. Im Bereich von 80 bis 115K bleibt der Film unverändert. Erst bei 115K nimmt die Mobilität der Wassermoleküle so sehr zu, dass einige Änderungen in den Spektren zu sehen sind:

Wurde der Film mit dem sich oberhalb des Wassers befindenden NaCl geheizt, so treten in beobachtetes Spektrum des Salzes die Peaks von Wasser auf. Bei 145K ist in MIES neben dem um ca. einen Faktor 2 abgeschwächten Peak von Cl, auch ein Peak von ca. einer Wasser-Monolage zu sehen. Zwar sind in UPS(HeI), wegen des Überlappens des Wasser-$1b_1$-Peaks mit dem Cl3p-Peak, die zwei aufgespalteten Komponenten des 3p-Peaks schwierig zu erkennen, jedoch lässt sich sagen, dass der 3pCl-Peak im Bereich 115-140K im Vergleich zu den anderen Temperaturen schmäler wird.

Obwohl beim Auftragen von H_2O/NaCl die Filme in anderer Reihenfolge vorbereitet wurden und vor dem Ausheizen eine Multilageschicht Wasser oben drauf bleibt, sieht bei 145K der Film fast wie im oben beschriebenen Fall aus. Bei dieser Temperatur wird die Wassermultilage bereits desorbiert und Chlor wird durch das restliche Wasser nur teilweise bedeckt. Es ist noch zu bemerken, dass das Auftauchen vom Chlorpeak bereits bei 115K anfängt, wo noch keine Desorption stattfindet.

Also, lässt sich aus dem 1. Fall schließen, dass die Wassermoleküle durch die NaCl-Schicht hindurchgehen, und aus dem 2. Fall, dass Chlor in die Wasserschicht eindringt. Dabei liegt Chlor, wie der schmale (typisch für dissoziierten Zustand) Cl3p-Peak zeigt, als Cl^--Ion. So folgt aus den Spektren, dass sich an der Schichtoberfläche NaCl in dissoziierter Form und Wasser befinden. Die Ergebnisse von theoretischen DFT-Rechnungen für ein Cl^--Ion in einem Wasserfilm zeigen, dass bei diesen Bedingungen das Cl-Ion solvatisiert wird. In einem MIES-Spektrum sollte ein so in die Wasserhülle eingepacktes Cl-Ion erkennbar sein. Das Verhältnis vom $1b_1$-Wasserpeak zum 3p-Peak von Chlor beträgt ca. 2:1. Da das Experiment gerade dasselbe zeigt, lässt es die folgenden Schlüsse zu: Bei Temperaturen zwischen 115-145K läuft die Wechselwirkung von NaCl mit Wasser darauf hinaus, dass NaCl dissoziiert und solvatisiert wird.

Während weiteren Heizens der Schicht wird bis 170K das ganze Wasser desorbiert, und wie die wieder auftretende Peakaufspaltung von Chlor zeigt, bleibt auf dem Substrat nur NaCl in molekularer Form zurück.

3 Kapitel III. Wechselwirkung von Benzolderivaten mit festem Wasser

3.1 The Interface between Benzenes (C_6H_6; C_6H_5Cl; 2-C_6H_4OHCl) and Amorphous Solid Water studied with MIES and UPS(HeI/II)

The interface between benzenes (C_6H_6; C_6H_5Cl; 2-C_6H_4OHCl) and amorphous solid water studied with metastable impact electron spectroscopy and ultraviolet photoelectron spectroscopy (HeI-II), A. Borodin, O. Höfft, U. Kahnert, S. Krischok, M. O. Abou-Helal and V. Kempter, Journal of Chemical Physics 120 (11): 5407-5413 (2004)

Interfaces between films of benzenes (C_6H_6; C_6H_5Cl; 2-C_6H_4OHCl) and solid H_2O on tungsten substrates were studied between 80 and 200K with metastable impact lectron spectroscopy (MIES) and ultraviolet photoelectron spectroscopy (UPS(HeI and II)). The following cases were studied in detail: (i) adsorption of the benzenes on solid water in order to simulate their interaction with ice particles, and (ii) deposition of water on benzene films in order to simulate the process of water precipitation. In all cases the prepared interfacial layers were annealed up to 200K under in situ control of MIES and UPS. The different behaviour of the interfaces for the three studied cases is traced back to the different mobilities of the molecules with respect to that of water. The interaction between H2O and the benzenes at the interfaces is discussed on the basis of a qualitative profile for the free energy of that component of the interface which has the larger mobility. Possible implications of the present results for atmospheric physics are brie y mentioned.

3.1.1 Introduction

The chemistry on molecular films, water in particular, is a challenging field for surface science because of the complexity of the three-dimensional system under study. The chemistry occurs here in a highly dynamic, quasi-liquid molecular environment where the balance between solvation, chemical reactions, stabilization of the solute and the reaction products are important factors [1, 2, 3, 4, 5]. In fact, the ice/frozen water interface is constantly changing as water molecules adsorb and desorb. Adsorbing species may become solvated quickly and encapsulated into a water matrix [6, 7].

Persistent, bioaccumulative, and toxic substances (PBT's) are of global and local concern: photochemical reactions involving PBT's play a mayor role in the atmosphere, in natural water, on soil, and in living organisms [8]. Snow and ice are important components of cold ecosystems and influence the fate and the reactions of PBT's. The process of uptake of these chemicals into nascent water crystals can take place either by adsorption onto the surface of precipitating snow crystals or through co-deposition with water into growing crystals or films. Our present understanding of how PBT's interact with frozen water is relatively limited, and the study of the interaction has only recently become a subject of detailed investigations. A quantitative model to assess and evaluate the environmental fate and behaviour of PBT's in cold ecosystems would include to know about [8].

- the efficiency and the mechanism of snow scavenging from the atmosphere by the chemicals,
- the behaviour (migration, solvation, etc.) of the chemicals within snow or ice particles, and
- the release, i.e. the desorption of chemicals, products from photochemical reactions in particular, into the ecosystem. The photolysis of the substances in

ice yielded photoproducts very different from those observed in liquid water [8]: the observed preferential formation of dimers of
the starting molecules gives evidence for their high concentration in the reaction region. This was explained in terms of an effective reaction cavity which restricted the reactions between the host water molecules and the guest organic substances. In order to shed more light into the origin of the different photochemistry of PBT's in solid and liquid water, we have applied the ultra-surface sensitive Metastable Impact Electron Spectroscopy (MIES), in combination with photoelectron spectroscopy (UPS with HeI and II), to the study of interfaces between the benzenes C_6H_6, C_6H_5Cl, and 2-(or ortho-) C_6H_4OHCl and solid water between 80 and 200K. In contrast to C_6H_6 and C_6H_5Cl, 2-C_6H_4OHCl may interact with water comparatively strongly via its OH-group. In order to obtain information on the PBT-water interaction under atmospheric conditions, we studied (i) the adsorption of the benzenes on solid water, simulating the interaction of the chemicals with ice and snow particles, and (ii) the deposition of water on films of the benzenes, simulating the process of water precipitation. (ii) may also provide a better understanding of the interaction of water with soot particles in aircraft contrails [9]: the films of organic rings serve as a model for the soot particle's surface while the ligands form functional groups for the interaction with water molecules.

3.1.2 Experimental Remarks

The experiments were carried out under ultra high vacuum (UHV) conditions (base pressure < $4 \cdot 10^{-10}$Torr) equipped with low energy electron diffraction (LEED), X-ray and ultraviolet photoelectron spectroscopy (XPS and UPS(HeI and II)), Auger electron spectroscopy (AES), and MIES, and are described in detail elsewhere [10, 11]. In MIES metastable helium atoms ($2^3S/2^1S$) of thermal kinetic energy are utilized to eject electrons from the uppermost layer of the

surface. The application of MIES to surface spectroscopy is well documented [4, 12]. Previous applications of MIES, in combination with UPS, to the characterization of films of solid water and to the study of processes taking place on these films as a consequence of the adsorption of atoms and molecules can be found elsewhere [5, 13, 14, 15, 16].

The energy scales in the figures are adjusted in such a way that electrons emitted from the Fermi level, i.e. electrons with the maximal kinetic energy, appear at the binding energy E_B=0eV. The position of the Fermi level is determined from MIES spectra for Na-covered tungsten [14, 17]. In the following, all binding energies refer to the Fermi level (E_B=0eV). The low-energy cut-off in the spectra gives directly the surface work function, irrespective of the actual interaction process which produces the electrons.

The employed benzenes were dosed to the surface by backfilling the chamber with the desired molecules at a pressure of about $2 \cdot 10^{-8}$Torr. The procedure for obtaining an estimate of the molecular coverage is discussed in more detail in Ref.[15]. Brie y, we benefit from the fact that the MIES signal saturates after completion of the first molecular adlayer, and that in UPS(HeI) the emission at the Fermi level disappears roughly at a coverage of two complete adlayers for the chemicals under consideration. The exposure is given in units of monolayer equivalents (MLE). At 1MLE the surface would be covered by one molecular adlayer; penetration of the molecules into the host solvent film may however modify the coverage. The amount of surface-adsorbed water can be estimated on the basis of earlier work with TPD and MIES [11, 13]. The surface temperature can be varied between 80 and 700K; the absolute value of the temperature is known within +/-10K. The surface was exposed to water by backfilling the chamber at a substrate temperature between 110 and 130K. This ensures the formation of a dense, non-porous and amorphous film of solid water [18]. The formation of an ordered film would require a certain degree of mobility of the water molecules; below 140K this mobility does not exist anymore. No extra

spots were observed with LEED when dosing the tungsten substrate with water; no substrate spots are seen anymore when the coverage exceeds 5MLE.

3.1.3 Results

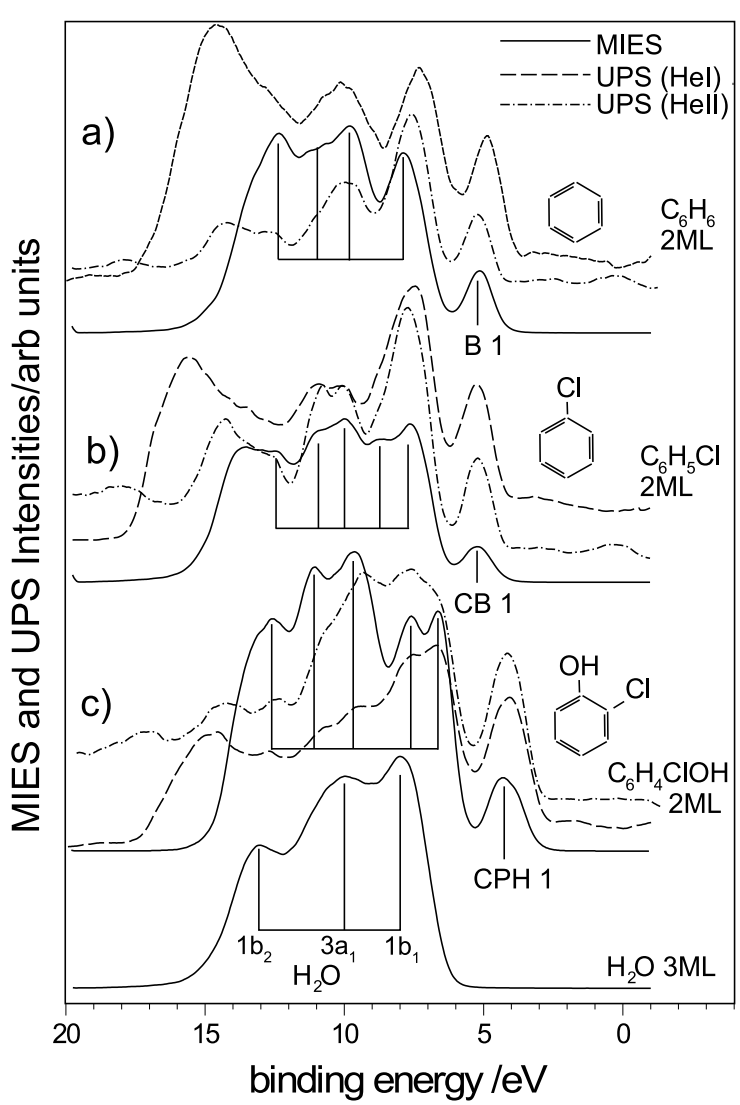

Fig. 1(a): MIES spectra for the adsorption of water on tungsten (80K), and MIES and UPS(HeI and II) spectra for benzene (B) (2ML) on water films (80K; 3BL). See text for the identification of the structures labeled by vertical bars.

Fig. 1(b): As fig. 1(a), but for chlorobenzene (CB)

Fig. 1(c): As fig. 1(a), but for chlorphenol (CPH)

Fig.1 (a) to (c) compare MIES and UPS(HeI/II) spectra for benzene (B) (fig.1(a)), chlorobenzene (CB) (fig.1(b)), and 2-chlorophenol (CPH) deposited on a solid water film supported by a tungsten substrate. Also shown are MIES spectra for water adsorbed on tungsten; UPS data for water can be found elsewhere [5, 11, 19, 20]. Water, when adsorbed molecularly, produces three peaks identified as emission from the three uppermost occupied water orbitals $1b_1$, $3a_1$, and $1b_2$ [19, 20] (E_B=7.8; 10.0; 13.2eV, respect.). In contrast, the adsorption of water onto partially alkalated titania, leading to water dissociation, yields peaks at E_B=7.0 and 11.2eV from the ionization of the OH 1π and the 3c orbitals, respectively [19, 20]. In the present work we see only the emission from molecular water. The emission from $3a_1$ is comparatively broad and, apparently, reflects contributions to this MO from intra-molecular mixing, i.e. this MO consists of contributions from the wave functions of adjacent water molecules that interact via hydrogen bonding [21].

The B spectra display 5 spectral features in MIES, B1 to B5, at E_B=5.1; 7.9; 9.8; 11.0; 12.4eV, respect. (fig.1(a), see vertical bars). They are due to the ionization of the benzene MO's $1e_{1g}(\pi_3/\pi_2)$ (B1), $1a_{2u}(\pi_1)/3e_{2g}(\sigma)$ (B2), $1b_{2u}(\sigma)/3e_{1u}(\sigma)$ (B3), and $2b_{1u}(\sigma)$ (B4) $3a_{1g}(\sigma)$ (B5) [22]. It is of considerable importance for the data reduction leading to the graphs of figs. 2 and 3, that no contribution from the ionization of water interfers with B1. The peak-like emission seen at the largest binding energies in MIES and UPS(HeI) is due to secondary and/or scattered electrons with small kinetic energies.

The CB spectra display 6 features, CB1 to CB6, at E_B=5.1; 7.3; 8.8; 9.9; 10.9; 12.4eV (fig.1(b), see arrows). Penning ionization of C_6H_5X (X= F, Cl, Br, I) molecules in the gas phase upon collisions with metastable He atoms was studied by Penning ionization electron spectroscopy (PIES) [23]. According to that work the following assignment can be given to the spectral features: $4b_1(\pi_3)/1a_2(\pi_2)$ (CB1), $9b_2(n_\perp)/3b_1(n_\parallel)$ (CB2), $2b_1(\pi_1)$(CB3), $14a_1/7b_2$(CB4), $6b_2/13a_1$ (CB5), and $12a_1$ (CB6). Again, as for B, the emission from the

ionization of the lowest π MO's is well separated from any water emission, in particular from $1b_1$. CB2 stems from those MO's that are most strongly affected by an admixture of states with Cl3p character [23].

The CPH spectra display 6 features, CPH1 to CPH6, at E_B=4.3; 6.8; 7.6; 9.9; 11.0; 12.5eV (fig.1(c), see arrows). On the basis of molecular structure calculations the following MO's can be expected to contribute strongly to the observed spectral features [24]: π_3/π_2 (CPH1), $n_\perp(Cl)/n_\parallel(Cl)$ (CPH2), $n_\perp(O)/\pi_{CCl}$ (CPH3), π_1 (CPH4), σ_{CC}/σ_{CO} (CPH5), σ_{CC}/σ_{CH} (CPH6). CPH1 is again well separated from any water emission.

All labeled features are seen both in the MIES, HeI and II spectra. We have not made any attempt to identify additional feature seen at larger binding energies with HeII. This suggests that the MIES spectra are due to the Auger deexcitation process in which one electron from water or benzene valence band states fills the 1sHe vacancy while the 2sHe takes over the excess energy and is ejected in the Auger process [4, 12]. However, the relative intensities in MIES and UPS spectra may differ [4, 12]: in MIES the spectra reflect the density of the respective molecular states prior to ionization by Auger deexcitation, while the UPS spectra depend upon the density of states of both the initial and final states involved in the photoionization process, and thus on the so-called joint density of states. Furthermore, we can expect that those MO's that extend outside the repulsive molecular surface, as estimated from the Van der Waals radii of the atoms in the molecule, give strong contributions to the MIES spectra [23]. For this reason π-bands will manifest themselves strongly in MIES in accordance with other conjugated molecules. Furthermore, n-bands should appear enhanced in MIES because, having Cl3p and O2p character, they will contribute strongly to the charge density that extends outside the repulsive molecular surface, and, thus, are not efficiently shielded by the charge density of the benzene ring. The same arguments apply to the MO's that form σ_{CCl}, σ_{CO} bonds. Figs. 2(a) to (c) show the temperature dependence of the $1b_1$ and B1 (CB1; CPH1)-intensities in

the MIES and UPS spectra for monolayers of benzenes deposited on solid water films.

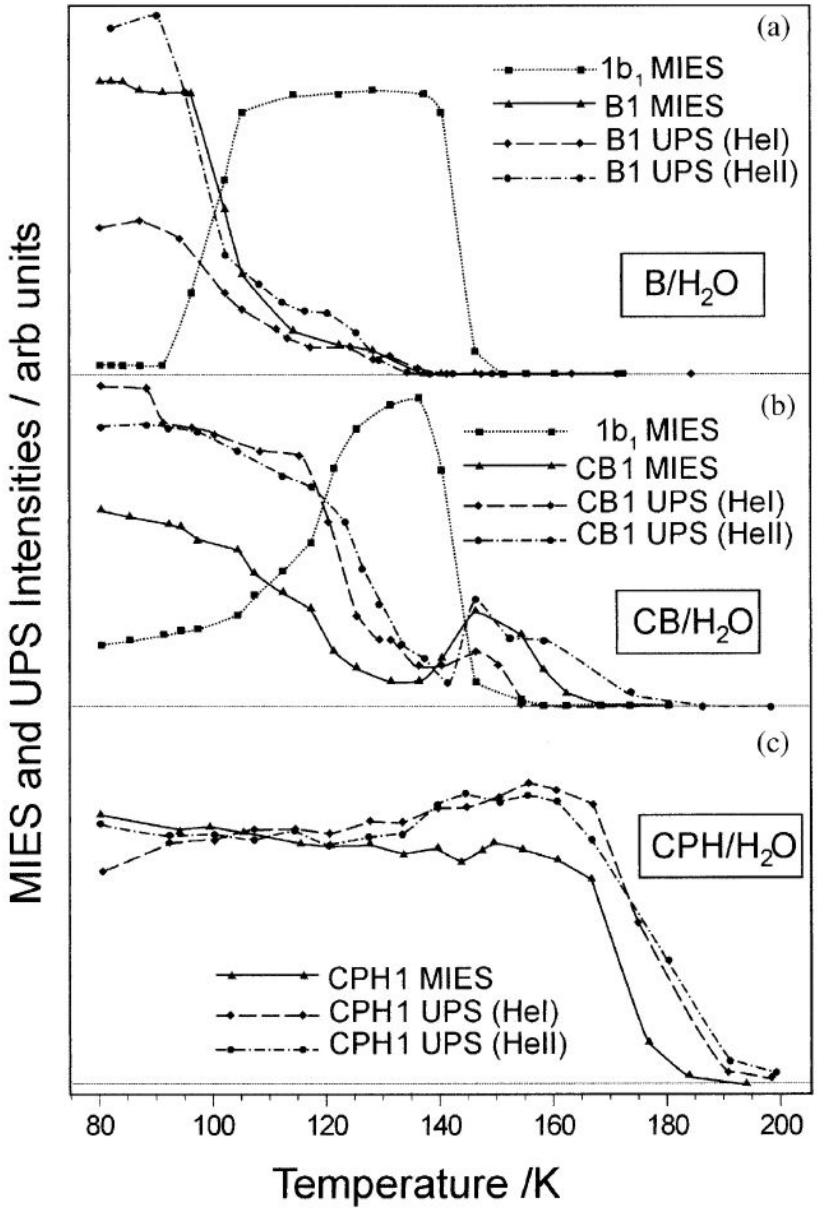

Fig. 2(a) to (c): Intensity changes of various spectral features ($H_2O(1b_1)$ in MIES; B1 (CB1; CPH1) in MIES, HeI and II) during the annealing of a film of benzene (1ML) (a), chlorobenzene (1ML) (b), and chlorphenol (3ML) (c) deposited on a water film (80K; 3BL)

Fig.2(a) shows the results for benzene (B)(denoted by B/H2O) as a function of the annealing temperature. At first, B is adsorbed atop. The simultaneous decrease of B1 in MIES and UPS seen above 95K suggests that B starts to desorb from the water film, and has practically disappeared at 130K. If B would penetrate into the water film, B1 should disappear in MIES, but would still be present in the UPS spectra which is not the case. With the onset of B desorption $1b_1$ starts to rise because the shielding of water by B against the interaction with He* becomes less efficient. Around 140K water starts to desorb, and, according to MIES and UPS, desorption is complete around 150K.

Fig.2(b) presents the corresponding results for chlorobenzene (CB) deposited on solid water (denoted by CB/H_2O). The simultaneous decrease of CB1 in MIES and UPS and the rise of $1b_1$ seen between 115 and 140K indicate that the desorption of CB species becomes sizeable above 115K. However, although CB1 has become rather small around 135K in MIES, desorption is not complete at that point because CB reappears both in MIES and UPS at T > 140K during water desorption. The small CB1 signal between 120 and 140K suggests, in particular, that CB is shielded from the interaction with He*, and, consequently, implies that in this temperature range the toplayer consists of water mainly. The CB species that are bound to the tungsten substrate are seen up to 165K.

Fig.2(c) displays the corresponding results for a 2-chlorophenol (CPH) film (denoted by CPH/H_2O). CPH covers the water film as signaled by the absence of water-induced features in both MIES and UPS. No significant change of the CPH1 intensity has yet occurred at 150K where water should have desorbed to a large extent; CPH desorption becomes significant above 170K. No water-induced emission is seen in the entire studied range of temperatures. Apparently, the high temperature for CPH desorption originates from an increased interaction among the CPH molecules, probably caused by H-bonding, involving the OH-group of CPH.

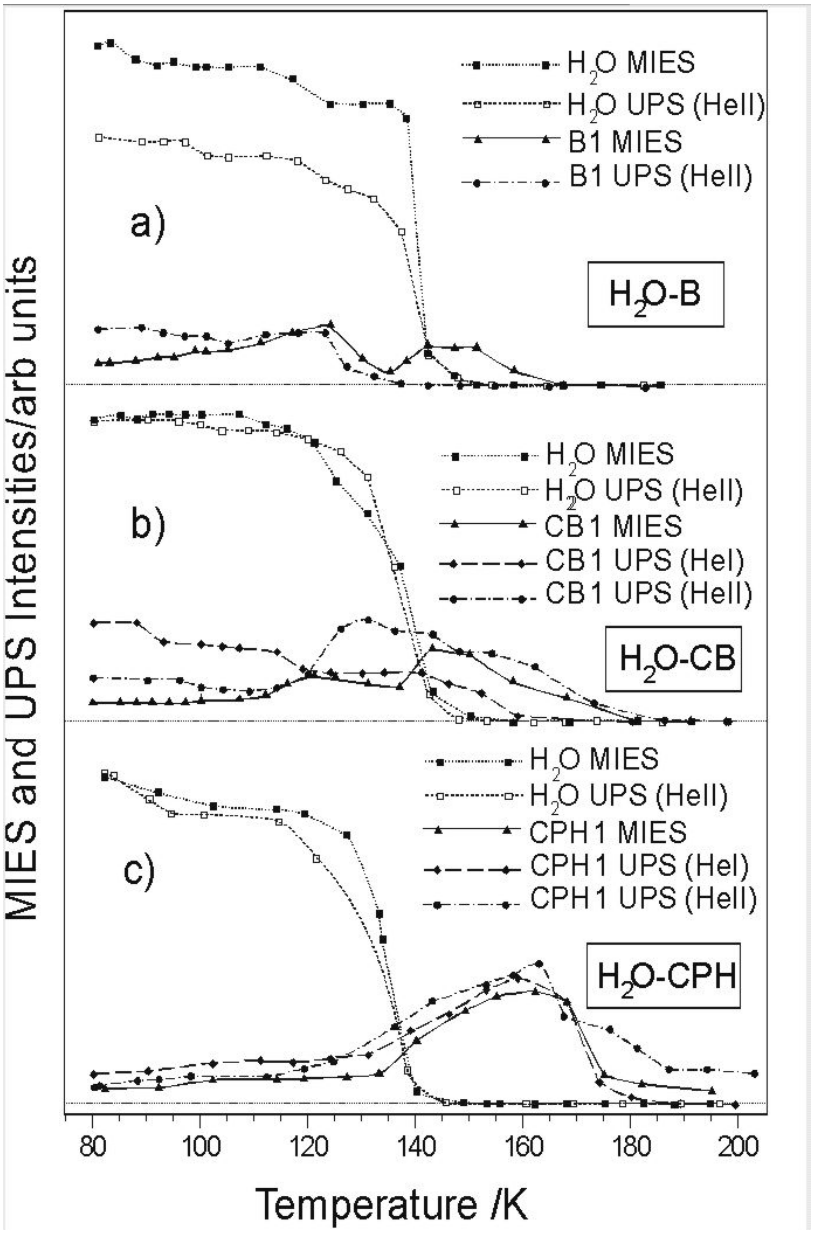

Fig. 3 (a) to (c): Intensity change of the MIES signals B1 (CB1; CPH1) and $H_2O(1b_1)$ during annealing a water film (2BL) deposited on films (about 3ML thick) of benzene (a), chlorobenzene (b), and 2-chlorophenol (c) (80K)

Figs. 3(a) to (c) show the temperature dependence of the $1b_1$ and B1 (CB1; CPH1)- intensities in the MIES and UPS spectra when water overlayers deposited on films of the benzenes are heated between 80 and 200K. In all cases

water desorption takes place at about the same temperature (around 140K); no significant influence of the ligands can be noticed. In particular, no indication of an eventual H-bonding is apparent for CPH. Fig.3(a) shows the results for a water overlayer (2BL) on benzene (B) (denoted by H_2O/B). Initially, water forms the top layer as judged from the fact that only very weak B1 emission, besides the spectral features from molecular water, can be noticed, i.e. efficient shielding of B by the water molecules takes place. The rise of B1 in MIES, noticeable already below 100K, cannot simply be attributed to water desorption. Considering the absolute surface sensitivity of MIES, we conclude that some B species have moved closer to the surface of the water film, and, to some extent, become accessible to MIES. A second maximum in the B1 signal occurs when most of the water has desorbed, i.e. around 150K, and the remaining B species are not shielded anymore efficiently. The B species responsible for this rise are directly bound to the tungsten substrate as is also suggested by the fact that the position of B1 is shifted by 0.5eV towards smaller binding energies. The comparison with the spectra collected during the deposition of B (before offering water) indicates that at 145K the B coverage of the substrate is only of the order of 20 percent (too low to be detected with He(II)). B desorption is impeded by about 15K as compared to B/H2O when the B layer is water-covered.

Fig.3(b) shows the corresponding results for H_2O/CB; parameters are as given in fig.3(a). At a first glance, the results appear to be qualitatively similar as for B. However, the decrease of $H_2O(1b_1)$ is more gradual and sets in earlier (around 120K, instead of 137K for B); the CB1 emission seen after water desorption (at 150K) is still about 50 percent of that before exposure of the CB film to water. Not before 190K all CB species have desorbed from the tungsten substrate.

The results for H_2O/CPH (Fig.3(c)) are qualitatively different: CPH1 rises in MIES and UPS as soon as the shielding of CPH by water molecules becomes

reduced, i.e. beyond 130K. At 160K the entire amount of CPH deposited prior to water exposure is still present.

For the following discussion we note from figs.2 and 3 that desorption from tungsten takes place between T_D=160 and 190K for all studied benzenes. On the other hand, desorption from water occurs earlier, at T_D=110 and 130K for B and CB, respectively. Here T_D denotes the temperature at which the intensities of B1 and CB1 have decayed to 1/e. For H_2O/CPH, multilayers are still stable on tungsten after the water has desorbed; for H_2O/B and /CB part of the underlying B and CB films has desorbed together with the water.

3.1.4 Discussion

The interaction of an adsorbate, in particular its penetration into the solvent, is often discussed in terms of the free energy (FE) behaviour of the adsorbate as a function of its distance from the solvent surface [2, 25]. As discussed in more detail in ref. [2], the FE-profile can be expressed as the sum of the average kinetic and potential energies and an entropy term, related to the disorder caused by the presence of the adsorbate. When the adsorbate approaches the surface, the potential energy term decreases monotonously, and reaches a minimum close to the surface. This is due to the increasing coordination number of the water molecules surrounding the adsorbate and/or to (hydrogen) bond formation. Qualitatively, the entropic contribution follows the behaviour of the potential energy, indicating an entropy loss caused by the increase of order when the adsorbate, entering the surface, becomes trapped by solvent molecules. Inside the solvent, the profile depends on subtle changes in the potential energy and the entropy of the system, and, thus, on the solvation ability of the solvent, i.e. on the type of the adsorbate-solvent interaction.

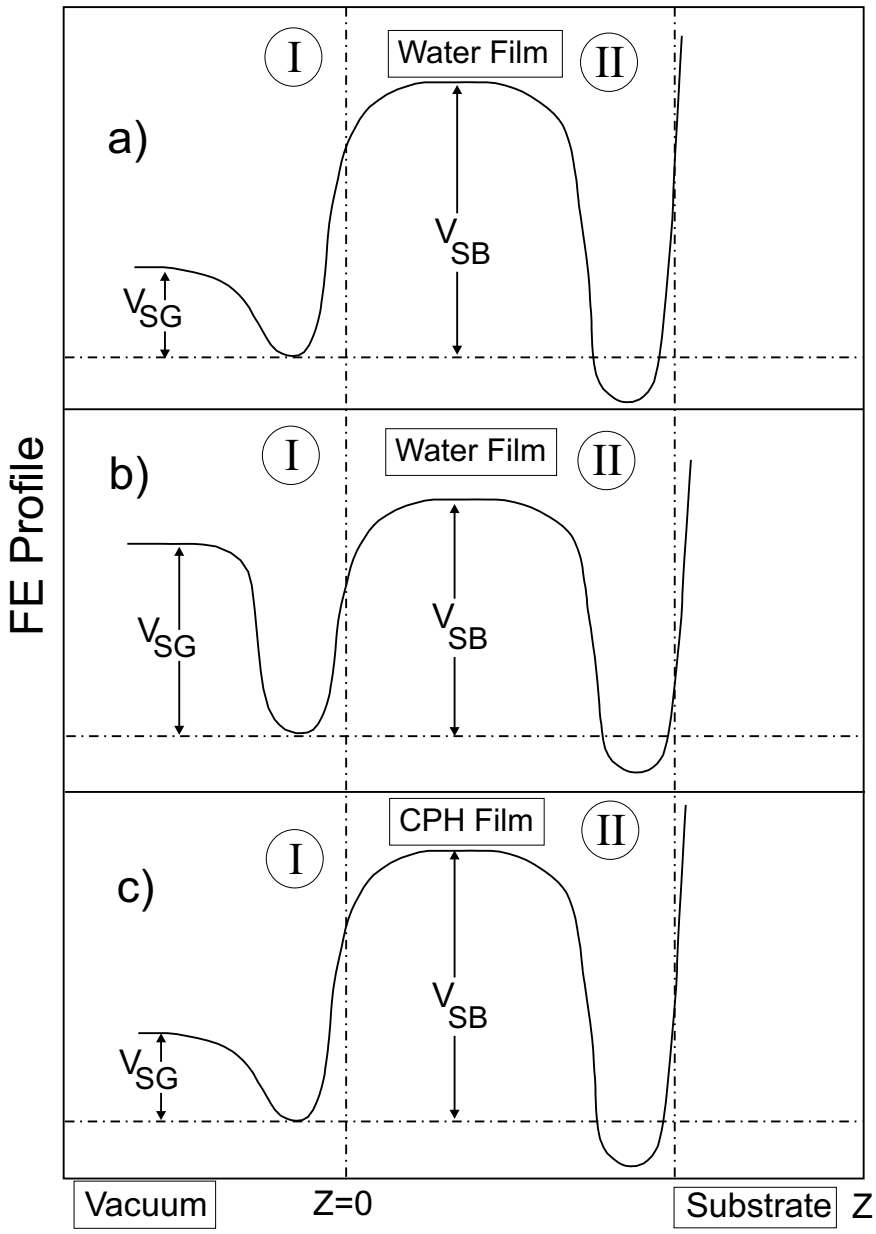

Fig. 4 (a) to (c): Free energy profiles (qualitatively) for the interaction at interfaces between water and the benzenes (a) C_6H_6, (b) C_6H_5Cl and (c) 2-C_6H_4OHCl. VSG and VSB are the barrier heights for desorption into the vacuum and migration into the solvent film, respectively; z = 0 is at the interface between film and vacuum.

For B/H_2O water will be considered as the solvent because B desorbs from water at 105K while a water film on tungsten is stable up to about 140K. The interaction at the (H_2O-B)-interface will be discussed with the help of Fig. 4(a). It presents, qualitatively, the FE profile of a B molecule as a function of its

distance z from the water surface. Minimum (I) (depth VSG) is responsible for the on-top adsorption at 80K. The rise of FE during the penetration of B into the solvent ($z < 0$) reflects the fact that no bond formation nor an appreciable energy gain from an increase of the coordination number of the water molecules takes place under these circumstances. Instead, the large value of VSB is attributable to the geometric reason that for penetration the large B molecule need to push-out water molecules from their lattice sites. VSB is a function of temperature, and will decrease with increasing water mobility.

Another well (II) (fig.4(a)) is noticed at the H_2O-substrate interface. This stable site for B adsorption arises from the B-substrate interaction which, in general, can be stronger than the water-water or water-B interaction. The observed temperature dependence of B1 and $1b_1$ simply implies that VSG << VSB; as explained above, the large B species are unable to enter the rather dense water lattice at temperatures much below TD of water. As soon as the temperature becomes larger than $T_D(B)$, the probability for B desorption from well (I) into the vacuum becomes rather high while that for migration into the film and to the tungsten substrate remains low. Consequently, B desorption causes the strong decrease of B1, seen both with MIES and HeII above 105K, connected with the strong rise of $1b_1$. Clearly, all B species have desorbed before water desorption becomes significant. For H_2O/B the B species are located in (II) initially (see results of fig.3(a)). Fig. 2(a) suggests that between 80 and 120K the penetration of these B species into the water film is unlikely because of the large barrier VSB. We have to explain the findings that, on the one hand, only about 20 percent of the originally deposited B species are present when all water has desorbed, and, on the other hand, only a weak B1 signal is observed in MIES at any temperatures. Obviously, the mobility of the water molecules has increased drastically at 130K because of the shorter lifetime of the H-bonds. Thus, their larger mobility allows the water molecules to "uncover" the B species which, as a consequence, can desorb even though they were initially located underneath

the water film. However, desorption is delayed as compared to B/H2O (115K). By applying TPD, it was demonstrated for CCl4 and CD3Cl that desorption is indeed impeded by an overlayer of solid water [26, 27]. The probability for detecting B species at the surface for temperatures close to $T_D(H_2O)$ is however small: their residence time in (I) is short for T far above $T_D(B)$, probably between 10^{-12} and 10^{-9}s [2], because VSG is small, and instantaneous desorption occurs into the vacuum. The onset of the water desorption above 135K causes a rise of B1: those B species, still located in well (II), become now accessible to MIES. Indeed, we find that T > 165K is required to completely remove the B species deposited at 80K on the tungsten substrate.

For the discussion of the interaction at the (H_2O-CPH)-interface we interchange the role of solvent and solute, treating CPH as solvent. This makes sense because T_D for H_2O on CPH is about 135K, and CPH films are still stable on tungsten at this temperature. We arrive at the FE profile displayed in Fig.4(c). (I) allows for on-top water adsorption of water, as observed for 80K. For H_2O/CPH, water desorption becomes significant as soon as VSG can be surpassed (T > 130K). Caused by the water desorption, CPH becomes accessible to MIES; this explains the correlation between the decrease of $1b_1$ and the rise of CPH1 (see fig.3(c)). Other than for B/H_2O, we have assumed that the barrier VSB is low because the water molecules can move relatively freely through the comparatively open CPH lattice. Thus, for CPH/H_2O, water molecules will migrate from II to I through the CPH lattice, as soon as water becomes mobile. Because VSG is also low, the residence time of water species that have migrated through the CPH film to the surface is short (between 10^{-12} and 10^{-9}s [2]), and accounts for the absence of water-induced features in the spectra. By applying TPD it should be possible to verify at which temperature water desorption takes place for CPH/H_2O.

For the (CB-H_2O)-system both components become mobile at about the same temperature. Consequently, inter-penetration of the two components takes place

before desorption is complete. This is underlined by the fact that CB species, originally deposited atop of the water film, are found on the tungsten substrate after all water has desorbed. In the FE profile for (CB-H_2O) (Fig.4(b)) the choice VSG π VSB allows for the simultaneous occurrence of desorption and penetration. By applying TPD, it was demonstrated for CCl_4 and CD_3Cl that desorption is impeded by an overlayer of solid water [26, 27]. It was claimed that the formation of cages of the coadsorbates under water takes place on metallic surfaces [26]. No indication of caging is seen for the large organic molecules under study. For CCl_4 the desorption from underneath a water layer is correlated with the onset of water crystallization [27]. In concert with crystallization, the underlaying CCl_4 desorbs abruptly over a narrow temperature range. It was proposed that structural changes during crystallization may facilitate desorption pathways in the water overlayer. These pathways may arise from the formation of grain boundaries, cracks, and fissures, occurring during crystallization. This mechanism may contribute to the observed B desorption through water.

The conclusions of this paper can be generalized to other substrates as well because the temperature for film formation, both of water and the benzenes, will show little dependence on the actual substrate [19, 20]. Only the monolayer fraction that can be obtained above the temperature for desorption of the films does depend on the number and type of centers actively interacting with the benzenes. The density of active centers on substrates of interest for application, as f.i.functional groups on soot, point defects on oxides, will certainly be higher than on metals. Finally, we make an attempt to apply our results to interfaces between benzenes and water under atmospheric conditions, say at 220 to 250K:

(1) Exposure of the films of benzenes to water (precipitation of water on polluted surfaces): prior to water exposure, T is larger than the temperature for desorption from the substrate on which the benzenes are deposited. Consequently, films of the benzenzes cannot form; only molecules bonded

suficiently strongly to the substrate in well (II), in particular at substrate imperfections, are present. Following water exposure, there is little tendency of these, comparatively strongly bound molecules to migrate into the water toplayer. Therefore, under the conditions of (1), the benzenes will be found at the interface between the substrate and the water film. (2) Benzenes inside ice particles: due to the low solubility of benzenes in water, their frozen solution may be visualized as an ensemble of molecular agglomerates, embedded into ice cavities [28]. As suggested from the behavior observed for water deposited underneath CPH, water molecules from the surrounding cavity walls can be expected to pass freely through the relatively open agglomerate structure of the organic species. However, these species, although being mobile themselves, will not be able to enter the cavity walls to a large extent because of kinematic constraints
(see figs.4). Consequently, their motion, at high concentration, remains largely restricted to the volume of the cavities; the water concentration inside the cavities will greatly depend on temperature.
When ice particles are exposed to benzenes, a similar argumentation shows that the organic species will accumulate at the outside of the particles, embedded into the aqueous atmosphere above the particle surface. Thus, a high concentration of the solute species is possible at the water-benzenes interface; indeed, this was concluded from the high probability for dimer formation in photoreactions of CPH with ice [28].

3.1.5 Summary

The interaction of the benzenes C_6H_6, C_6H_5Cl, and 2-C_6H_4OHCl with solid H_2O, deposited on tungsten, was studied with metastable impact electron spectroscopy (MIES) and ultraviolet photoemission spectroscopy (UPS) with HeI/II. The conditions were (i) adsorption of the benzenes on solid water in order to simulate

the interaction of the chemicals with ice particles, and (ii) deposition of water on the organic films in order to simulate the process of water precipitation. In all cases, we studied the properties of the adsorbed layers during their annealing between 80 and 200K. At 80K, closed layers of all studied benzenes can be prepared on water with little mixing and vice versa.

For C_6H_6 on water (B/H_2O), desorption starts around 105K; no penetration of B into the water film could be detected. For H_2O/B, B desorption appears to be delayed and starts when the water molecules of the overlayer become sufficiently mobile (T > 120K). B desorption is complete when the B molecules interacting comparatively strongly with the tungsten substrate have desorbed (T=160K). For chlorobenzene on water (CB/H_2O), CB and water molecules both become mobile around 120K and desorb in the same temperature range. Not all CB molecules desorb with the water film; some CB molecules interact with the tungsten substrate, and finally desorb at 170K. For 2-chlorophenol on water (CPH/H_2O), all water has desorbed before CPH desorption sets in (T=170K). We suggest that, as soon as the H_2O molecules of the underlayer become sufficiently mobile, e.g. above 120K, water can migrate through the comparatively open CPH lattice. For H_2O/CPH water has desorbed before any desorption of CPH can be detected (around 170K).

Qualitative Free Energy profiles are proposed that can account for the experimental results. We predict that under atmospheric conditions the studied benzene species, when deposited on solid substrates, remain located at the interface under water exposure. On the other hand, benzenes will accumulate at the outside of benzenes-exposed ice particles. As solutes remain aggregated in ice cavities of frozen solutions.

3.1.6 References

[1] G.E. Brown et al.: Chem. Rev. 99 (1999) 77

[2] C. Girardet, C. Toubin: Surf. Sci. Rep. 44 (2001) 159

[3] M. Faubel, in: Photoionization and Photodetachment, Part 1 (Ed. C.Y. Ng, World Scientific, Singapore) (2000) 634

[4] H. Morgner: Adv. Atom. Molec. and Opt. Phys. 42 (2000) 387

[5] J. Günster, S. Krischok, V. Kempter, J. Stultz, D.W. Goodman: Surf. Rev. Lett. 9 (2002) 1511

[6] D.R. Haynes, N.J. Tro, S.M. George: J. Phys. Chem. 96 (1992) 8502

[7] L. Chaix, H. van den Bergh, M.J. Rossi: J. Phys. Chem. A 102 (1998) 10300

[8] P. Klan, I. Holoubek: Chemosphere 46 (2002) 1201

[9] D. Ferry, J. Suzanne, S. Nitsche, O.B. Popovitcheva, N.K. Shonija: J. Geophys. Res. Atmos. 107 (2002) 4734

[10] P. Stracke, S. Krischok, V. Kempter: Surf. Sci. 473 (2001)

[11] S. Krischok, O. Höfft, J. Günster, J. Stultz, D. W. Goodman, V. Kempter: Surf. Sci. 495 (2001) 211

[12] Y. Harada, S. Masuda, H. Osaki: Chem. Rev. 97 (1997) 1897

[13] J. Günster, S. Krischok, J. Stultz, D.W. Goodman: J. Phys. Chem. B 104 (2000) 7977

[14] S. Krischok, O. Höfft, J. Günster, R. Souda, V. Kempter: NIM in Phys. Res. B 203 (2003), 124

[15] A. Borodin, O. Höfft, S. Krischok, V. Kempter: NIM in Phys. Res. B 203 (2003), 205

[16] S. Krischok, O. Höfft, V. Kempter: Surf. Sci. 532-35 (2003) 370

[17] M. Brause, S. Skordas, V. Kempter: Surf. Sci. 445 (2000) 224

[18] K.P. Stevenson, G.A. Kimmel, Z. Dohnalek, R.S. Smith, B.D. Kay: Science 283 (1999) 1505

[19] P.A. Thiel, T.E. Madey: Surf. Sci. Rep 7 (1987) 211

[20] M. A. Henderson: Surf. Sci. Rep. 285 (2002) 1

[21] S. Casassa, P. Ugliengo, C. Pisani: J. Chem. Phys. 106 (1997) 9030

[22] K. Kimura et al.: Handbook of HeI Photoelectron Spectra of Fundamental Organic Molecules, Halsted Press, N.Y.

[23] K. Imura, N. Kishimoto, K. Ohno: J. Phys. Chem. A 105 (2001) 4189

[24] K. Ohno: priv. comm. (2003)

[25] H. Shinto, T. Sakakibara, K. Higashitani: J. Chem. Engin. Jap. 31 (1998) 771

[26] Y. Lilach, M. Asscher: J. Chem. Phys. 117 (2002) 6730

[27] R.S. Smith, C. Huang, E.K.L. Wong, B.D. Kay: Phys. Rev. Lett. 79 (1997) 909

[28] J. Klanova, P. Klan, D. Heger, I. Holoubek: Photochem. Photobiol. Sci. 2 (2003) 1023

3.1.7 Zusammenfassung von Kapitel 3

Die Attraktivität von Messungen mit Benzolderivaten gründet sich mit der wichtigen Rolle, welche sie in heutigen Ökosystemen spielen. Als Beispiel, eine Fragestellung im Rahmen dieser Arbeit kann so lauten: Es ist bekannt, dass sich unter der UV-Sonnenbestrahlung mehrere Chlorbenzolmoleküle bei einer Reaktion verbinden können, wodurch extrem giftige Dioxin-Verbindungen entstehen können. Normalerweise, ist in der Natur die Konzentration von Benzolderivaten so gering, dass sich mehrere Schadstoffmoleküle in der Atmosphäre kaum treffen können, sodass die Wahrscheinlichkeit einer Verbindung vernachlässigbar klein wird. Es ist auch bekannt, dass es in hohen Schichten der Atmosphäre eine Menge Eispartikel gibt. Es wäre gut zu wissen, ob die Oberfläche von diesen Eispartikeln als Substrat dienen kann, auf welchem sich die Moleküle sammeln könnten und die obige Reaktion stattfinden kann.

Die Prozesse zwischen Wasser und Benzolderivaten (Benzol, Chlorbenzol, 2-Chlophenol) wurden bei einem auf W(110) aufgebrachten Film untersucht. Bei der Präparation wurden auf einem auf bis zu 80K gekühlten W-Substrat in unterschiedlicher Reihenfolge (zuerst Wasser, oder z.B. Benzol) die Schichten von Wasser und von einem Benzolderivat aufgebracht. Weitere Untersuchungen des Films wurden im Temperaturintervall 80-200K durchgeführt. Die dafür benutzten Techniken waren MIES und UPS(HeI und HeII). Für das Beschreiben der Ergebnisse stellte es sich heraus, dass die Profile von freier Energie sehr nützlich sein können. So kann die Darstellung der Ergebnisse anschaulich werden.

Das Verhalten von Wasser zu den Benzolderivaten bei 80K ist gleich für alle untersuchten Systeme. Es gibt tatsächlich keine Wechselwirkung. Ob Wasser oberhalb der Schicht von Benzolderivaten angeboten wird oder Benzol auf

Wasser oben drauf kommt, ist irrelevant. Es findet nur ein normales Lagewachstum statt.

Beim Heizen der Probe nimmt mit steigender Temperatur die Mobilität der Wassermoleküle und der Benzolderivat-Moleküle zu, und bereits bei 105K sind einige Änderungen im Zustand des Films zu sehen:

1a) Benzol/Wasser: Bei 105K fängt die Desorption des Benzols von der Wasseroberfläche an. Bis zu 135K sind neben der Wasser- noch die geringe Benzolemission zu beobachten; ab 135K ist schon kein Spur von Benzol mehr zu finden.

1b) Wasser/Benzol: Wird in anderer Reihenfolge der Film aufgedampft, so lässt sich an der Oberfläche (in den MIES-Spektren) bis zu seiner Desorption nur Wasser erkennen. Wird Wasser bereits vollständig desorbiert (145K), so sind nur stark an das Substrat gebundenes Benzol-Moleküle zu bemerken. Die Information über die Desorption von Benzol liefern die UPS-Spektren. Sie zeigen eindeutig, dass es, obwohl Benzol durch Wasser bedeckt ist, die Benzoldesorption gar nicht stört. Dank der Mobilität von Molekülen dringen die Benzolmoleküle bereits ab 130K durch die Wasserschicht hindurch. Zur Zeit der vollständigen Wasserdesorption bliebt von Benzol nur die letzte mit dem Substrat verkuppelte Lage übrig, die erst bei 170K vollständig desorbiert wird. Die Zeit, während der sich Benzol bei der Desorption in der Filmoberfläche befindet, ist sehr klein ($1\cdot10^{-12}$-$1\cdot10^{-9}$s). Dies kann erklären, weshalb dabei in MIES keine Struktur von Benzol zu bemerken ist.

2a) Wasser/Chlorbenzol: In diesem System sind dieselben Effekte, wie die unter Punkt 1b) für Benzol/Wasser beschriebenen, zu sehen. Der Unterschied läuft darauf hinaus, dass die Temperatur der vollständigen Desorption von Chlorbenzol bei 180K liegt.

2b) Chlorbenzol/Wasser: Hier fängt die Desorption von Chlorbenzol bei 115K an, bereits bei 140K sind keine Spezies davon mehr in MIES zu sehen. Doch UPS zeigt, dass trotz der Desorption noch eine Menge von Chlorbenzol in

Wasser eingedrungen ist. Dies lässt die folgenden Schlüsse zu: Chlorbenzol kann sich ab 115K relativ frei in Wasser bewegen; neben der Desorption können die Chlorbenzolmoleküle auch zur Substratoberfläche gehen, wo sie (s. 2a) bis 180K bleiben.

3a) Wasser/2-Chlorphenol: In dem System ist keine Wechselwirkung zu erkennen. 2-Chlorphenol ist erst nach der Desorption von Wasser (140K) zu sehen, während weiteren Heizens beginnt 2-Chlorphenol bei 170K zu desorbieren.

3b) 2-Chlorphenol/Wasser: Da Wasser früher als 2-Chlorphenol desorbiert, und da Wasser sich unter dem 2-Chlorphenolfilm befindet und während des Heizen nichts von Wasser zu registrieren ist, bleibt die Frage, wann und wie Wasser desorbiert, immer noch offen. Um das sicher festzustellen, sollen weitere Versuche mit anderen Methoden (z.B. TPD) durchgeführt werden.

4 Kapitel IV. Wechselwirkung von Na mit Wasser, Methanol und Ammoniak

4.1 The Interaction of Na Atoms with the Molecular Surfaces H_2O and CH_3OH: The Role of Delocalized Na3s Electrons

The interaction of Na atoms with the molecular surfaces H_2O and CH_3OH: The role of delocalized Na3s electrons, A. Borodin, O. Höfft, U. Kahnert, V. Kempter, A. Allouche, Physical Surface Engineering Vol. 1 (2): 146-154 (2003)

The interaction of Na atoms with H_2O and CH_3OH films is studied with metastable impact electron spectroscopy (MIES) under UHV conditions. The films were grown at 90(+/-10)K on tungsten substrates, and exposed to Na. Na-induced water dissociation takes place whereby OH and CH_3OH-species are formed, and Na-atoms become ionized. At small Na exposures the outermost solvent layer remains largely intact as concluded from the absence of MIES signals caused by the reaction products. However, emission from OH and CH_3OH -species, located at the film surface, occurs at larger exposures. In the same exposure range also emission from Na3s-ionization can be detected. The corresponding spectral structure occurs at an energetic position different from that found on metals or semiconductors. For the (Na-water) system the results are compared with First-Principles calculations on $Na_2(H_2O)_{10}$ clusters concerned with the electron and proton exchange within the cluster. Experiment and theory agree in the energetic positions of the main spectral features from water and sodium ionization. The calculations suggest that the 3sNa emission observed experimentally is due to the ejection of solvated 3s electrons which are trapped between the Na-core and water molecules of the surrounding water

shell. The simultaneous emergence of dissociation products, OH and CH_3OH, and solvated 3s electrons suggests that the delocalization and, consequently, the solvation plays an important role in the Na-water(methanol) reaction.

4.1.1 Introduction

The chemistry on molecular films, water in particular, is a challenging field for surface science because of the complexity of the three-dimensional system under study: in the mobile molecular environment the balance between solvation, chemical reactions, stabilization of the solute and the reaction products are important factors. Although the reaction of Na atoms with water, yielding NaOH and H_2, is a well-known exothermic reaction, the underlying mechanism for this simple-looking process is not well understood. One particular reason is that it is not easy to obtain direct detailed information on the 3sNa electron which plays an active role in this process. In order to overcome this problem we have started to study the interaction of Na with films of amorphous solid water (SW) by combining the Metastable Impact Electron Spectroscopy (MIES) and UPS [1, 2, 3, 4]. As compared to UPS, MIES possesses a rather large sensitivity for the detection of the 3sNa electron, and its pronounced surface sensitivity allows, in combination with UPS, to distinguish between species adsorbed atop and underneath the surface under study. So far, the main findings are that Na-induced water dissociation is certainly efficient above 110K, and that the 3sNa electron is involved in the dissociation reaction. As compared to Na adsorption on solid surfaces, metals and semiconductors in particular, a peculiar shift of the Na3s-structure is seen in the MIES spectra [3, 4], namely for adsorption on water the 3s-ionization energy is smaller by 1eV. A qualitative explanation for the lowering of the 3s-ionization energy has been attempted [4] using Born's model in which Na is thought to be surrounded, at least partially, by water

molecules; this situation is modeled by embedding the Na in a cage formed by the surrounding dielectric medium.

Theory has studied the Na-water interaction by applying First-Principles and/or Molecular Dynamics methods to Na-water clusters [5, 6, 7, 8]. This work shows that the 3s-electron becomes delocalized from its respective core and is trapped between Na and the protons of the shell of hydrating water molecules pointing towards the Na. The electron distribution is unique in the sense that the electron becomes trapped by the surrounding (O-H)-bonds, and has no positive charge near the center of the charge distribution. It was demonstrated that the solvated 3s-electron plays an important role for the dissociation of the water [8]. In this last paper, First-Principles calculations were carried out on clusters consisting of one or two Na atoms and their water environment with the goal to shed light into the mechanisms for exchange of electrons and protons between the constituents of the cluster. In particular, the 3s molecular orbital energy becomes 0.9eV smaller after hydration.

The new detailed MIES data reported in the present paper were collected with the purpose to make a detailed comparison with the predictions of Ref.[8]. This required the extraction of density functional theory (DFT) density of states (DOS) information from Ref.[8]; this information, before and after the transfer of the delocalized electron to the protons of the surrounding water has taken place, is compared with the MIES spectra.

In addition, we present MIES data for the interaction of Na with methanol in order to check the predictions of theory concerning the mechanism for the Na-CH_3OH reaction.

4.1.2 Experimental Remarks

The experiments, described in detail elsewhere [9, 10], were carried out under ultra high vacuum (UHV) conditions (base pressure $<2\cdot10^{-10}$Torr). AES and

XPS are used to characterize the chemical composition of the tungsten substrate employed for the deposition of the molecular films. With LEED it was checked that the molecular films are amorphous. The electronic structure of the molecular films was studied by applying MIES and UPS(HeI and II). In MIES metastable helium atoms ($2^3S/2^1S$) eject electrons from the edge of the surface under study. The application of MIES to surface spectroscopy is well documented [11, 12]. If the Na adsorbate is not fully ionized, a spectral feature is expected from the presence of 3s-charge density at the Na core. With UPS(HeI) the partially occupied 3s-orbital is practically not seen due to its low photoionization cross section [13]. However, in MIES it causes a prominent feature, Na(3s), close to E_F which is clearly seen on metals and semiconductors for coverages larger than about 0.5ML [11, 12]. This underlines the power of MIES for investigating the chemistry between Na and water, which is driven by the 3s-valence electron. For the study of the Na-induced changes in the electronic structure of the molecular films we have confined ourselves to MIES because the UPS(HeI and II) spectra give no information on the 3sNa electron.

The primary result of the experiments are electron energy spectra versus the kinetic energy of the emitted electrons. By choosing a suitable bias voltage between the target and the electron energy analyzer, the energy scales in the figures are adjusted in such a way that electrons emitted from the Fermi level, denoted by E_F, i.e. electrons with the maximal kinetic energy, appear at 19.8eV (which is the potential energy of the metastable He atoms employed for MIES). With this particular choice of the bias voltage, the low-energy cutoff in the spectra gives directly the surface work function (WF), irrespective of the actual interaction process which produces the electrons. For a convenient comparison with theory we present our data as a function of the binding energy of the emitted electrons prior to their ejection. Electrons emitted from the Fermi level, i.e. those with the 19.8eV kinetic energy, appear at binding energy E_B=0eV with respect to the Fermi level.

Na atoms were dosed employing carefully outgassed commercial dispenser sources (SAES Getters). They operate at a rate of 0.05 ML/min, typically. The procedure for the calibration of the alkali coverage is described elsewhere [14]. The exposure is given in units of monolayer equivalents (MLE); at 1MLE the surface would be covered by one Na monolayer if penetration of the Na into the molecular films could be neglected.

The surface temperature can be varied between about 90 and 700K; at present the accuracy of the temperature calibration is 10K. The surface was exposed to water by backfilling the chamber at a substrate temperature between 110 and 130K. This ensures the formation of a closed, non-porous and amorphous SW film [15]. The formation of an ordered film would require a certain degree of mobility of the water molecules; below 140K this mobility does not exist anymore. The relative amount of surface-adsorbed water can be estimated on the basis of earlier work with TPD and MIES [1, 10]. Prior to Na exposure the surface prepared as described above was cooled to the desired temperature.

4.1.3 Computational Details

The method of computation was fully exposed in [8]. A Density Functional Theory (DFT) calculation was carried out at the B3LYP/6-31+g(d,p) level of approximation. This was performed on several cluster models in order to investigate the potential energy surfaces associated to neutral sodium hydrolysis. The first model included only one sodium atom in a cluster consisting of seven water molecules. The calculated barrier of activation was equal to 31.6 $kJ \cdot mol^{-1}$ after correction of the zero point energy. The two others clusters involved two atoms embedded into clusters of seven and ten water molecules, respectively. The associated barriers of activation were 37.2 and 33.2 $kJ \cdot mol^{-1}$, respectively, i.e. the barriers decrease with the number of hydrating molecules.

The calculation of the free activation energies shows that at low temperature the two Na mechanism is more easy. However, all the investigated models involve the 3sNa electron solvation, and are strongly dependent of the electrostatic fields generated by the water cluster.

It was established previously that the interaction of He* with clean and Na covered water films is via the Auger deexcitation process. This implies that the MIES spectra image the surface density of states (SDOS) directly [11, 12]. The SDOS, needed for the comparison with the MIES spectra, have been obtained by dressing the DFT molecular energy level distributions with Lorentzian functions of arbitrary height and an half width of 0.25 eV.

4.1.4 Results

The following spectral features are expected when Na and water interact with surfaces [1, 2, 3, 4]: the 2pNa-orbital, due to its high ionization energy, is not accessible by the chosen techniques. If the Na adsorbate is not fully ionized, a spectral feature is expected from the presence of 3s-charge density at the Na core. It causes a prominent feature, Na(3s), close to E_F which is clearly seen on metals and semiconductors for coverages larger than about 0.5ML [11, 12].

Molecularly adsorbed water produces three peaks, both in MIES and UPS, identified as emission from the three uppermost occupied water orbitals $1b_1$, $3a_1$, and $1b_2$ [16, 17] (binding energies 7.8, 10.0, and 13.2eV, respectively). In contrast, the adsorption of water onto partially alkalated titania leads to water dissociation provided the precoverage is larger than about 0.5 monolayers [10]. The ionization of the OH 1π and the 3σ orbitals yields peaks at E_B=7.0 and 11.2eV, respectively [16, 17]. On metal substrates the Na-H_2O interaction can lead to complete dissociation of H_2O. In this case atomic oxygen species, stabilized by Na^+ ions, will be seen. As a particular example, the ionization of O_2^- species will give rise to a single peak around E_B=3.6eV [18].

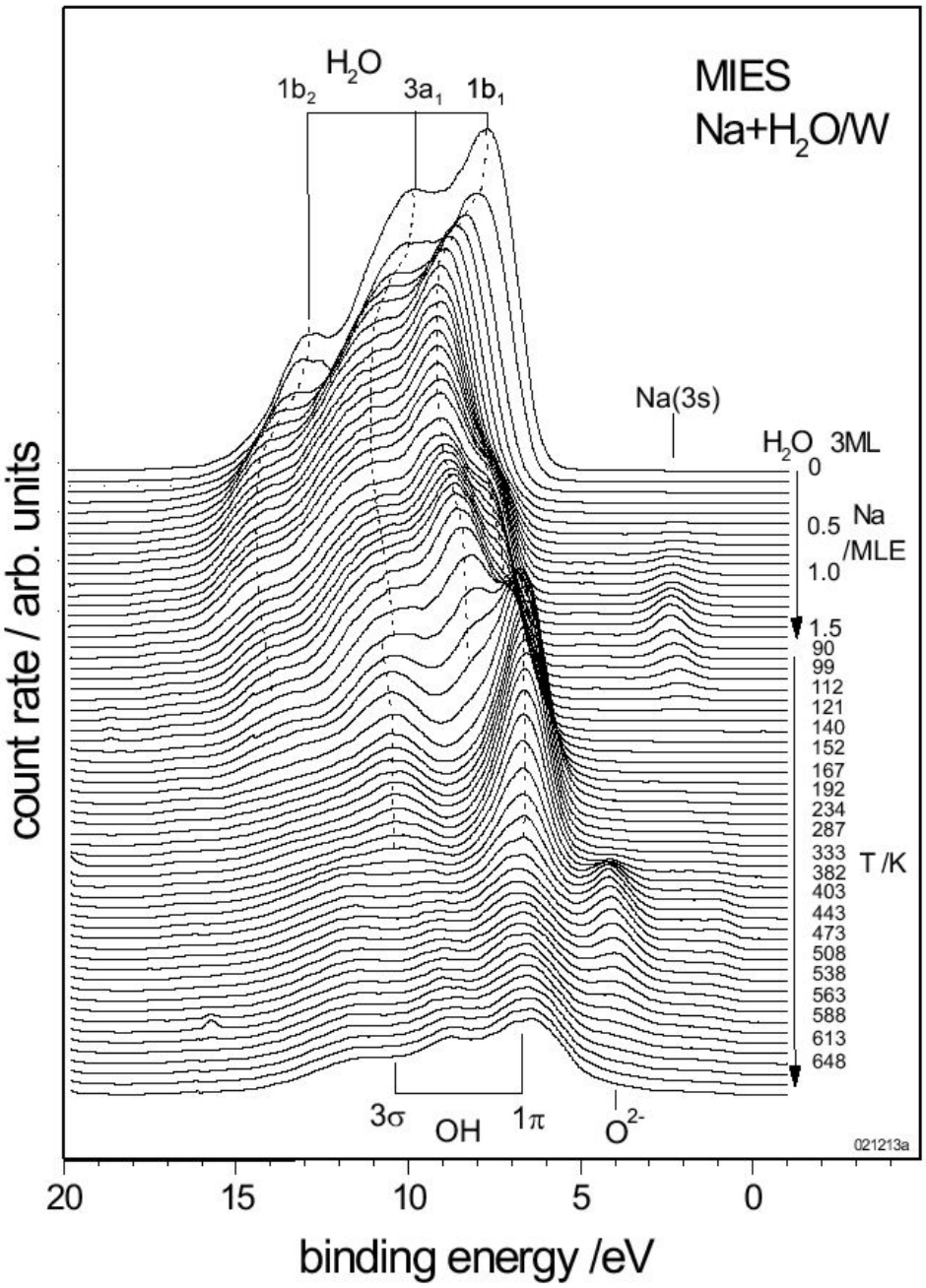

Fig. 1. MIES spectra for the adsorption of Na on solid water (3 layers) prepared on tungsten (90K) (upper set of spectra), and the spectral changes resulting from annealing the Na/H_2O system over the indicated temperature range (lower set of spectra) (see text for the acronyms employed in the figure).

Fig.1 (upper set of spectra) presents the MIES results obtained during Na deposition on a water film (3 bilayers of water) held at 90K. For pure water we see indeed the structures orbitals $1b_1$, $3a_1$, and $1b_2$ from the ionization of the

three highest occupied water MO's (top spectrum). Under Na exposure the spectra remain unchanged initially except for a change of the peak positions simultaneously with the observed Na-induced WF decrease (1eV), and a smearing-out of the water features $1b_1$, $3a_1$, and $1b_2$.

Above 0.5MLE a shoulder emerges at the position where emission from 1π of OH is expected [16, 17]. Accordingly, we have denoted the shoulder by 1π. The contribution expected from the ionization of 3σ of OH at a binding energy larger by 3.7eV [16, 17] is obscured by the emission from $3a_1$. In the same exposure range emission, labeled Na(3s), appears. It resembles closely to the Na-induced emission seen with metals and semiconductors for coverages larger than about 0.5ML. In these cases, the emission is due to the presence of s-charge density at the alkali core, i.e. the Na adsorbate is not fully ionized anymore. We assume that Na(3s) has the same origin. However, the emission is peaked at E_B=2.3eV which is about 1eV larger than on solid surfaces. This binding energy is with respect to E_F. As determined from the onset of the MIES spectra at low kinetic energies, the work function (WF) is 2eV, and thus E_F is located 2eV below the vacuum level. Thus, under the present conditions the 3s-ionization energy is (E_B+WF)eV=4.3eV. Although no Na signature is seen in the early stage of exposure, Na species must become adsorbed/incorporated into the water film as suggested by the decrease of WF and the concomitant shift of the water spectra. Since no 3s-emission is seen, we conclude that no 3s electrons are present at the film surface.

Compared to 130K [3,4], Na(3s) appears already at lower exposures, and, thus, Na penetration into the water film is less likely. In addition, other than at 130K, H_2O and OH features appear simultaneously over the entire studied range of exposures, indicating that the (Na-water) reaction is blocked before the entire film surface is converted into NaOH complexes. The present results are rather similar to the 10K results [3] where little reaction was seen, and the Na species stayed at the surface.

The surface prepared by Na exposure was heated stepwise between 90 and 650K. The results (lower set of spectra in fig.1) support the interpretation given to the feature 1π: the molecular water desorbs at 155K while OH-species can be detected on the surface up to 390K as suggested by the presence of the two peaks 1π and the 3σ at a distance of 3.7eV at positions that agree well with [16, 17]. The 1π shoulder develops smoothly into the peak labeled 1π, suggesting that 1π, seen before the water desorption, is indicative for OH-species from the reaction of Na with water molecules.

When annealing further, the OH-features disappear at 390K. Apart from the tungsten substrate emission, seen between about 5 and 13eV, a prominent peak appears at 4eV; it persists up to 600K. This finding is consistent with OH-decomposition whereby atomic oxygen remains at the surface. The energetic position is characteristic for O_2^- species, stabilized by Na ions.

Na disappears from the surface when heating from 90 to 110K, presumably because the mobility of the water molecules increases which leads to the solvation of Na in the film.

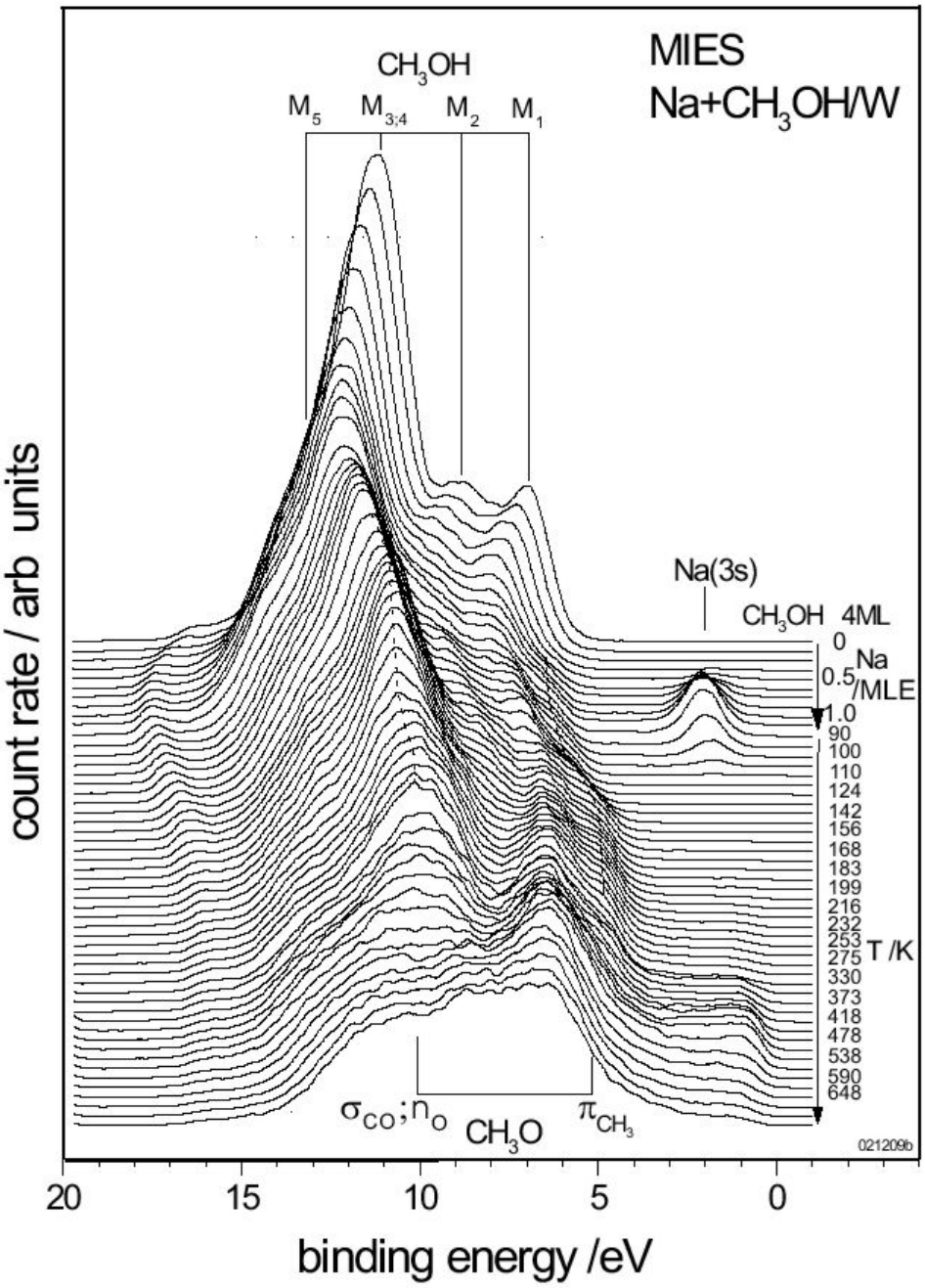

Fig. 2. MIES spectra for the Na-exposed film of solid CH_3OH (4 layers prepared on tungsten (90K) (upper set of spectra), and the spectral changes resulting from annealing the Na/CH_3OH system over the indicated temperature range (lower set of spectra) (see text for the acronyms employed in the figure).

Fig.2 presents MIES results for CH_3OH, obtained in the same manner as described above (fig.1) for water. The tungsten substrate is held at 90K during the film preparation. The top spectrum is for the methanol film (4 layers thick)

prior to Na exposure. The upper set of spectra is obtained during the Na exposure of the film. According to Refs.[2, 19, 20], M1 to M5 $n_{O\perp}$, $n_{O\parallel}$, σ_{CO} ; π_{CO}, and σ_{OH} character, respectively. As a consequence of the exposure to Na M1 to M5 shift to larger E_B's simultaneously with the observed decrease of WF by 1.3eV. In addition, the structure, labeled π_{CH3}, develops. In studies which concentrate on the electronic structure of CH_3OH-ice, we established that π_{CH3} together with σ_{CO}; n_O, overlapping with M3;4, must be attributed to methoxy, CH_3O, species from the dehydrogenation of CH_3OH by Na [21]: the structures π_{CH3} and σ_{CO}; n_O, separated by about 5eV, result from the ionization of the antibonding π-MO's, located at the CH_3-group and the oxygen core π_{CH3} and n_O, and from the σ-MO along the (C-O)-direction. Support for this identification comes from the study of the oxygenation of CH_3OH on a oxygen precovered Cu(111) surface [22]. The structure Na(3s) at E_B=2eV develops as a consequence of the Na-exposure, and can clearly be noticed above 0.4MLE; the WF of the Na-exposed film saturates after a WF decrease of 1eV.

The lower set of spectra in fig.2 was obtained when heating from 90 to 650K. M1 to M5 from CH_3OH disappear when annealing to 165K while the structures attributed to CH_3O, in particular π_{CH3}, persist up to 460K. We attribute the emission seen between 5 and 13eV at higher temperatures to the tungsten substrate. During annealing Na(3s) behaves similar as for water, shifts to smaller E_B's and disappears at 110K. In auxiliary experiments on films prepared at 120K we have established that there is no Na desorption at these temperatures; instead Na penetrates into the CH_3OH film.

4.1.5 Discussion

A qualitative explanation of the observed lowering of the 3sNa ionization energy in aqueous environment has been attempted [4] using Born's model, applied previously to explain photoelectron spectra from liquid water [23]: the Na atom is thought to be surrounded, at least partially, by water molecules. In Born's model this situation is modeled by embedding the Na in a cage formed by the surrounding dielectric medium. This leads to a decrease of the 3s-ionization energy by

$$\delta W = {}^{1}\!\!\diagup\!\!{}_{8\pi\varepsilon_0 r_0}(1 - 1/\varepsilon)$$

where r_0 is the cage radius (about 0.2nm for water [23]) and ε the dielectric constant of water. Using $\varepsilon = 1.5$ [23], one obtains an 1eV reduction of the 3s-ionization energy for the embedded Na atom, in reasonable agreement with experiment [4]. Of course, this naive model gives no hint how to explain the observed Na-induced water dissociation.

The sodium interaction with water ice will now be discussed on the basis of the theory results for sodium hydroxyl formation in water clusters [8]. The key point was to consider the consequences of the hydrolysis of a single Na atom as well as of Na_2 dimers interacting with water clusters. The role of 3s Na electrons solvated by three surrounding water molecules was studied. As a consequence, the 3s-electrons are located very far from their original nuclei. The fundamental role of the electric field generated by the metal atoms inside the water cluster was also pointed out. A major effect of the Na trapping is the strong perturbation of the molecular energy levels distribution, narrowing the DOS bands. The following considerations go beyond ref. [8] in as much as a DOS, suitable for comparison with the MIES spectra, has been generated from the energy levels of the sodium-water clusters considered in ref. [8].

As pointed out in section 3, significant Na(3s) and 1π emission (attributed to the reaction product OH) is not seen below 0.5MLE. This could be indication that this minimum Na concentration is required for the water dissociation to occur. Indeed, the First-Principles calculations carried out on clusters consisting of one and two Na atoms and their water environment [5, 6, 7, 8] suggest that the presence of Na dimers (or even trimers [6]) facilitates the water dissociation.

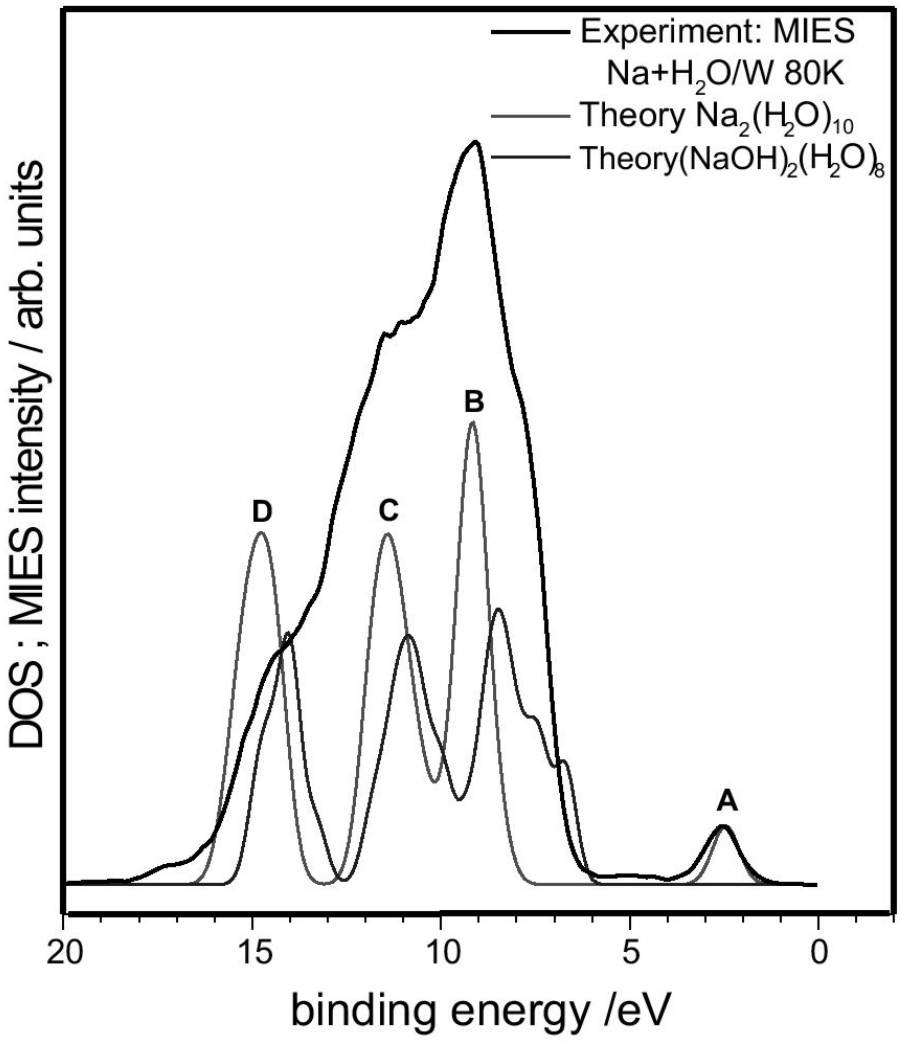

Fig. 3. DOS of the $Na_2(H_2O)_{10}$-cluster defined in the text and comparison with the results of fig.1 (heavy spectrum).

We show now that the MIES spectra and the DFT results for the DOS for two sodium atoms trapped in a $(H_2O)_{10}$ cluster before and after Na_2 hydrolysis are consistent (Fig.3). As suggested by the results of section 4, we suppose in the

following that unreacted, but solvated Na-species (prior to the reaction) and OH-species from the Na-induced hydrolysis are both present at the surface. The DFT-DOS before Na-ionization shows 4 peaks in the 0 to 20 eV window labeled A, B, C and D as in ref.[8]. Peak A corresponds to the solvated electron (denoted by Na(3s) in the MIES spectra). Peaks B and C correspond mainly to the π and σ water lone pairs of electrons involved in OH bonds (denoted $1b_1$ and $3a_1$ in MIES). Peak D (labeled $1b_2$ in MIES) is the antisymmetric OH contribution. B is well reflected in the experimental spectrum. C is also seen in the MIES spectrum, but overlaps with the contribution of the "ionized" system, consisting of Na^+, the solvated electron and the water cluster, since as mentioned before, the MIES DOS is a superposition of "ionized" and "non-ionized" (before the transfer of the solvated electron to nearby protons takes place) species. D is also present in the experimental DOS, but merely as a shoulder.

After hydrolysis, the solvated electron signal disappears from the DFT-DOS. Two shoulders appear in the DFT-DOS corresponding to the shift of the two water LP's combined to the two hydroxyl groups issued from Na_2 ionization; a larger cluster would have produced a broad band analogous to the shoulder in the MIES pattern in the same energy region. The former peaks B, C and D are shifted towards the Fermi level, and the overall combination is well reflected in the experimental curve. The σ hydroxyl OH, located around 25eV, is not displayed in this figure.

From the present experiment it is not possible to determine unambiguously whether the active Na species are single atoms, dimers (as assumed in the present work) or, as proposed in ref.[6], as trimers. Nevertheless, the comparison between theory and experiment appears to be meaningful enough to support the reaction pathway involving Na dimers: in the first step, after film adsorption, Na is trapped inside the cluster. This perturbs strongly the original water DOS in mixing more intimately the lone pair and antisymmetric water OH wave functions. Therefore, the proton tunneling from one water molecule to a

neighbouring one is greatly facilitated. The acceptor molecule releases one of its own protons to another neighbour. This process continues from site to site until the end of the H-bonded chain is reached. This happens at the protons pointing toward the solvated electrons. Such a proton is therefore able to capture one of these electrons producing, in the first step, an H radical atom, and then a H_2 molecule.

When heating beyond 115K Na species disappear from the surface, becoming solvated in the water film. Therefore, a comparison of MIES results and theory is limited to temperatures below 115K.

A few comments are in order concerning the mechanism for the interaction of Na with methanol. The experiment demonstrates that, as for water, delocalization of the 3s-electron takes place, and plays an important role in producing H radical atoms by dehydrogenation of methanol as documented by the formation of CH_3O-species. In analogy to water, we expect that the 3s-electron is trapped between the Na-core and protons of the OH-group of CH3OH molecules surrounding the Na^+ core. A possible reaction path that resembles that of the single Na case discussed in Ref. [8] for the reaction of Na with water, is as follows: the delocalized electron is transferred to one of the protons of the methanol molecules surrounding the Na species. The particular proton that captured the solvated electron is released from its molecule, and leaves CH_3O^- species behind. The Na^+ core and the CH_3O^- species form $(Na^+CH_3O^-)$-complexes. This is in agreement with MIES which simultaneously detects 3sNa, CH_3OH (prior to the reaction), and CH_3O^- species (after the reaction) at the surface.

4.1.6 Conclusions

The present study, employing the Metastable Impact Electron Spectroscopy (MIES), gives insight into the chemistry between Na and water (methanol) ice films held at 80K. It concentrates on the role of the Na3s electron for the reaction between Na and the molecular films. For water the interaction leads to OH-formation which, at 80K, appears to be confined to the film surface mainly. This is in contrast with previous results at 130K film temperature where the reaction involves the entire film. For methanol the reaction products are identified as CH_3O-species. As for water, at 80K the reaction is mainly confined to the film surface. For water the MIES spectra are in good agreement with the density of the states in $Na_2(H_2O)_{10}$ clusters as obtained from First-Principles DFT calculations. In particular, theory and experiment agree well in the energetic position of the 3s electron. Theory predicts that the 3s electron is delocalized from its Na^+ core, and is trapped between the core and surrounding solvent molecules. It is therefore suggested that in both cases, water and methanol, the 3sNa electrons are solvated in the respective molecular surroundings. Calculations and experiment both underline that the delocalized electron triggers the Na-water reaction leading to the formation of NaOH.

On the basis of the available theory results for the Na-water system and the comparison of the experimental results for Na-water and -methanol we propose a scenario for the Na-methanol reaction. As for water, it is initiated by delocalized 3sNa electrons which become transferred to one of the protons of surrounding CH_3OH molecules leading to its dehydrogenation.

4.1.7 References

[1] J. Günster, S. Krischok, J. Stultz, D. W. Goodman: J. Phys. Chem. B 2000, 104, 7977

[2] J. Günster, S. Krischok, V. Kempter, J. Stultz, D. W. Goodman: Surf. Rev. Lett. 2002, 9, 1511

[3] S. Krischok, O. Höfft, J. Günster, R. Souda, V. Kempter: NIM B 2003, 203, 124

[4] S. Krischok, O. Höfft, V. Kempter: Surf. Sci. 2003, 532--535, 370

[5] R. N. Barnett, U. Landman: Phys. Rev. Lett. 1993, 70, 1775

[6] C. J. Mundy, J. Hutter, M. Parinello: J. Am. Chem. Soc. 2000, 122, 4873

[7] T. Tsurusawa, S. Iwata: J. Chem. Phys. 2000, 112, 5705

[8] Y. Ferro, A. Allouche: J. Chem. Phys. 2003 , 118, 10461

[9] P. Stracke, S. Krischok, V. Kempter: Surf. Sci. 2001 , 473, 86

[10] S. Krischok, O. Höfft, J. Günster, J. Stultz, D. W. Goodman, V. Kempter: Surf. Sci. 2001 , 495, 211

[11] Y. Harada, S. Masuda, H. Osaki: Chem. Rev. 1997 , 97, 1897

[12] H. Morgner: Adv. At. Molec. Opt. Phys. 2000 , 42, 387

[13] W. C. Price, in: Electron Spectroscopy: Theory, techniques and applications, Vol. 1 (C.R. Brundle, A.D. Baker, eds., Academic Press, N.Y., 1977) 151

[14] M. Brause, S. Skordas, V. Kempter: Surf. Sci. 2000 , 445, 224

[15] K. P. Stevenson, G. A. Kimmel, Z. Dohnalek, R. S. Smith, B. D. Kay: Science 1999 , 283, 1505

[16] P. A. Thiel, T. E. Madey: Surf. Sci. Rep. 1987 , 7, 211

[17] M. A. Henderson: Surf. Sci. Rep. 2002 , 285, 1

[18] W. Maus--Friedrichs, S. Dieckhoff, M. Wehrhahn, S. Pülm, V. Kempter: Surf. Sci. 271 (1992) 113

[19] K. Kimura et al.: Handbook of HeI Photoelectron Spectra of Fundamental Organic Molecules , Halsted Press, N.Y.

[20] H. Yamakado, M. Yamauchi, S. Hoshino, K. Ohno: J. Phys. Chem. 1995 , 99, 17093

[21] A. Borodin, O. Höfft, S. Krischok, V. Kempter: J. Phys. Chem. 2003 , xxx, in preparation

[22] S. Pöllmann, A. Bauer, C. Ammon, H.--P. Steinrück: Spring Meeting of the DPG, Dresden 2003 , Book of Abstr., p.378

[23] M. Faubel, in: Photoionization and Photodetachment, Part I (World Scientific, Singapore, 2000) 634

4.1.8 Zusammenfassung des Unterkapitels 4.1

Obwohl über die Wechselwirkung von Natrium mit Wasser ziemlich viel bekannt war, war es wirklich interessant, die Reaktion bei tiefer Temperatur zu beobachten. Das System wurde auch von Theoretikern berechnet und die Frage nach der Übereinstimmung der Ergebnisse der Theorie mit dem Experiment, war auch damals aktuell. Außerdem standen Messungen zur Verfügung, die bei 130K durchgeführt wurden. Was ändert sich in dem System bei der Erniedrigung der Temperatur auf 90K?

Die Filme wurden bei 90K auf einem W(100)-Substrat präpariert. Es wurde oberhalb einer 3ML dicken Wasserschicht Natrium aufgebracht. Das Angebot verursacht eine Verschiebung der Spektren zusammen mit der Abnahme der Austrittsarbeit. Ab 0.5MLE Na ist schon der Peak vom Na3s-Elektron zu sehen, die Lage von dem Peak entspricht der vom solvatisierten 3s-Elektron.

Es ist bekannt, dass Natrium mit flüssigem Wasser sofort reagiert. Die Ergebnisse von 130K zeigen dasselbe. Jedoch bei 90K ist nur ein wenig von den Reaktionsprodukten zu bemerken. Eine Struktur von der so entstandenen OH-Gruppe zeichnet sich relativ schwach ab. Viel spricht dafür, dass bei dieser Temperatur Natrium nicht in festes Wasser eindringen kann. Die Reaktion beschränkt sich auf die letzte Lage des Films.

Wird der Film auf T>105K geheizt, reagiert das Natrium; bei 145K wird Wasser desorbiert und bis 390K lässt sich in den Spektren nur OH erkennen.

Es ist schon gesagt, dass ein im AD-Prozess erzeugtes MIES Spektrum mit der theoretisch berechneten Dichteverteilung direkt verglichen werden kann. Von der Theorie wurde ein Wassercluster mit eingekapseltem Natrium in zwei Zuständen berechnet: vor der Reaktion ($Na_2(H_2O)_{10}$) und nach der Wechselwirkung von Natrium mit Wasser ($(NaOH)_2(H_2O)_8$). Der Vergleich zeigt eine gute Übereinstimmung von gemessenen und berechneten Spektren, wenn man davon ausgeht, dass in einem gemessenen Spektrum beide Anteile zu sehen sind.

4.1.9 References

[1] J. Günster, S. Krischok, J. Stultz, D. W. Goodman: J. Phys. Chem. B 2000, 104, 7977

[2] J. Günster, S. Krischok, V. Kempter, J. Stultz, D. W. Goodman: Surf. Rev. Lett. 2002, 9, 1511

[3] S. Krischok, O. Höfft, J. Günster, R. Souda, V. Kempter: NIM B 2003, 203, 124

[4] S. Krischok, O. Höfft, V. Kempter: Surf. Sci. 2003, 532--535, 370

[5] R. N. Barnett, U. Landman: Phys. Rev. Lett. 1993, 70, 1775

[6] C. J. Mundy, J. Hutter, M. Parinello: J. Am. Chem. Soc. 2000, 122, 4873

[7] T. Tsurusawa, S. Iwata: J. Chem. Phys. 2000, 112, 5705

[8] Y. Ferro, A. Allouche: J. Chem. Phys. 2003 , 118, 10461

[9] P. Stracke, S. Krischok, V. Kempter: Surf. Sci. 2001 , 473, 86

[10] S. Krischok, O. Höfft, J. Günster, J. Stultz, D. W. Goodman, V. Kempter: Surf. Sci. 2001 , 495, 211

[11] Y. Harada, S. Masuda, H. Osaki: Chem. Rev. 1997 , 97, 1897

[12] H. Morgner: Adv. At. Molec. Opt. Phys. 2000 , 42, 387

[13] W. C. Price, in: Electron Spectroscopy: Theory, techniques and applications, Vol. 1 (C.R. Brundle, A.D. Baker, eds., Academic Press, N.Y., 1977) 151

[14] M. Brause, S. Skordas, V. Kempter: Surf. Sci. 2000 , 445, 224

[15] K. P. Stevenson, G. A. Kimmel, Z. Dohnalek, R. S. Smith, B. D. Kay: Science 1999 , 283, 1505

[16] P. A. Thiel, T. E. Madey: Surf. Sci. Rep. 1987 , 7, 211

[17] M. A. Henderson: Surf. Sci. Rep. 2002 , 285, 1

[18] W. Maus--Friedrichs, S. Dieckhoff, M. Wehrhahn, S. Pülm, V. Kempter: Surf. Sci. 271 (1992) 113

[19] K. Kimura et al.: Handbook of HeI Photoelectron Spectra of Fundamental Organic Molecules , Halsted Press, N.Y.

[20] H. Yamakado, M. Yamauchi, S. Hoshino, K. Ohno: J. Phys. Chem. 1995 , 99, 17093

[21] A. Borodin, O. Höfft, S. Krischok, V. Kempter: J. Phys. Chem. 2003 , xxx, in preparation

[22] S. Pöllmann, A. Bauer, C. Ammon, H.--P. Steinrück: Spring Meeting of the DPG, Dresden 2003 , Book of Abstr., p.378

[23] M. Faubel, in: Photoionization and Photodetachment, Part I (World Scientific, Singapore, 2000) 634

4.1.10 Zusammenfassung vom Unterkapitel.

Obwohl über die Wechselwirkung von Natrium mit Wasser ziemlich viel gesagt wurde, war es wirklich interessant, die Reaktion bei tiefer Temperatur zu beobachten. Das System wurde auch von Theoretikern berechnet und die Frage nach der Übereinstimmung der Ergebnisse der Theorie mit dem Experiment, war auch damals aktuell. Außerdem standen Messungen zur Verfügung, die bei 130K durchgeführt wurden. Was ändert sich in dem System bei der Erniedrigung der Temperatur auf 90K?

Die Filme wurden bei 90K auf einem W(100)-Substrat präpariert. Es wurde oberhalb einer 3ML dicken Wasserschicht Natrium aufgebracht. Das Angebot verursacht eine Verschiebung der Spektren zusammen mit der Abnahme der Austrittsarbeit. Ab 0.5MLE Na ist schon der Peak vom Na3s-Elektron zu sehen, die Lage von dem Peak entspricht der vom solvatisierten 3s-Elektron.

Es ist bekannt, dass Natrium mit flüssigem Wasser sofort reagiert. Die Ergebnisse von 130K zeigen dasselbe. Jedoch bei 90K ist nur ein wenig von den Reaktionsprodukten zu bemerken. Eine Struktur von der so entstandenen OH-Gruppe zeichnet sich relativ schwach ab. Viel spricht dafür, dass bei dieser Temperatur Natrium nicht in festes Wasser eindringen kann. Die Reaktion beschränkt sich auf die letzte Lage des Films.

Wird der Film geheizt, reagiert erst das Natrium durch; bei 145K wird Wasser desorbiert und bis 390K lässt sich in den Spektren nur OH erkennen.

Es ist schon gesagt, dass ein im AD-Prozess erzeugtens MIES Spektrum mit der theoretisch berechneten Dichteverteilung direkt verglichen werden kann. Von der Theorie wurde ein Wassercluster mit eingekapseltem Natrium in zwei Zuständen berechnet: vor der Reaktion ($Na_2(H_2O)_{10}$) und nach der Wechselwirkung von Natrium mit Wasser ($(NaOH)_2(H_2O)_8$). Der Vergleich zeigt eine gute Übereinstimmung von gemessenen und berechneten Spektren, wenn man davon ausgeht, dass in einem gemessenen Spektrum beide Anteile zu sehen sind.

4.2 Electron Solvation by Polar Molecules: The Interaction of Na Atoms with Solid Methanol Films Studied with MIES and Density Functional Theory Calculations

Electron Solvation by Polar Molecules: The Interaction of Na Atoms with Solid Methanol Films Studied with MIES and Density Functional Theory Calculations, A.Borodin, O. Höfft, U. Kahnert and V. Kempter, Y. Ferro, A. Allouche, Journal of Chemical Physics 120(18): 8692-8697 (2004)

The interaction of Na atoms with CH_3OH films was studied with metastable impact electron spectroscopy (MIES) under UHV conditions. The films were grown at 90(+/-10)K on tungsten substrates, and exposed to Na. Na-induced formation of methoxy (CH_3O) species takes place, and Na-atoms become ionized. At small Na exposures the outermost solvent layer remains largely intact as concluded from the absence of MIES signals caused by the reaction products. However, emission from CH_3O, located at the film surface, occurs at larger exposures. In the same exposure range also Na-species can be detected at the surface. The spectral feature from 3sNa ionization occurs at an energetic position different from that found for metals or semiconductors. The results are compared with DFT calculations (see preceding paper in the same issue [1]). Experiment and theory agree in the energetic positions of the main spectral features from the methanol and sodium ionization. The calculations suggest that the 3sNa emission observed experimentally originates from solvated 3s electrons which are located far from the Na-core and become stabilized by solvent molecules. The simultaneous emergence of emission from CH_3O and from solvated 3s electrons suggests that the delocalization and, consequently, the solvation play an important role in the Na-induced formation of CH_3O from CH_3OH.

4.2.1 Introduction

Although the exothermic reaction of Na atoms with liquid methanol, yielding Na ions and methoxy, CH_3O, species, is well-known, the underlying mechanism for this simple-looking process is not well understood. One particular reason is that it is not easy to obtain direct detailed information on the 3sNa electron which plays an active role in this process. Methoxy species have found considerable interest because of their role in the methanol conversion into dimethyl ether (DME) or formaldehyde which represent important routes to non-pollutant fuel production [2, 3, 4]. It is generally accepted that the first step in the conversion of Methanol To Gasoline (MTG) is the dehydration of CH_3OH to dimethyl ether (DME). Although the MTG process has been studied extensively, few studies exist on low-temperature routes to CH_3OH dehydration.

Methoxy species can be created as a stable intermediate in heterogeneous reactions of methanol on surfaces; they have been characterized by a variety of surface-analytical techniques including photoemission [5, 6, 7, 8, 9, 10]. As an example, the CH_3O species can be formed on copper surfaces by de-protonation of methanol with preadsorbed atomic oxygen [6, 7]. Furthermore, when adsorbed onto Cu(111), partially covered by Na, or onto closely packed Na films, CH_3OH reacts to CH_3O; the species is stable up to 450K [9].

Previously, we have studied the interaction of Na with films of amorphous solid water by combining the Metastable Impact Electron Spectroscopy (MIES) and UPS [11, 12, 13, 14, 15, 16]. As compared to UPS, MIES possesses a rather large sensitivity for the detection of the 3sNa electron; consequently, it allows, in combination with UPS, to distinguish between species located atop and underneath the surface under study. In these studies we have concentrated on the role played by the 3sNa electron for the water dissociation process. First-principles DFT cluster calculations suggest that the 3sNa electron becomes

solvated [17], i.e. is delocalized from its Na^+ core and trapped between the Na^+ and surrounding water molecules. Indeed, by combining MIES with first-principle calculations we arrive at the conclusion that the peculiar structure seen in the spectra near the Fermi level is characteristic for solvated 3sNa electrons [15, 16]. Furthermore, the calculations indicate that the solvated electron plays a key role in the water dissociation reaction. In the present paper we apply MIES to the study of the interaction of Na with films of solid methanol held at T=90 and 120K. By confronting the experimental results with those from DFT cluster calculations (preceding paper [1]), we conclude that the 3sNa becomes solvated and initiates CH_3O formation. The calculations shed light into the underlying mechanism for this process. Two reaction channels were considered: the Na-induced de-hydrogenation of methanol, and the de-hydration of methanol by (C-O) bond breaking. Moreover, the calculations seem to explain the Na-induced dissociation of the CH_3O-H bond reported in ref. [9].

4.2.2 Experimental Remarks

The experiments, described in detail elsewhere [18, 19], were carried out under ultra high vacuum (UHV) conditions (base pressure < $2 \cdot 10^{-10}$Torr). AES and XPS are used to characterize the chemical composition of the tungsten substrate employed for the deposition of the molecular films. With LEED it was checked that the molecular films are amorphous. The electronic structure of the molecular films was studied by applying MIES and UPS(HeI and II). In MIES metastable helium atoms ($2^3S/2^1S$) eject electrons from the edge of the surface under study. The application of MIES to surface spectroscopy is well documented [20, 21]. If the Na adsorbate is not fully ionized, a spectral feature is expected from the presence of 3s-charge density at the Na core. With UPS(HeI) the partially occupied 3s-orbital is practically not seen due to its low photoionization cross section [22]. However, in MIES it causes a prominent feature, Na(3s), close to EF which is clearly seen on metals and semiconductors for coverages larger than about 0.5ML [20, 21]. This underlines the power of MIES for investigating the chemistry between Na and molecular films, which can be expected to be driven by the 3s-valence electron. For the study of the Na-induced changes in the electronic structure of the molecular films we have confined ourselves to MIES because the UPS(HeI and II) spectra give no information on the 3sNa electron.

The primary result of the experiments are energy spectra of the emitted electrons versus their kinetic energy. By choosing a suitable bias voltage between the target and the electron energy analyzer, the energy scales in the figures are adjusted in such a way that electrons emitted from the Fermi level (denoted by E_F), i.e. electrons with the maximal kinetic energy, appear at 19.8eV (which is the potential energy of the metastable He atoms employed for MIES). With this particular choice of the bias voltage, the low-energy cut-off in the spectra gives

directly the surface work function (WF), irrespective of the actual interaction process which produces the electrons. For a convenient comparison with theory we present our data as a function of the binding energy of the emitted electrons prior to their ejection. Electrons emitted from the Fermi level appear then at binding energy E_B =0eV.

Na atoms were dosed employing carefully out gassed commercial dispenser sources (SAES Getters). They operate at a rate of 0.05 ML/min, typically. The procedure for the calibration of the alkali coverage is described elsewhere [23]. The exposure is given in units of monolayer equivalents (MLE); at 1MLE the surface would be covered by one Na monolayer if penetration of the Na into the molecular films could be neglected.

The surface temperature can be varied between about 90 and 700K; at present the accuracy of the temperature calibration is 10K. The surface was exposed to CH_3OH by backfilling the chamber at a substrate temperature of 90K. The amount of surface-adsorbed water can be estimated on the basis of earlier work with MIES on CH_3OH multilayers [11, 19]. Prior to Na exposure the surface prepared as described above was brought to the desired temperature.

4.2.3 Theoretical Considerations

The method of computation was fully exposed in Ref. [17] (see also ref.[1]). A Density Functional Theory (DFT) calculation was carried out at the B3LYP/6-31+g(d,p) level of approximation. This was performed on several cluster models in order to investigate the potential energy surfaces associated to neutral sodium ionization by solvation. The solvation of the sodium atom by methanol has been studied by an analogous strategy [1]. It is demonstrated that Na is solvated by six methanol molecules and that its 3s electron is trapped/solvated between the sodium core and two solvent molecules. This process induces a large mixing of the non-bonding oxygen and OH energy

levels. Two reactive pathways were proposed in the preceding paper, de-hydrogenation by (O-H) bond breaking, and dehydration by (C-O) bond breaking:

i) The de-hydrogenation reaction involves one single methanol molecule, its OH bond breaking and the capture of the solvated 3sNa electron by the ejected proton. The associated activation energy is 56.1 $kJ \cdot mol^{-1}$, uncorrected for the zero point energy.

ii) The de-hydration reaction is associated with the (C-O) methanol bond breaking. The final products are CH_3O, the methyl radical CH_3 and a water molecule. The (C-O) breaking is therefore equivalent to the dehydration process. The corresponding calculated barrier of activation is 62.6 $kJ \cdot mol^{-1}$.

At the present level of approximation, these two reactions are equally probable, not taking into consideration the dynamical and entropic aspects, outside the possibilities of this study. It must be underlined that CH_3O is among the final products of both proposed reactions, but the second one could be the precursor reaction for DME formation because CH_3 radical formation occurs.

It was established previously that the interaction of He^* with clean and Na covered CH_3OH films is via the Auger deexcitation process [12]. This implies that the MIES spectra image the surface density of states (SDOS) directly [20, 21]. The SDOS, needed for the comparison with the MIES spectra, have been obtained by dressing the DFT molecular energy level distributions, obtained in ref. [1], with Lorentzian functions of arbitrary height and an half width of 0.25eV.

4.2.4 Results and Discussion

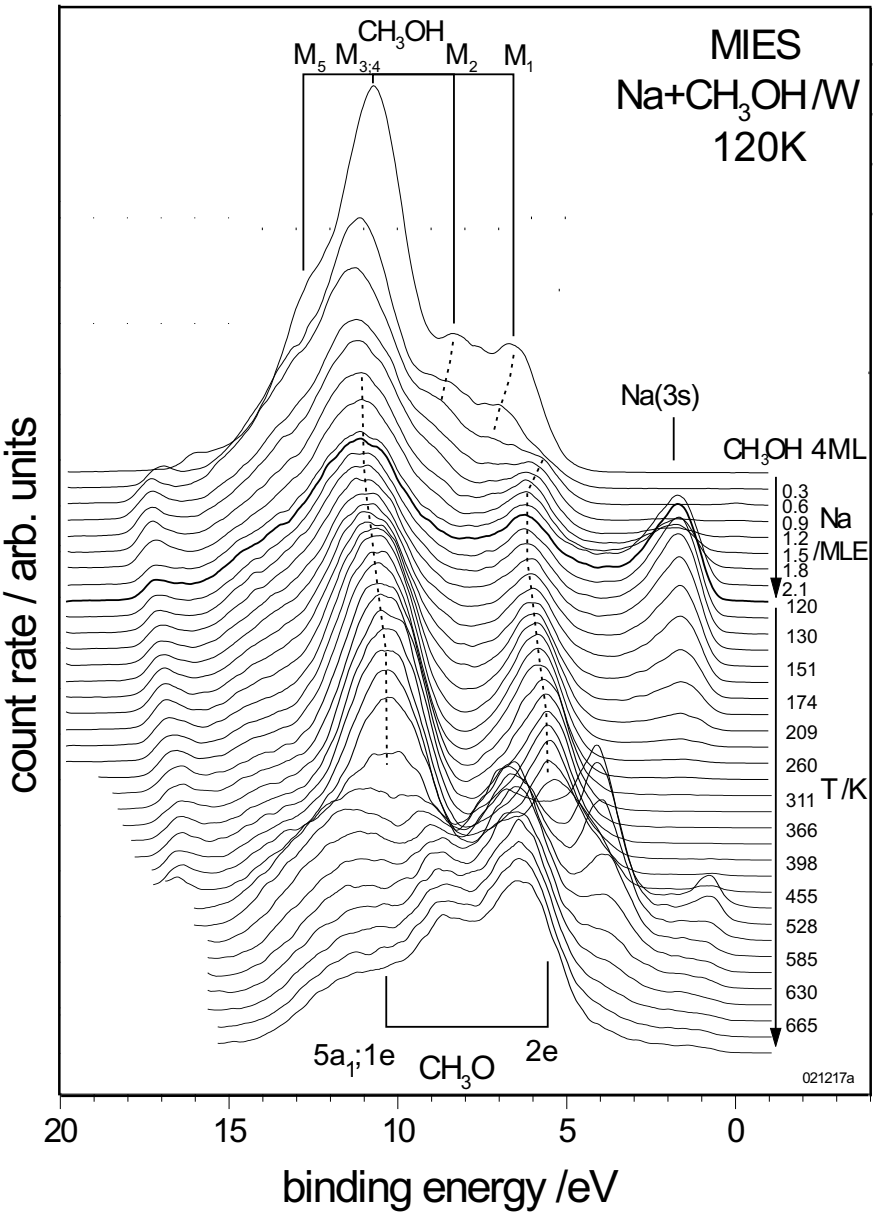

Fig.1: MIES spectra for the adsorption of Na on solid methanol (3 layers) prepared on tungsten (120K) (upper set of spectra), and the spectral changes resulting from annealing over the indicated temperature range (lower set of spectra) (see text for the acronyms employed in the figure).

Fig. 1 presents MIES results for the interaction of Na with a CH_3OH film held at 120K. The top spectrum is for the methanol film (4 layers thick) prior to Na exposure. The upper set of spectra is obtained during the Na exposure of the

film. According to Refs. [12, 24, 25], M1 to M5 have $n_{O\perp}$, $n_{O\parallel}$, σ_{CO} ; π_{CO} , and σ_{OH} character, respectively. During Na exposure M1 to M5 shift to larger E_B 's; simultaneously, a decrease of WF by 1.3eV is noticed. The methanol features M1 to M5 become weaker during the Na exposure and disappear around 0.5MLE. Instead, a two-peaked structure, labeled 2e and $5a_1$;1e, appears. The identification of the species responsible for this structure can be made on the basis of previous photoemission studies and first-principles calculations carried out on surface-adsorbed CH_3O [5, 6, 9]. According to Ref.[9], CH_3O is formed when coadsorbing Na and CH_3OH on Cu(111). The photoelectron spectra attributed to Na-stabilized CH_3O consist of two peaks at (4.6-5.7) and (9.3-10.5)eV binding energy, their exact peak energy depending on the Na precoverage. Based on Hartree-Fock calculations for the MOs of small clusters simulating the Na-bound CH_3O, they can be attributed to the ionization of the 2e and $5a_1$;1e CH_3O MOs, respectively. The contributions from $5a_1$ and 1e cannot be resolved. In Ref. [6] CH_3O species were prepared by first exposing a Cu(111) surface to oxygen and subsequently to methanol. The resulting photoemission spectra show three adsorbate-induced features at E_B =5.3, 9.5, and 15.5eV. The feature at 15.5eV is seen for special geometries only. First-principle calculations indicate that the adsorbate induced features at E_B =5.3 and 9.5eV are due to the ionization of the 2e, $5a_1$;1e MOs of CH_3O species [6]. Again, the contributions from $5a_1$ and 1e cannot be resolved. We note that the formation of a Na-CH_3O complex [9] appears to enlarge the distance between 2e and $5a_1$/1e by about 0.5eV (energy separation 4.7eV) as compared to the interaction with bare copper [6]. The identification of the spectral features made in Ref. [6, 9] is supported by a comparison with the UPS(HeI) spectra for CH_3F (which is isoelectronic with the CH_3O^- anion). Indeed, the photoemission spectra for CH_3F and CH_3O are very similar, both as far as the position and the shape of the spectral features are concerned. In the present work the two Na-induced features from the reaction with CH_3OH appear at E_B=(5.5-6.1) and (10.3-10.8)eV (energy separation

4.7eV). Summarizing, there is ample evidence that Na-CH_3O complexes are the primary result of the interaction of Na with solid methanol at 120K.

The lower set of spectra (heating from 120 to 665K) shows that, as a consequence of the heating, the CH_3O structure becomes more pronounced up to 260K while Na(3s) decreases monotonously and disappears around 260K. This implies that above this temperature no neutral Na species are present at the surface. Around 450K the CH_3O structure disappears. The close agreement of the temperature for the disappearance of the species attributed to CH_3O in Ref. [9] and the present work is further support for our identification of the Na-CH_3OH reaction product as CH_3O species. For CH_3O on Cu, formaldehyde is formed during CH_3O dissociation [7].

However, in the present case the new structure emerging at 450K, consisting of the three peaks at E_B=3.8, 6.5, and 8.5eV, cannot be attributed convincingly to formaldehyde species because the distance between the first two peaks is about 1eV smaller than expected (3.7eV). Moreover, the three peaks display a different temperature dependence. Neither can the observed structure be attributed convincingly to carbon monoxide formation, observed during the thermal composition of CH_3O on Ni(100) [8]. The spectrum reminds to the UPS(HeI) spectrum for Na-W-bronze, Na_xWO_3 with $x > 0.4$, consisting of peaks at E_F, 4, 6.5 and (weakly) 9eV [26]. This would imply that the observed CH_3O dissociation yields atomic oxygen that becomes stabilized at the tungsten surface by the available Na species. The geometric configuration could indeed resemble to that of the Na_xWO_3 surface.

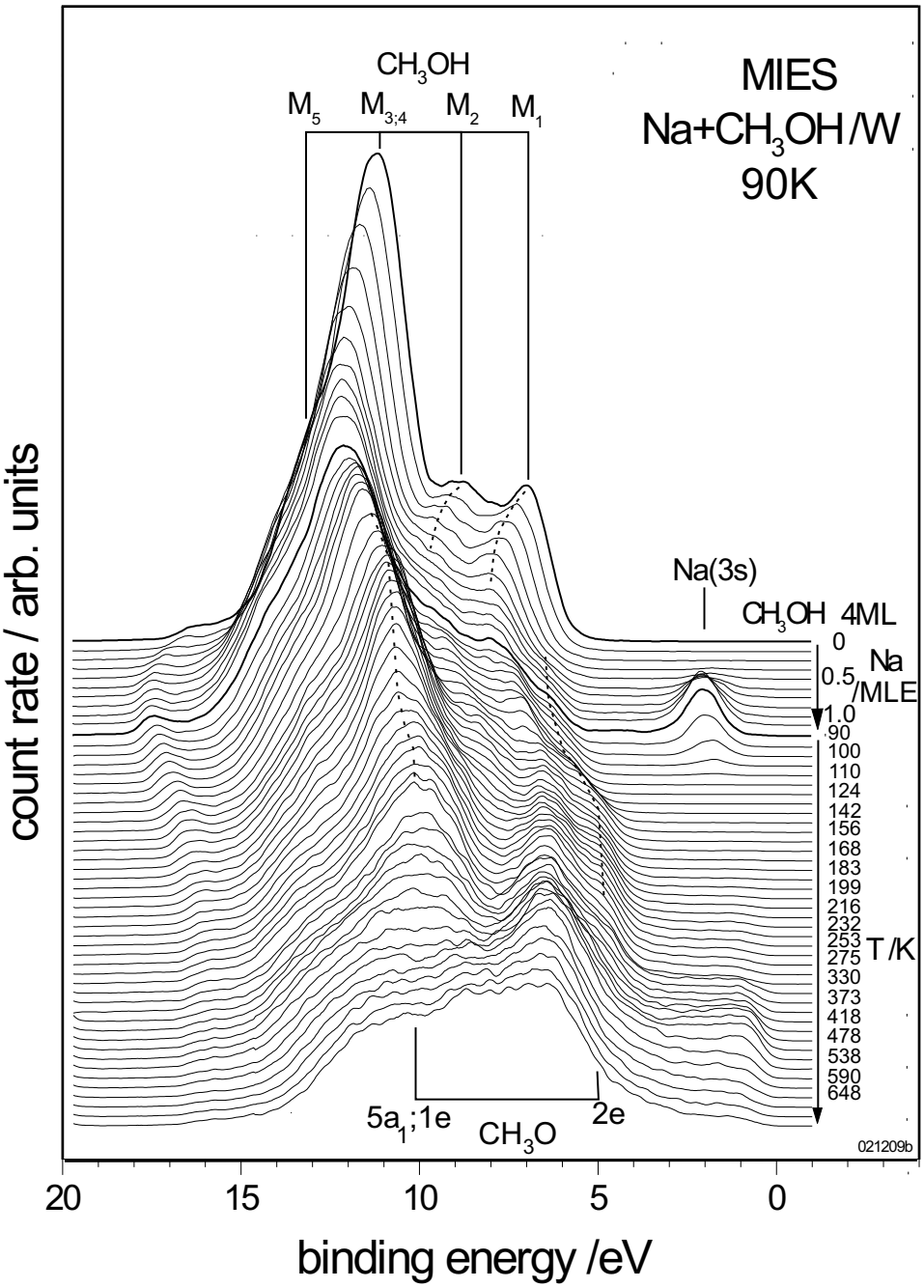

Fig.2: MIES spectra for the Na-exposed film of solid CH_3OH (4 layers prepared ontungsten (90K) (upper set of spectra), and the spectral changes resulting from annealing over the indicated temperature range (lower set of spectra) (see text for the acronyms employed in the figure).

The results obtained for Na deposition on a CH_3OH film held at 90K (Fig.2) differ in some respects: Na(3s) appears considerably more narrow, and, upon heating, disappears already at 110K, instead at 260K for deposition at 120K.

The surface cannot be converted completely into a CH_3O film, because methanol species remain visible throughout the Na exposure. As for the interaction of Na with water ice [14, 15], Na(3s) occurs at about E_B =2.3eV, at about 1eV larger binding energy than on metals, and the reaction product in both cases results from de-hydrogenation of the film molecules.

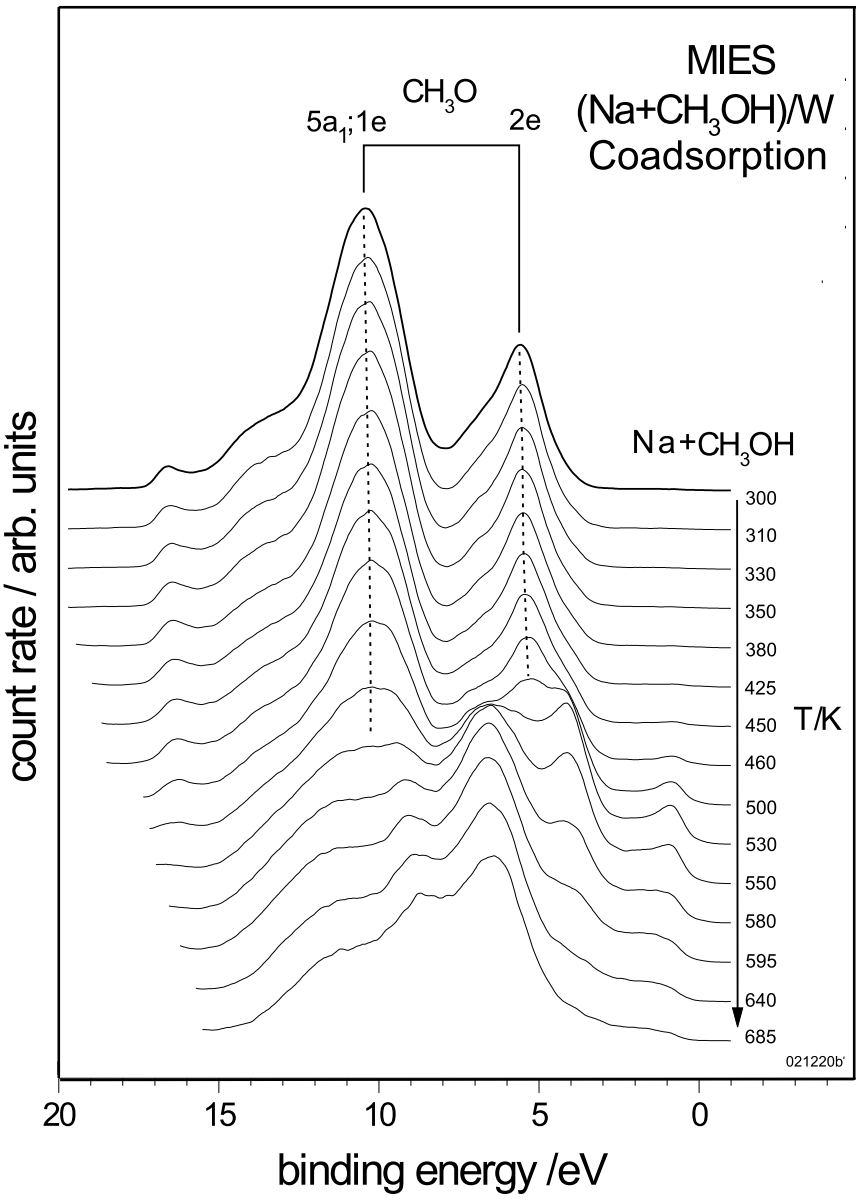

Fig.3: Codeposition of Na and CH_3OH on tungsten held at room temperature (top spectrum), and the spectral changes during annealing over the indicated temperature range (see text for the acronyms employed in the figure).

In order to mimick the interaction of Na with liquid CH_3OH we have co-adsorbed Na and CH_3OH on tungsten at room temperature (Fig.3). An equivalent of 1.5 MLE Na and 6 MLE CH_3OH were offered. As the inspection of fig.1 shows, the resulting spectrum (top spectrum in fig.3) is very similar to the spectra in fig.1 when all surplus CH_3OH species have desorbed (above 260K). Also the change with temperature seen in fig.3 is practically identical with that in fig.1. This suggests that during co-deposition at room temperature Na and CH_3OH indeed react under the formation of (Na-CH_3OH) complexes.

A detailed discussion of the DFT results for the interaction of Na with CH_3OH clusters can be found in the preceding paper [1]. Here, only a short summary will be presented: the 3sNa becomes solvated, both in the $Na(CH_3OH)_6$ and the $Na_2(CH_3OH)_{10}$ clusters modeling Na solvation. As compared to a free Na atom, the ionization energy of 3sNa when solvated in CH_3OH is reduced by 1.62 and 1.0eV, respectively. As fig. 5a and b of ref.[1] show, the corresponding MO is delocalized far from the Na^+ core and is stabilized by CH_3OH molecules; a significant charge fraction is located on the OH bonds pointing towards the solvated electron. In the de-hydrogenation reaction, studied for the $Na(CH_3OH)_6$ cluster, the reaction coordinate is the (O-H) bond distance in the OH-group pointing toward the solvated electron (fig. 5a of ref.[1]). When this distance increases, the proton departs from its original location at the CH_3OH molecule, taking with itself the complete electron spin density. The process under discussion involves only one particular methanol molecule. However, the CH_3OH molecules of the cluster are involved through the H-bonded network. In particular, the amount of energy lost during OH bond breaking is overcompensated by a rearrangement of the H-bonds within the solvent medium. The Na atom acts as provider for the electron required for the electron transfer, and, in addition, contributes to the electrostatic field responsible for electron solvation and the organization of the H-bonded network. The barrier associated with the reaction is $56 kJ \cdot mol^{-1}$.

In the de-hydration reaction, having an activation energy of 63kJ·mol^{-1} , all spin density prior to the reaction is on the Na atom [1]. After passing the reaction barrier, the spin density is at the C-atom only. This implies that the (C-O) bond breaking takes place as (CH^+_3-OH^-) dissociation. The CH^+_3 ion captures the solvated electron, forming $CH_3^{\cdot}$. On the other hand, the OH^- ion captures a proton from a neighboring CH_3OH molecule, thereby producing a H_2O molecule and a CH_3O^- ion.

Obviously, the Na atom acts as donator, while the H-bonded network is responsible for the transfer of energy and charge. As shown in refs.[1, 17], H_2O molecules, being part of the molecular network, undergoes Na-induced hydrolysis when close to a solvated Na species. Therefore, it appears possible that in the final step of the reaction the H_2O molecule from the dehydration of CH_3OH can give OH^- and H.

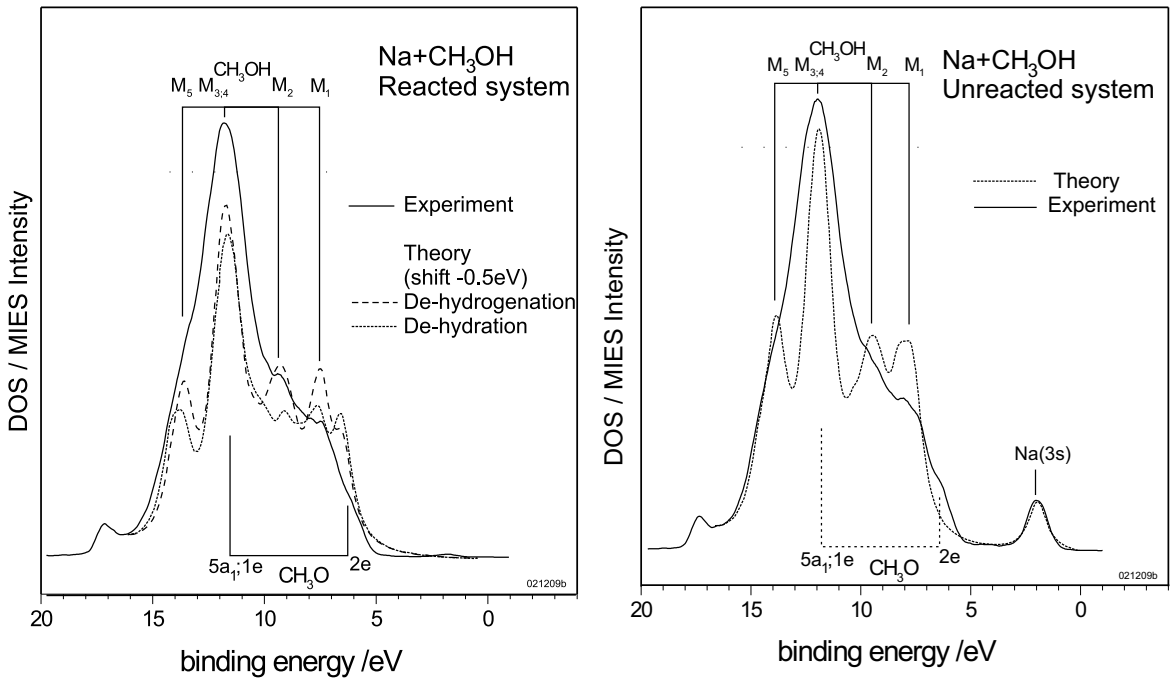

Fig.4: DOS of the Na-methanol-cluster defined in the text and comparison with the MIES results: DFT-DOS for Na-CH_3OH (unreacted system) and MIES results at 90K before heating (fig.2, see text)(a), DFT-DOS for Na-CH_3OH (reacted system) for the de-hydrogenation and dehydration channels (b).

Fig. 4 compares appropriate MIES spectra with the DOS of (a) the Na-CH_3OH cluster prior to the reaction and (b) with that after the de-hydrogenation and de-hydration reactions have taken place. For the comparison shown in fig.4(a) we have assumed that the MIES spectra for about 0.75MLE Na exposure at 90K film temperature, to a first approximation, represent the system prior to the reaction between Na and methanol. This is suggested by the comparatively weak signal from 2e, attributed to CH_3O formation. Thus, we can compare these results with the density of states in the Na-methanol cluster prior to the reaction. If necessary, the DFT-DOS was shifted slightly (0.2eV) in order to align its main peak to the structure M3;4. The good agreement with experiment suggests that signal Na(3s) is due to solvated electrons and not simply caused by surface-adsorbed Na-atoms.

The comparison with the predictions of theory for the reacted system is shown in fig.4(b). It compares the DOS of the reacted Na-$(CH_3OH)_6$ cluster with the spectrum obtained for 0.6MLE Na exposure from fig.1. We choose this spectrum for comparison because the absence of the feature Na(3s) indicates that all Na species take part in the CH3O formation, manifesting themselves in the shoulder 2e. For larger exposures the entire surface layer is converted into CH_3O; this situation cannot be modeled by the present calculations which take into account only well-separated Na atoms or Na_2 dimers. Included in fig.4(b) are the DOS of the eracted systems, after dehydrogenation and dehydration have taken place. The predictions of theory for the reacted system can also be tested by comparison with the results of fig.2, lower set of curves, at temperatures above 110K where Na(3s) has disappeared completely; hereby we suppose that all solvated electrons contribute CH_3O formation. The result of this comparison is very similar to fig.4(b), and therefore is not displayed here. For the de-hydrogenation reaction the DOS is composed from contributions of CH_3O and the surrounding shell of methanol molecules. In particular, CH_3O accounts for the additional peak in the DOS seen around 6.5eV and contributes to the large

peak at 11.4eV. For the de-hydration channel, in addition, the products CH_3 and H_2O give contributions to the DOS; they overlap with those from the CH_3OH network. For both reaction channels good qualitative agreement is obtained with the MIES spectra, in particular as far as the location of the feature 2e is concerned. However, the comparison of MIES and DOS alone does not allow to distinguish in a unique way between the two reaction channels. We can state that, at present, there is no indication for the presence of H_2O (or OH^- after its reaction with Na) which would establish the presence of the de-hydration channel. In the future, TPD will be available to get additional information on the reaction products, CH_3 species in particular.

Theory suggests the following explanation for the different temperature dependence of Na(3s) seen at different film temperatures: at 90K Na stays initially at the surface without reacting with methanol, but becomes solvated which causes the peak at 2.3eV. When heating beyond 110K, the solvated 3s electron starts to react with surrounding methanol species, and, for this reason, Na(3s) disappears. On the other hand, at 120K film temperature all methanol species in the surface layer react readily, provided enough Na is available. Na(3s) appears only after the entire surface layer has been converted into CH_3O. As a consequence of this conversion, Na species cannot be solvated anymore; surplus Na stays at the surface, forming metallic regions, and desorbs above 260K. On the other hand, Na species bound to CH_3O remain at the surface. Even after at 450K the CH_3O features have disappeared, Na species remain at the tungsten probably in a configuration resembling to the surface of Na-W-bronze (see above).

Finally, we discuss the findings of ref.[9]using the results of the present calculations: a thick film of methanol was adsorbed at 100K onto Na-predosed Cu(111) and ashed to 270K (fig.5 of ref.[9]). The UPS spectra obtained after recooling were characteristic for CH_3O. It is evident that, as a consequence of the annealing, only the reaction products, (Na^+-CH_3O)-complexes, remain on the

substrate; unreacted methanol has desorbed around 160K. Considering the chosen preparation conditions, namely Na species which very likely become embedded into their methanol environment during the annealing to 270K, it appears likely that the mechanism proposed by us does also apply: formation of solvated 3sNa electrons, trapped between the Na^+ core and surrounding methanol molecules, takes place and constitutes the first step in the Na/CH_3OH reaction.

In another set of experiments a close-packed Na film was produced at 100K (fig.8 of ref.[9]). Methanol exposure at 100K produced a 2D layer on top of the Na film. UPS spectra were measured at 100K, again after annealing to 270K. Only emission from CH_3O groups was observed. As a consequence of the heating the surface becomes transformed into $(Na\text{-}CH_3O)$-complexes. Hereby, the 3sNa electron becomes solvated, and the reaction scheme proposed in ref. [1], leading to CH_3O formation, can be applied.

4.2.5 Conclusions

The present study, combining the Metastable Impact Electron Spectroscopy (MIES) with DFT cluster calculations, gives insight into the chemistry between Na and films of methanol ice at temperatures between 90 and 120K. It concentrates on the role played by the Na3s electron for the reaction between Na and CH_3OH molecules. The MIES spectra at 90K, i.e. before the Na-induced reaction becomes efficient, are in good agreement with the density of the states of Na-CH_3OH clusters as obtained from the Density Functional Theory (DFT). In particular, theory and experiment agree well in the ionization energy of the 3s electron in the CH_3OH environment. Theory predicts that the 3s electron is delocalized from its Na^+ core, and is trapped between the core and surrounding solvent molecules; this reduces the ionization energy by 1eV as compared to isolated Na species. It is suggested that the 3sNa electrons become solvated by the surrounding molecules. Methoxy (CH_3O) species are identified as products of the Na-induced reaction which takes place with large probability already at 120K. Calculations and experiment both underline that the delocalized 3s electron triggers the formation of CH_3O. Two channels with similar activation energies , both leading to CH_3O formation, namely de-hydrogenation and de-hydration of CH_3OH were considered theoretically. At present, the qualitative agreement of the MIES spectra with the predictions of both channels does not allow to distinguish conclusively between them.

4.2.6 References

[1] Y. Ferro, A. Allouche, and V. Kempter, J. Chem. Phys. xxx, xxxx (2003)

[2] S.R. Blaskowski and R.A. van Santen, J. Am. Chem. Soc. 118, 5152 (1996)

[3] S. Ruf, A. May, and G. Emig, Appl. Cat. A213, 203 (2001)

[4] Wei Wang, M. Seiler, and M. Hunger, J. Phys. Chem. B 105, 12553 (2001)

[5] P. Hofmann and D. Menzel, Surf. Sci. 191, 353 (1987)

[6] M. Witko, K. Hermann, D. Ricken, W. Stenzel, H. Conrad, and A.M. Bradshaw, Chem. Phys. 177, 363 (1993)

[7] C. Ammon, A. Bayer, G. Held, B. Richter, Th. Schmidt, and H.-P. Steinr. uck, Surf. Sci. 507-10, 845 (2002)

[8] R. Neubauer, C.M. Whelan, R. Denecke, and H.-P. Steinr. uck, Surf. Sci. 507-10, 832 (2002)

[9] J.Paul, Surf. Sci. 160, 599 (1985)

[10] M.A. Henderson, S. Otero-Tapia, and M.E. Castro, Faraday Disc. 114, 313 (1999)

[11] J. Günster, S. Krischok, J. Stultz, and D. W.Goodman, J. Phys. Chem. B 104, 7977 (2000)

[12] J. Güunster, S. Krischok, V. Kempter, J. Stultz, and D. W. Goodman, Surf. Rev. Lett. 9, 1511 (2002)

[13] S. Krischok, O. Höfft, J. Günster, R. Souda, and V. Kempter, NIM B 203, 124 (2003)

[14] S. Krischok, O. Höfft, and V. Kempter, Surf. Sci. 532-535, 370 (2003)

[15] A. Borodin, O. Höfft, U. Kahnert, V. Kempter, and A. Allouche, Phys. Surf. Eng. 1, (2003) 146

[16] A. Borodin, O. Höfft, U. Kahnert, V. Kempter, and A. Allouche, Vacuum xx, in print

[17] Y. Ferro and A. Allouche, J. Chem. Phys. 118, 10461 (2003)

[18] P. Stracke, S. Krischok, and V. Kempter, Surf. Sci. 473, 86 (2001)

[19] S. Krischok, O. Höfft, J. Günster, J. Stultz, D. W. Goodman, and V. Kempter, Surf. Sci. 495, 211 (2001)

[20] Y. Harada, S. Masuda, and H. Osaki, Chem. Rev. 97, 1897 (1997)

[21] H. Morgner, Adv. At. Molec. Opt. Phys. 2000, 42, 387

[22] W. C. Price, in Electron Spectroscopy: Theory, techniques and applications, edited by C.R. Brundle, A.D. Baker (Academic Press, New York, 1977), Vol. 1, p. 151

[23] M. Brause, S. Skordas and V. Kempter, Surf. Sci. 445, 224 (2000)

[24] K. Kimura et al., Handbook of HeI Photoelectron Spectra of Fundamental Organic Molecules, (Halsted Press, New York, 1990)

[25] H. Yamakado, M. Yamauchi, S. Hoshino, and K. Ohno, J. Phys. Chem. 99, 17093 (1995)

[26] R.G. Egdell, H. Innes, and M.D. Hill, Surf. Sci. 149, 33, 1985

4.2.7 Zusammenfassung des Unterkapitels 4.2

Es ist bekannt, dass zwischen Methanol und Natrium bei normalen Bedingungen eine exoterme Reaktion abläuft. Als Hauptprodukt der Reaktion entsteht dabei Methoxy (CH_3O), dessen Produktion kann als erster Schritt für die Herstellung eines ökologisch sauberen Kraftstoffes betrachtet werden. Die Umwandlung von Methanol zu Methoxy kann in dünnen Filmen erforscht werden. Die dabei ablaufenden Prozesse sind bereits mehrmals mit verschiedenen Methoden wie z.B. UPS untersucht worden.

Die Ergebnisse dieser Arbeit wurden mit MIES als Haupttechnik erzielt; im Gegensatz zu UPS liefert MIES eine ausführliche Information über die Oberfläche und Prozesse darin, und, was in den Experimenten besonders wichtig ist, erlaubt MIES, das 3s-Elektron gut zu beobachten. Die Rolle von dem Elektron scheint entscheidend für mehrere Reaktionen mit Na zu sein. Folgende Fragen waren zu untersuchen: 1) Die Untersuchung der Wechselwirkung von Natrium mit Methanol bei tiefer Temperatur (90K) und während weiteren Heizens; 2) Die Untersuchung der Rolle des 3s-Elektrons von Natrium bei der Reaktion.

Um die Spektren korrekt zu interpretieren, wurden die Ergebnisse von den DFT-Rechnungen des Systems herangezogen. Ein direkter Vergleich eines MIES-Spektrums mit einem gerechneten ist immer möglich, und so kann man feststellen, wofür der eine oder andere Anteil des gemessenen Spektrums verantwortlich ist.

Die Experimente wurden auf einem W(110)-Substrat durchgeführt. Der Film mit den in verschiedener Reihenfolge angebotenen Natrium und Methanol wurde bei unterschiedlichen Temperaturen (90, 120, 300K) präpariert. Nach der Präparation kam das Heizen.

Die Strukturen in den Spektren lassen die untersuchten Spezies erkennen:

Methanol – vier Peaks bei 6.7, 8.5, 11.0, 12.9eV, die während des Na-Angebots um bis zu 1eV verschoben sein können;

Methoxy – zwei Peaks bei 5.5-6.1 und 10.3-10.8eV (Energiedifferenz 4.7eV);

Natrium – eine Struktur vom 3s-Elektron an der Fermikante. Das 3s-Elektron von Natrium in einem Na-Cluster gibt einen relativ breiten Peak bei 1eV. Wird das 3s-Elektron vom Na-Atom delokalisiert und solvatisiert, so ergibt sich ein Peak bei 2eV und keine Emission an der Fermikante.

Über die Ergebnisse lässt sich das Folgende sagen:

1) Beim Angebot von Natrium bei 120K auf den 4ML-dicken Methanolfilm wird unter dem Na-Einfluss Methanol zu Methoxy umgewandelt. Bis zu 1ML lässt sich Na nicht beobachten; nur die von Na verursachte Verschiebung der Austrittsarbeit ist zu bemerken. Es ist zu vermuten, dass das ganze Natrium für das Entstehen des Methoxy verbraucht wird. Wird das ganze Methanol in Spektren durch Methoxy ersetzt, taucht ein Peak bei 2eV von Natrium auf. Der gehört zum solvatisierten 3s-Elektron. Bei weiterem Na-Angebot wird die Methoxy-Struktur abgeschwächt und der Na-Peak entwickelt sich weiter zur Struktur vom Na-Film: Es gibt ein normales Schichtwachstum von Na oberhalb der Methoxyschicht. Beim Heizen desorbiert erst (170K) der restliche (nichtreagierte) Anteil von Methanol. Oberhalb 160K gibt es kein neutrales Natrium mehr bzw. es ist keine Struktur davon zu sehen. Ab 450K desorbiert Methoxy.
2) Wenn der Film bei 90K präpariert wird, reagiert Methanol mit Natrium nicht vollständig. Neben der Struktur von Methoxy ist bis zu 170K auch die von Methanol zu sehen. Der weitere Verlauf sieht aus wie von der oben beschriebenen Messung.
3) Eine Koadsorption von Na mit Methanol bei Raumtemperatur zeigt nur Methoxy.

Die Theorie beschreibt zwei mögliche Wege für die Reaktion zwischen Methanol und Natrium: Deprotonation und Dehydratation.

1) Beim ersten Prozeß wird durch die Wechselwirkung von Methanol mit einem delokalisiertem 3s-Elektron ein Proton von einem Methanolmolekül abgezogen. Dabei nimmt das Proton die komplette Elektrondichte von 3s mit. So entsteht CH_3O – Methoxy.
2) Bei der Dehydration handelt es sich um die Dissoziation des Methanolmoleküls durch den Bruch der CH_3^+–OH^- Bindung. Vor dem Bruch lokalisiert die ganze Elektrondichte vom Na3s am C-Atom, dann kann OH^- abgespalten werden. Das OH^- kann von einem anderen CH_3OH-Molekül ein Proton übernehmen; so wird ein CH_3O^- und ein Wasser-Molekül gebildet.

Welcher von den Prozessen in Wirklichkeit stattfindet, ist mit den genutzten Messmethoden nicht zu erkennen. Die Rechnungen geben fast gleiche Wahrscheinlichkeiten für die Prozesse (56 zu 63kJ·mol^{-1}), und die Spektren der durchreagierten Schichten unterscheiden sich sehr wenig. Es ist zu vermuten, dass weitere Experimente mit TPD die Frage klären können.

4.3 Electron Delocalization by Polar Molecules: Interaction of Na Atoms with Solid Ammonia Films Studied with MIES and Density Functional Theory

Electron Delocalization by Polar Molecules: Interaction of Na Atoms with Solid Ammonia Films Studied with MIES and Density Functional Theory, A.Borodin, O. Höfft, V. Kempter, and Y. Ferro, A. Allouche, Journal of Chemical Physics 120(18): 8692-8697 (2004)

The interaction of Na and NH_3 on tungsten was studied with metastable impact electron spectroscopy (MIES) under UHV conditions. NH_3-(Na) films were grown at 90(+/-10)K on tungsten substrates and exposed to Na(NH_3). No Na-induced reaction involving NH_3 takes place. At small Na exposures a Na-induced shift of the NH_3 spectral features is seen, in parallel with a decrease of the surface work function. At larger exposures three 3sNa-related spectral structures are seen, two of them at energetic positions different from that found for Na on metals or semiconductors. The main additional peak is attributed to delocalized Na species. A small additional feature is attributed to simultaneous ionization and excitation of partially ammoniated Na_2 species. The results are compared with DFT calculations which suggest that the 3sNa emission at small exposures appears to originate mainly from delocalized 3sNa electrons; they are located far from the Na-species and become stabilized by solvent molecules. When depositing NH_3 molecules onto Na films, metallic-like Na patches and delocalized Na species coexist. The delocalization of 3sNa is seen up to T=130K where the NH_3 species desorb.

4.3.1 Introduction

Electron solvation during the interaction of Na with liquid ammonia is well established. However, despite of many efforts, the structure and the localization mode of the solvated electrons is still subject of intense discussions. One particular reason is that it is not easy to obtain direct detailed information on the 3sNa electron which plays an active role in this process. Recently, the study of solvated electrons in finite clusters has furnished information on the microscopic aspects of the solvated states. Neutral and negatively charged hydrated and ammoniated Na clusters were prepared by the capture of low-energy electrons. The properties of ammoniated Na monomer and dimer clusters have been studied, as a function of cluster size, by photoelectron, photoion and related spectroscopies as well as by first-principles Density Functional Theory (DFT) [1, 2, 3, 4, 5].

Another promising approach appears to be the study of the interaction of Na species with solid molecular films [6, 7]. Previously, we have studied the interaction of Na with films of solid water and methanol by combining Metastable Impact Electron Spectroscopy (MIES) and UPS [6, 8, 9, 10, 11, 12]. As compared to UPS, MIES possesses a rather large sensitivity for the detection of the 3sNa electron, and its pronounced surface sensitivity allows, in combination with UPS, to distinguish between species adsorbed atop and underneath the surface under study. These studies concentrated on the role played by the 3sNa electron for the Na-induced water dissociation and methoxy formation. First-principles DFT calculations on Na-water clusters suggest that the 3sNa electron becomes delocalized from its Na^+ core and is trapped between the Na^+ (and eventually Na^+_2) species and surrounding water molecules [13]. A peculiar structure seen in the MIES spectra near the Fermi level appears to be characteristic for delocalized 3sNa electrons [7, 11]. The extension of this work

to Na-ammonia and methanol clusters [14] indicated that the delocalized electrons play a key role in the de-protonation of water and methanol.

In the present paper we apply MIES to the study of the interaction of Na and ammonia on a cold tungsten substrate. By combining the experimental results with the above-mentioned DFT calculations [14], we conclude that the 3sNa electrons become delocalized. The combined results from theory and experiment shed light into the underlying mechanism for this process. It is suggested that Na_2 dimers are involved in the solvation process.

4.3.2 Theoretical Details and Results

The method of computation was fully exposed and applied to the solvation of the sodium atom by water in Refs.[13, 14]. The solvation of Na by ammonia and methanol has been studied by an analogous strategy and compared with hydration [14]. Briefly, DFT calculations were carried out at the B3LYP/6-31+g(d,p) level of approximation. This was performed on several cluster models in order to investigate the potential energy surfaces associated to neutral sodium ionization by solvation. Two models were considered: solvation of a single sodium atom or of a sodium dimer. In both cases we tried to embed the sodium into the solvent cluster as completely as possible. The DFT functional, the orbital basis set and all the computational ingredients can be found in Ref.[13].

It was established by the comparison of the MIES with UPS spectra that the interaction of He* with clean and Na covered ammonia films is via the Auger de-excitation process [6]. This implies that the MIES spectra image the surface density of states (SDOS) directly [15, 16]. The SDOS, needed for the comparison with the MIES spectra, have been obtained by dressing the DFT molecular energy level distributions with Lorentzian functions of arbitrary height and an half width of 0.25eV.

In the case of monomer solvation, a $Na(NH_3)_6$ cluster was treated (see fig.1(a) of ref. [14]. The ammonia molecules organize themselves in two layers: (i) In the first layer, the nitrogen atoms are located at nearly equal distances from Na (between 2.464 and 2.539A). All the N-H bonds point toward the outside of the cluster and no hydrogen bond is established between the solvent molecules. (ii) The sixth ammonia has been introduced in the model in an attempt to surround the Na atom more completely. This "extra" molecule bonds to the first solvent layer by a hydrogen bond.

For $Na_2(NH_3)_{11}$ the metal dimer was embedded, as completely as possible, into the solvent cluster (see fig.1(b) of ref. [14]. Eleven NH_3 solvent molecules were required for this purpose. The whole system consists of two subsystems, each one centered in the vicinity of the two alkali atoms found at a distance of 3.95A from each other. In the larger subsystem, the Na is at distances of about 2.5A from its closer NH_3 neighbors. This ensemble is surrounded by a second shell of NH_3 molecules that interact via H-bonds. The other Na is bonded to a single ammonia. As in the hydration case, a tendency is found for the second alkali to remain at the "surface" of the cluster. The DOS from the cluster DFT calculations for a pure $(NH_3)_{10}$ cluster and the solvated cases $Na(NH_3)_6$ and $Na_2(NH_3)_{11}$ will be compared with the MIES spectra for Na adsorbed on NH_3 films (fig.4).

4.3.3 Experimental Details and Results

The apparatus and the experimental procedures are described in detail elsewhere [11, 17, 18]. The electronic structure of the molecular films produced on a tungsten substrate was studied by applying MIES and UPS(HeI and II). In MIES metastable helium atoms ($2^3S/2^1S$) eject electrons from the edge of the surface under study. The application of MIES to surface spectroscopy, and its combination with UPS(HeI and II) is well documented [15, 16].

The primary result of the experiments are energy spectra of the emitted electrons versus their kinetic energy. By choosing a suitable bias voltage between the target and the electron energy analyzer, the energy scales in the figures are adjusted in such a way that electrons emitted from the Fermi level, denoted by E_F, i.e. electrons with the maximal kinetic energy, appear at 19.8eV (which is the potential energy of the metastable He atoms employed for MIES). With this particular choice of the bias voltage, the low-energy cut-off in the spectra gives directly the surface work function (WF), irrespective of the actual interaction process which produces the electrons. For a convenient comparison with theory we present our data as a function of the binding energy of the emitted electrons prior to their ejection. Electrons emitted from the Fermi level, i.e. those with the 19.8eV kinetic energy, appear at binding energy E_B=0eV with respect to the Fermi level. The surface temperature can be varied between about 90 and 700K; at present the accuracy of the temperature calibration is 10K. The surface was exposed to NH3 by backfilling the chamber at a substrate temperature of 90K. The Na exposure is given in units of monolayer equivalents (MLE); at 1MLE the surface would be covered by one Na monolayer if penetration of the Na into the molecular films could be neglected. The amount of surface-adsorbed ammonia can be estimated from the variation of the tungsten substrate intensity at the Fermi edge in the UPS(HeI and II) spectra. If the Na adsorbate is not fully ionized, a strong spectral feature from the presence of 3s-charge density at the Na core is seen with MIES, but not UPS. For the study of the Na-induced changes in the electronic structure of the molecular films we have therefore confined ourselves in reporting the MIES results.

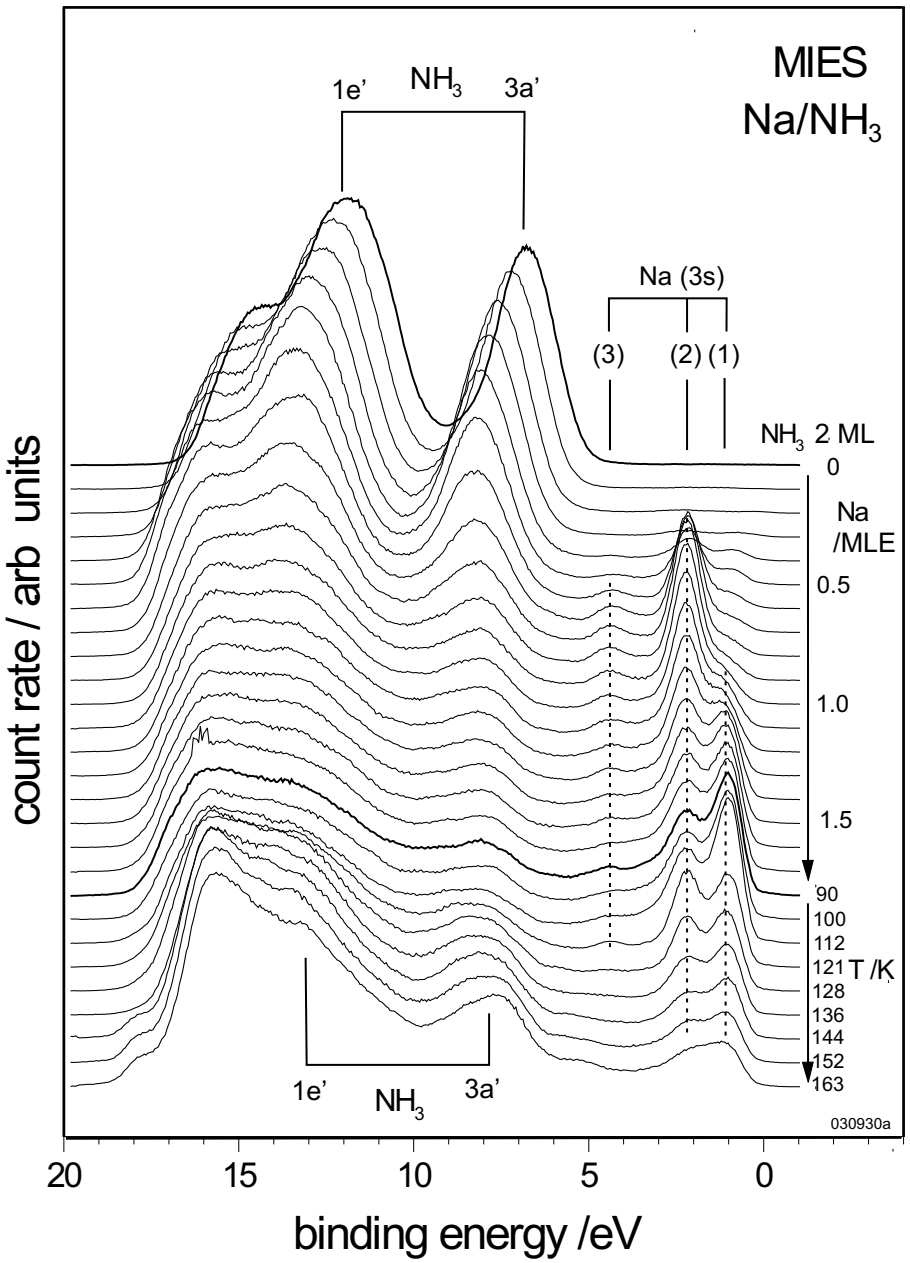

Fig.1: MIES spectra for the adsorption of Na on solid NH_3 (3 layers) prepared on tungsten (90K) (upper set of spectra), and the spectral changes resulting from annealing in the indicated temperature range (lower set of spectra) (see text for the acronyms employed in the figure).

Fig.1 presents MIES results for the interaction of Na with a NH_3 film held at 90K. The top spectrum is for the ammonia film (2 layers thick) prior to Na exposure. The upper set of spectra is obtained during the Na exposure. The lower set of spectra displays the spectral changes observed during film

annealing in the indicated temperature range. According to Ref.[19] the two broad features observed at E_B=6.5; 11.3eV in the MIES spectra of the ammonia film are due to the ionization of the 3a'(n_N) and 1e'($\pi(NH_2)$), respectively. A shift of these features takes place, correlated with the Na-induced decrease of WF. With increasing Na exposure three Na-induced structures (1) to (3) appear, located at 1.3, 2.3, and 4.5eV with respect to the Fermi level (E_B=0eV). At low exposures we attribute (1), by comparison with the corresponding feature for Na adsorption on metals and semiconductors, to 3sNa ionization from neutral isolated Na atoms; at larger exposures (1) comes from patches with metallic-like properties. By comparison with the interaction of Na with water and methanol ices [7, 10, 11], we attribute (2) (at 2.3eV) to delocalized electrons (see fig.4 for a comparison with theory). When heating from 90K to 163K 3a' NH_3, (2) and (3), but not (1), pass through maxima around 120K, and finally decay with temperature (for details see fig.2). According to MIES, NH_3 has practically sublimated from bare tungsten at 130K; it is obvious from fig.1 that, due to its interaction with Na, sublimation is delayed by at least 30K.

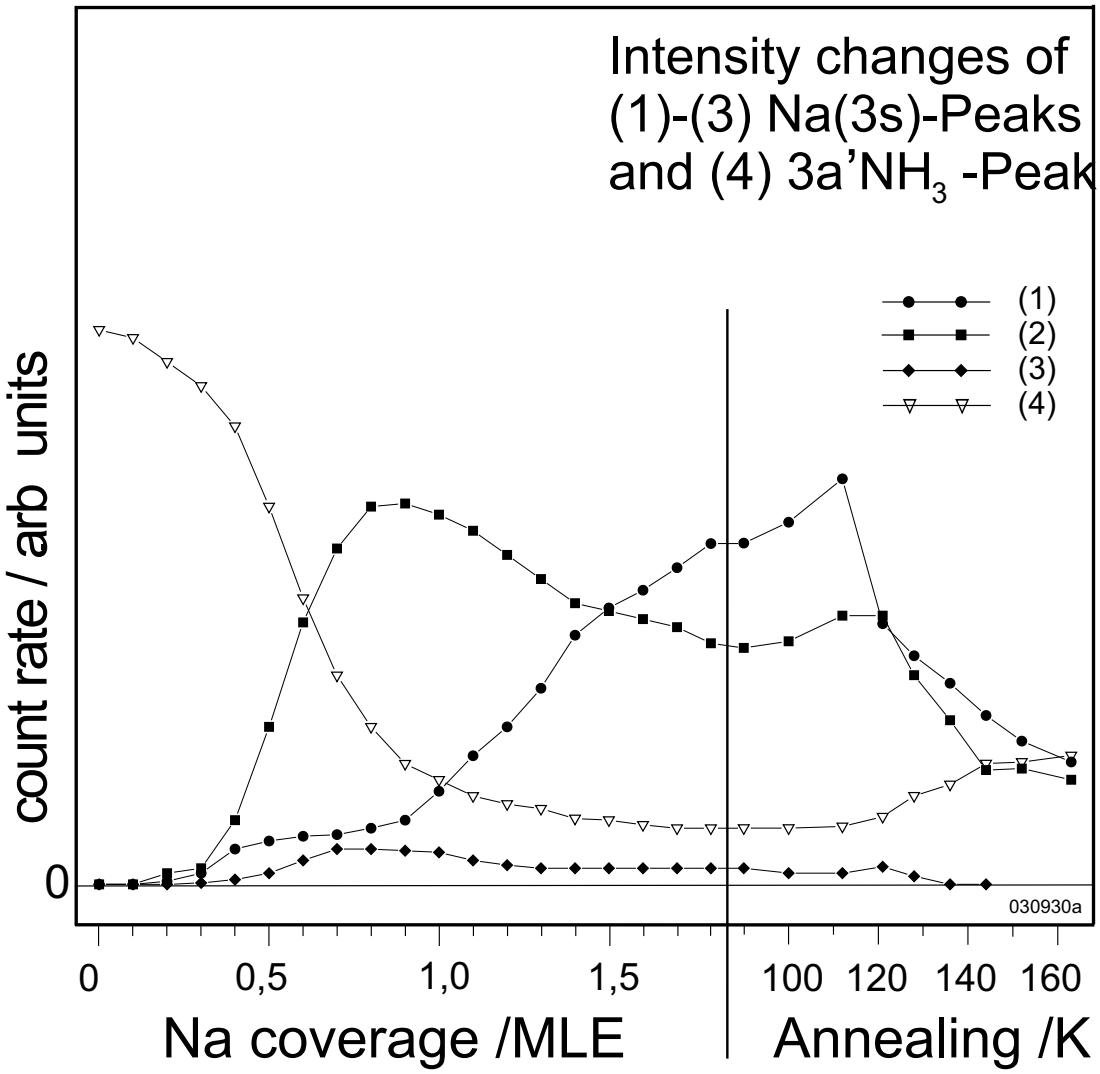

Fig.2: Intensities of the Na-induced peaks (1) to (3) (localized and solvated 3sNa, and the satellite of (2), respect.) and of 3a'NH_3 (4) versus the Na exposure and during the heating of the Na/NH_3 system (data from fig.1).

Fig.2 displays the exposure dependence of the intensities of the Na-induced peaks (1) to (3), seen between E_B=0 and 5eV, and of 3a' NH_3 (curve (4))(data from fig.1). Peaks (1) to (3) become sizeable around 0.3MLE whereby (2) and (3) display a similar exposure dependence, suggesting that the emission has a common origin. In the following (3) is considered as a satellite of (2) (see section 3.3). A clear correlation appears to exist between the three Na-induced

signals and 3a' NH_3 (peak (4)): when (2) saturates, (4) has essentially decayed. On the other hand, (1) rises after (2) and (3) have levelled off, and (4) has decayed. Also included is the change of the signals intensities upon heating. All Na-induced signals display a sharp break around 120K, close to the temperature where thermal desorption of ammonia films takes place (125K)[20].

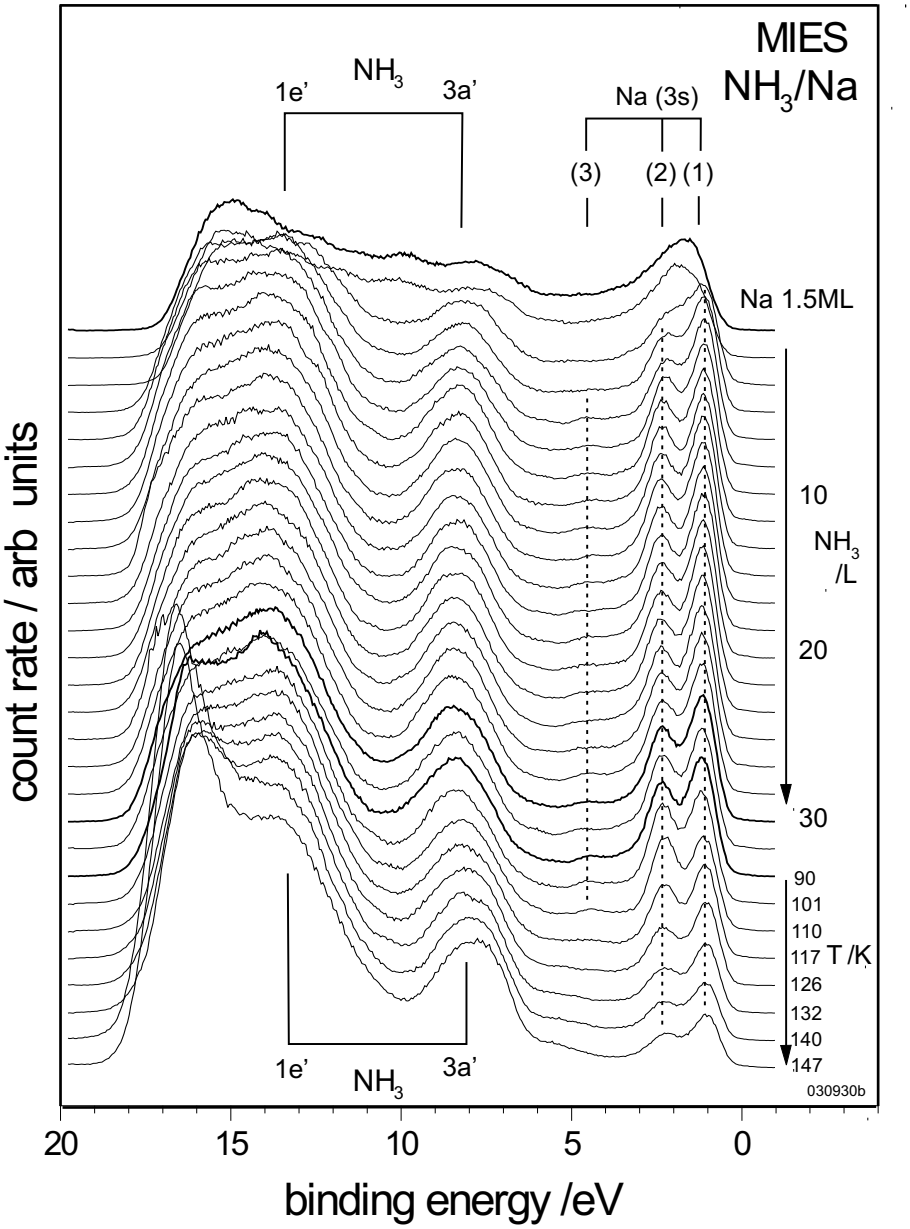

Fig.3: MIES spectra for the Na film (2 layers prepared on tungsten (90K) (upper set of spectra) exposed to NH_3 molecules, and the spectral changes resulting from annealing over the indicated temperature range (lower set of spectra) (see text for the acronyms employed in the figure).

Fig.3 presents MIES results for NH_3 molecules interacting with a Na film held at 90K. The top spectrum is for the Na film (saturation coverage at 90K; 1ML minimum) prior to NH_3 exposure. The upper set of spectra is for NH_3 exposure at 90K. The lower set of spectra displays the spectral changes observed during film annealing in the indicated temperature range. As a consequence of the exposure, the NH_3 structures 3a' and 1e' appear at E_B=7.8 and 13.2eV, respectively. Initially, the 3sNa electron in metallic environment manifests itself by the comparatively broad structure just below EF which is known to be due to the Auger de-excitation process involving the 3sNa electrons. Following ammonia exposure, a peak appears at 1.3eV which, as for the clean Na film, is due to the interaction of the He* probe atom with the 3sNa electron; however, because the surface work function has reduced 0.5eV to below 2eV, it is now mainly due to autodetachment of He* temporary negative ions formed by the resonant capture of a 3s electron by the probe atom [15, 16].

Peak (2) (2.3eV), appearing together with his satellite (3), is again attributed to ammoniated Na; the structures attributed to the delocalized species weaken as a consequence of film annealing.

4.3.4 Interpretation and Discussion

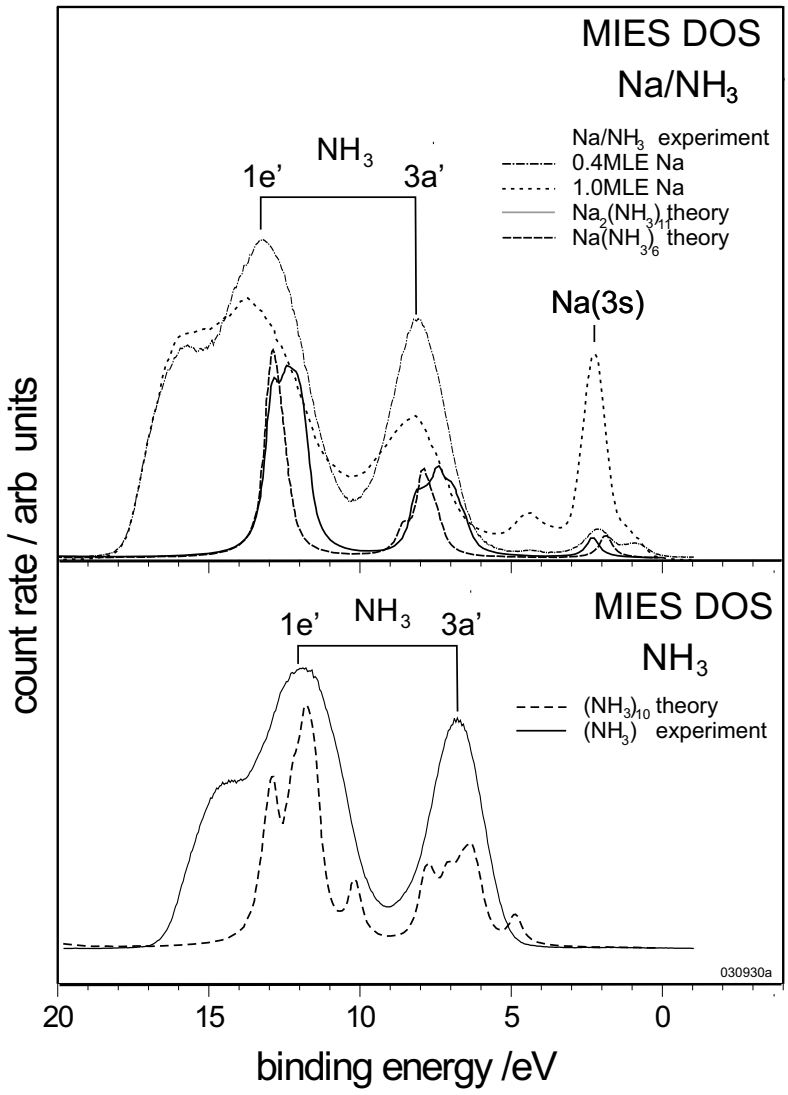

Fig.4: Comparison of the DOS results for various clusters with selected MIES spectra (fig. 2). Bottom: bare NH_3 film and $(NH_3)_{10}$ cluster. Top: Na/NH_3 and the clusters $Na(NH_3)_6$ and $Na_2(NH_3)_{11}$.

Fig.4 summarizes the computational and experimental results by comparing the DOS of the cluster DFT calculations and the MIES spectra. For pure NH_3 the DOS displays the structures from the 1e' and 3a' derived states in the energy range films accessible to MIES; in the solvated cases also the contribution,

originating from the delocalized 3sNa electron, is seen. General agreement with experiment exists in the positions of the observed main features, namely those from the ionization of the NH_3 MOs and the peak (2), attributed to 3sNa delocalization (2.3eV). Peak (1), attributed to emission from 3s electrons localized at the Na core, is not reproduced by the chosen model. The calculations do also not reproduce structure (3) centered around 4.5eV. The good general agreement noticed otherwise between theory and experiment suggests that (3) may not be a feature of the DOS of the system (see below). The inspection of the results without and with Na confirms that, as under liquid conditions, no Na-induced reaction takes place. Theory correctly predicts, but underestimates the shift of 3a' and 1e' of NH_3 towards larger binding energies as a consequence of the Na adsorption. The agreement in the position of the Na-derived peak (2), with respect to the valence band maximum, for both the Na monomer and dimer cases provides evidence for the presence of delocalized 3sNa electrons at the film surface. However, the presence of peak (2) does not necessarily imply that the Na species are fully solvated; there is ample evidence that 3sNs delocalization takes already place when Na interacts with a single NH_3 molecule [1, 2, 3, 4, 5]. After an Na exposure of 1.5MLE a rather dense Na layer is obtained on top of the ammonia film as judged from the decay of the 3a' NH_3 signal. The large intensity of (2) suggests that strong interaction exists between Na and NH_3 in the toplayer. We tend to believe that Na does not become fully solvated as a consequence of the annealing because (2) remains strong up to 160K where part of the NH_3 has already desorbed. On the other hand, it cannot be excluded that some 3sNa charge density "leaks through" an eventual solvation shell, and, thus, becomes accessible to MIES [21].

Peak (3), the satellite of (2), deserves some additional considerations. In order to arrive at a convincing explanation for its origin, we anticipate that partially ammoniated Na_2 species are produced during the Na exposure onto the solid ammonia film. This may happen quite naturally by attaching an additional Na

atom to an existing $Na(NH_3)_n$ cluster. The interaction of Na atoms with hydrated Na-clusters was studied previously by inserting a neutral Na atom next to $Na(H_2O)_n$ (n = 6; 8) [22]. Wave function minimization leads to the formation of a so-called dipolar sodium anion: the negative charge in the HOMO becomes localized between the two Na atoms, close to, but not coinciding with the core of the un-solvated one, hence giving it its dipolar character. We suppose that the Na interaction with $Na(NH_3)_n$ takes place in a similar way as for the hydrated case, and leads to ammoniated $Na_2(NH_3)_{11}$ complexes whose charge distribution is similar as in fig.2(b) of ref. [14]. As for hydration, a clear tendency of the second Na to remain at the "surface" of the ammoniated cluster can be anticipated. In order to explain the occurrence of the satellite, we assume that simultaneous excitation and ionization of the ammoniated Na_2 takes place in MIES during its ionization in the Auger de-excitation process. Hereby, a transition takes place to excited states of the ammoniated Na^+_2 system during the ionization process. This process sequence was studied for ammoniated Na^*_2 anions by combining first-principles calculations with photoelectron spectroscopy [1]. Spectral contributions are seen which correspond to transitions from the ground state of ammoniated Na^*_2 to excited states of ammoniated neutral Na_2, i.e. - to electron detachment accompanied by excitation of the cluster. The 3s-solvation leads to large red shifts of the energies for the transitions from the anionic ground state to excited states correlating with (Na(2S) + Na(2P)). It appears not unreasonable to expect that, as in the case of simultaneous ionization and excitation of the ammoniated anion [1], the spectral features from simultaneous excitation and ionization of the Na_2 ground state to excited states of Na^+_2 are located about 1.5 to 2.5eV above the peak attributed to the Na_2 ground state. Thus, the comparison with the photoelectron spectra for solvated Na^*_2 [1] gives confidence that peak (3) is due to processes involving (partially) ammoniated Na_2 species. Consequently, the existence of the satellite can be considered as evidence that ammoniated dimers are formed during the Na

interaction with solid NH_3 films. Finally, the interaction of NH_3 molecules with the Na adlayer will be discussed (fig.3). Even after an exposure of 30L NH_3 the Na film is not entirely covered by NH_3. As was discussed above, some 3sNa charge density may be seen through a NH_3 adlayer. However, it appears safe to conclude, on the basis of the strong Na(3s) signal seen at all temperatures, that no NH_3 multilayers are formed at 90K on top of the Na film. Upon annealing, (2) becomes more pronounced relative to (1) before it fades away with the onset of NH_3 desorption, suggesting that a temperature-induced rearrangement takes place within the Na-NH_3 system.

4.3.5 Conclusions

The present study, combining Metastable Impact Electron Spectroscopy (MIES) with DFT calculations, is devoted to the Na interaction with ammonia ice. It concentrates on the role played by the Na3s electron in the interaction process. The MIES spectra from pure ammonia ice at 90K are in good agreement with the DFT cluster density of the states of NH_3. Two models for the Na-ammonia interaction were considered, solvation of a single Na atom and of Na dimers. Theory and experiment agree that no Na-induced reaction takes place. The agreement of the MIES spectra with the predictions of both solvation models is rather satisfactorily, in particular concerning the ionization energy of the 3s electron in the NH_3 environment. This suggests that MIES detects 3s electrons, delocalized from their Na^+ core and trapped between the core and surrounding solvent molecules; this reduces the ionization energy by about 1eV as compared to isolated Na species. A satellite, correlated with the main peak from delocalized 3sNa, is seen in the experiment. We attribute it to the simultaneous excitation and ionization of delocalized electrons in Na dimers during their interaction with the He^* probe atoms in MIES. This provides evidence that dimers play a role in the Na-NH_3 interaction.

4.3.6 References

[1] R. Takasu, K. Hashimoto, R. Okuda, K. Fuke: J. Phys. Chem. A 103 (1999) 349

[2] K. Hashimoto, T. Kamimoto, K. Fuke: Chem.Phys.Lett. 266 (1997) 7

[3] K. Hashimoto, T. Kamimoto, N. Miura, R. Okuda, K. Daigoku: J. Chem. Phys. 113 (2000) 9540

[4] P. Brockhaus, I.V. Hertel, C.P. Schulz: J. Chem. Phys. 110 (1999) 393

[5] C.P. Schulz, A. Scholz, I.V. Hertel: Israel J. Chem. xx (2004) submitted

[6] J. Günster, S. Krischok, V. Kempter, J. Stultz, D. W. Goodman: Surf. Rev. Lett. 2002, 9, 1511

[7] A. Borodin, O. Höfft, U. Kahnert, V. Kempter: Vacuum 73 (2004) 15

[8] J. Günster, S. Krischok, J. Stultz, D. W. Goodman: J. Phys. Chem. B 2000, 104, 7977

[9] S. Krischok, O. Höfft, J. Günster, R. Souda, V. Kempter: NIM B 2003, 203, 124

[10] S. Krischok, O. Höfft, V. Kempter: Surf. Sci. 2003, 370, 532-535

[11] A. Borodin, O. Höfft, U. Kahnert, V. Kempter, A. Allouche: Phys. Surf. Engin. 2004, 1, 146

[12] A. Borodin, O. Höfft, U. Kahnert, V. Kempter, Y. Ferro, A. Allouche: J. Chem. Phys. 2004, 120, in print

[13] Y. Ferro, A. Allouche: J. Chem. Phys. 2003, 118, 10461

[14] Y. Ferro, A. Allouche, V. Kempter: J. Chem. Phys. 2004, 120, 1

[15] Y. Harada, S. Masuda, H. Osaki: Chem. Rev. 1997, 97, 1897

[16] H. Morgner: Adv. At. Molec. Opt. Phys. 2000, 42, 387

[17] P. Stracke, S. Krischok, V. Kempter: Surf. Sci. 2001, 473, 86

[18] S. Krischok, O. Höfft, J. Günster, J. Stultz, D. W. Goodman, V. Kempter: Surf. Sci. 2001, 495, 211

[19] K. Kimura et al.: Handbook of HeI Photoelectron Spectra of Fundamental Organic Molecules 1990, Halsted Press, N.Y.

[20] S. Raunier, T. Chiavassa, F. Marinelli, A. Allouche, J.-P. Aycard: J. Phys. Chem. 2003, A 107, 9335

[21] A. Borodin, O. Höfft, U. Kahnert, V. Kempter, A. Poddey, P. Blöchl: J. Chem. Phys. 2004, submitted

[22] F. Mercuri, C.J. Mundy, M. Parrinello: J. Phys. Chem. A 2001, 105, 8423

4.3.7 Zusammenfassung des Unterkapitels 4.3

Die Elektronensolvatisierungsprozesse bei der Wechselwirkung von Natrium mit flüssigem Ammoniak sind schon lange bekannt. Aber es ist nicht einfach ausführliche experimentelle Information zu bekommen. Der Einsatz von MIES, dank seiner guten Empfindlichkeit zum 3s-Elektron von Natrium, ist eine gute Möglichkeit, die Eigenschaften und das Verhalten von diesem Elektron zu untersuchen.

Die Versuche wurden auf einem W(110)-Substrat durchgeführt. Beim Auftragen der Schichten wurden Natrium und Ammoniak in verschiedener Reihenfolge auf bis zu 90K gekühltes Substrat aufgedampft.

1) Beim Angebot des Natriums auf den 2ML dicken Ammoniakfilm lassen sich keine Änderungen der Struktur vom Ammoniak beobachten. Da durch Natrium der Ammoniakfilm abgeschirmt wird, nimmt die Höhe der NH_3-Peaks bei weiterem Na-Angebot ab. Die Strukturen von Natrium treten erst nach 0.5MLE auf, obwohl die Verschiebung der Austrittsarbeit von Beginn an zu sehen ist. Das weist auf das Eindringen der Natrium-Moleküle in die Ammoniakschicht hin. Die Hauptstruktur von Natrium ist ein Peak (Peak 2) bei 2eV; er gehört zum solvatisierten 3s-Elektrom. Die Peakintensität nimmt ab, wenn das Angebot von Na 1MLE erreicht, dabei steigt die Intensität eines Peak (1eV) (Peak 1), der zum neutralen Natrium gehört. Neutrales Natrium kann z.B. dann gebildet werden, wenn Na-Cluster gebildet werden.

   Weil sich bei weiterem Angebot diese zwei Peaks immer beobachten lassen, ist zu sagen, dass Na auf der Ammoniakoberfläche in Form von Inseln wächst.

   Ein weiterer Peak, der von Natrium verursacht wird, tritt bei 4eV auf. Der Peak (Peak 3) taucht mit Peak 2 zusammen auf und ab 1MLE bleibt seine Höhe ungefähr konstant.

2) Wird auf einem Natriumfilm Ammoniak angeboten, so bildet sich bei 90K keine Multilageschicht von Ammoniak. Die 3s-Struktur des geschlossenen Na-Films wird sofort verändert: Anstatt eines breiten 3s-Peaks entstehen die drei weiter oben erwähnten Peaks: Von neutralem Natrium, von solvatisiertem Natrium und noch ein Peak von 4eV.

Zur Erklärung des 4eV-Peaks wurde ein Modell entwickelt. Man geht davon aus, dass im Ammoniakfilm Na-Dimere existieren. Wie Rechnungen zeigen, sind die 3s-Elektronen der Na_2-Dimere in einem Ort lokalisiert. Wenn jetzt im AD-Prozeß ein 3s-Elektron abgelöst wird, kann ein angeregtes Na_2^{+*}-Ion entstehen, falls das zweite 3s-Elektron gleichzeitig angeregt wird. Die dafür benötigte Energie (ca. 2eV) wird vom ausgelösten Elektron aufgenommen. So entsteht ein Peak von 4eV ins Spektrum.

5 Zusammenfassung

In der vorliegenden Arbeit wird die Wechselwirkung von verschiedenen Adsorbaten mit Lösungsmitteln in festem Zustand (meistens Wasser, auch Methanol und Ammoniak) untersucht.

Bei Untersuchungen der Solvatation von Alkali-Halogeniden in Wasser wurde CsCl und, als Vergleich, NaCl untersucht. Die Filme wurden *in situ* bei 80 und 130K unter MIES/UPS Kontrolle präpariert und einschließlich bis auf 300-450K geheizt. Es wurde festgestellt, dass bis 110K keine Reaktion zwischen Salzen und Wasser stattfinden. Erst ab 110K dissoziieren die Salze in die Ionen. Dies lässt sich besonders gut durch ein Aufspalten vom Cl5p-Peak bei NaCl beobachten. Ab 145K fängt Wasserdesorption an. Beim Lösen der Salze im Wasser lässt sich auch eine kritische Konzentration beobachten. Wird die Salz-Sättigungskonzentration noch nicht erreicht, so besteht der Film aus den solvatisierten Ionen, und es gibt keine Möglichkeit, Salz in Ionen- oder Molekularform auf der Wasseroberfläche zu sehen. Es ist auch interessant, dass die Eigenschaften der Wasseroberfläche sogar durch nur eine kleine Menge vom Salz wesentlich geändert werden. Dies betrifft insbesondere die Ausbildung des Wassernetzwerkes über H-Brückenbindungen.

Untersuchungen zur Wechselwirkung zwischen verschiedenen Benzolderivaten (Benzol, Chlorbenzol und 2-Chlorphenol) und festem Wasser wurden auch im Temperaturintervall 80-200K durchgeführt. Die Filme wurden bei 80K in verschiedener Reihenfolge aufgebracht und danach bis 200K geheizt. Die Schichten von Wasser und Benzolderivaten wurden im verschiedenen Reihenfolgen aufgebracht.

Von Benzol auf Wasser lässt sich sagen, dass bei 80K kein Eindringen von Benzol und seiner Derivate in den Wasserfilm zu sehen ist. Ab 105K fängt

schon Benzoldesorption an. Wird Wasser auf Benzol angeboten, scheint Benzoldesorption bis 115K (wenn die Wassermoleküle schon mobil sind) durch den Wasserfilm verhindert zu werden. Desorbiert Wasser vollständig (155K), so verbleiben auf dem Substrat noch einige Moleküle Benzol; sie desorbieren bei 160K. Für Chlorbenzol auf Wasser sieht das Bild ähnlich aus; nur ist die Restschicht von Chlorbenzol dichter. Die Desorptionstemperatur für diese Schicht beträgt 170K. Für 2-Chlorophenol auf Wasser findet erst die Wasserdesorptoion statt. Das lässt den Schluss zu, dass, sobald die Wassermoleküle genügend beweglich werden (110-120K), Wasser durch den Chlorphenolfilm hindurchgehen kann.
Für das Beschreiben der Eigenschaften von den Systemen wurden qualitative Profile der freien Energie vorgeschlagen.

Die wichtigste Frage bei den Untersuchungen von Natrium-Wechselwirkungen mit Wasser, Methanol und Ammoniak war: Welche Rolle hat das 3s-Elektron von Natrium bei den Reaktionen in einem gefrorenen (90K) Film? Um die richtigen Schlüsse zu machen, braucht man Unterstützung von der Theorie. Der Vergleich der mit MIES gemessenen und mit DFT berechneten Spektren zeigt, dass die theoretischen Ergebnisse mit MIES übereinstimmen. Mit der Hilfe der Theorie kann man dann bestimmen, wie die Wechselwirkungsprozesse zwischen Na und dem Film ablaufen.
Die Theorie sagt voraus, dass das 3s-Elektron von seinem Na^+-Kern delokalisiert wird. Das Elektron befindet sich zwischen dem Na^+-Kern und den Molekülen aus der Umgebung. Die Ionisierungenergie des Elektrons ist um 1eV kleiner als die von neutralem Natrium.
Wie es weit bekannt ist, verursacht das Na-3s-Elektron beim flüssigen Wasser die Abspaltung eines H-Atoms, so wird OH gebildet. Bei 90K beschränkt sich die Reaktion auf die letzte Lage des Wasserfilms. Na-Atome, welche an der Reaktion nicht teilnehmen, sind nur im solvatisierten Zustand zu sehen. Das

gemessene Spektrum von solchem Na-Wasser Film stimmt am bestem mit einem gerechneten überein, das besteht aus zwei Anteilen: Ein Anteil stammt vom solvatisierten Natrium in Wasserumgebung und ein anderer von dem Reaktionsprodukt (NaOH) in Wasserumgebung.

Bei Methanol wird bereits ab 120K von dem 3s-Elektron eine bemerkbare Reaktion verursacht. Das Reaktionsprodukt ist Methoxy (CH_3O). Nach der Theorie kann die Reaktion auf zwei Wegen stattfinden: Deprotonation und Dehydratation. In diesen Experimenten ist nicht festzustellen, welchen Mechanismus es in Wirklichkeit gibt.

Bei Ammoniak gibt es überhaupt keine Reaktion mit Natrium. Es lassen sich aber detaillierte Aussagen zu Prozessen der Delokalisierung des 3s-Elektrons machen. Die Theorie sagt einen Peak vom delokalisierten und solvatisierten 3s-Elektron voraus. In den gemessenen Spektren lassen sich noch zwei zusätzliche Peaks beobachten. Eine Struktur kann man dem Na-3s-Elektron aus Na-Clustern zuordnen. Das dient als Beweis, dass Na auf einem Ammoniak-Film in Inseln wächst. Ein weiterer Peak weist auf kollektive Effekte mit Na-Dimeren hin. Wenn sich beim Auftragen neben den Na-Clustern auch Natrium-Dimere im Ammoniak-Film bilden, können die 3s-Elektronen von beiden Na-Atomen aus Na_2 in einem Ort lokalisieren. Wird beim AD-Prozess ein Elektron ausgelöst, so kann das zweite auf ein höheres Niveau übergehen und es wird ein angeregtes Na-Dimer-Ion (Na_2^+*) gebildet. Das ausgelöste vom Na-Dimer Elektron besitzt eine um ca. 2eV kleinere kinetische Energie, als Na-3s-Elektronen von solvatisierten Na-Monomeren.

Bei den in dieser Arbeit vorgestellten Untersuchungen hat sich gezeigt, dass es sinnvoll ist, die Methoden MIES/UPS mit TPD und Infrarot-Spektroskopie (IR) zu kombinieren und die Ergebnisse mit jenen der Theorie (MIES↔DOS, IR↔IR-gerechnete Spektren) zu vergleichen.

TPD lässt sowohl Informationen über die gebildeten Reaktionsprodukte (z.B. bei Na/CH_3OH) als auch Bindung zwischen den Reaktionsprodukten und Film bekommen.
IR oder HREELS können hilfreich bei der Feststellung der Bindungsverhältnisse zwischen Adsorbat- und Filmmolekülen sein.
Am Beispiel der Wechselwirkung zwischen Ameisen- oder Essigsäure und festem Wasser kommen alle Techniken, mit Unterstützung durch die Theorie, zum Einsatz.

Die Erfahrungen dieser Arbeit haben zur Entwicklung eines TPD-Systems geführt (Diplomarbeit S. Bahr).
IR-Spektroskopie an Ameisensäure auf Wasser wird im weiterem in Zusammenarbeit mit der Université de Provence durchgeführt werden.

6 Verzeichnis der Abbildungen

Zum Kapitel I.

Zum Kapitel II. Unterkapitel 2.1.

Zum Kapitel II. Unterkapitel 2.2.

Zum Kapitel III.

Zum Kapitel IV. Unterkapitel 4.1.

Zum Kapitel IV. Unterkapitel 4.2.

Zum Kapitel IV. Unterkapitel 4.3.

Eidesstattliche Erklärung

Hiermit erkläre ich an Eides statt, dass ich die vorliegende Arbeit selbständig ohne unerlaubte Hilfe verfasst und die benutzten Hilfsmittel vollständig angegeben habe.

Andriy Borodin

Eidesstattliche Erklärung

Hiermit erkläre ich an Eides statt, dass ich noch keine früheren Promotionsversuche unternommen habe.

Andriy Borodin

Lebenslauf

Persönliche Daten:

Vorname, Name:	Andriy Borodin
Anschrift:	Hoher Weg 12 38678 Clausthal-Zellerfeld
Telefonnummer	05323-72-3626 (d)
Geburtsdatum:	21. September 1976
Geburtsort:	Stariy Oskol, Rußland
Familienstand:	ledig
Staatsangehörigkeit:	Ukraine

Schulischer Werdegang

1983-1993:	Grundschule in Slaviansk, Ukraine

Studium

1993-1998:	Studium der Physik an der Karasin Kharkiv National Universität, Ukraine
1998:	Diplom Thema der Diplomarbeit: *Dimensionseffekt der Benetzbarkeit auf deformierten Unterlagen* Bewertung der Diplomarbeit: ausgezeichnet

wissenschaftlicher Laufbahn

1998-1999:	Angestellter am Zentrum für wissenschaftliche physikalische Technologien an der Karasin Kharkiv National Universität
1999-2003	Angestellter am Labor dünner Schichten an der Karasin Kharkiv National Universität
2002-2004	wissenschaftlicher Angestellter an der Technischen Universität Clausthal

Andriy Borodin